

School of Molecular and Life Sciences

**Morphology and ecology of fishery important,
cryptic teleosts in Australia**

Miwa Takahashi

0000-0001-8952-051X

**This thesis is presented for the degree of
Doctor of Philosophy
Of
Curtin University**

September 2021

Declaration

To the best of my knowledge and belief this thesis contains no material previously published by any other person except where due acknowledgement has been made.

This thesis contains no material which has been accepted for the award of any other degree or diploma in any university.

The research presented and reported in this thesis was conducted in compliance with the National Health and Medical Research Council Australian code for the care and use of animals for scientific purpose 8th edition (2013). Prior to the commencement of the study ethical approval and guidelines were waived by the Curtin University Human Research Ethics Committee (EC00262), as samples used in this study were collected for different projects at the Western Australian Fisheries and Marine Research Laboratories, Department of Primary Industries and Regional Development, Government of Western Australia (DPIRD) with the appropriate government permits.

Signature:

Date: 23 September 2021

Abstract

Cryptic species are morphologically alike, despite being genetically distinct. Cryptic species targeted by commercial and recreational fishers pose several challenges to biological and ecological studies and fishery assessments. Firstly, accurate species identification is critical for fisheries assessments. However, studies on cryptic species are confronted by the difficulties of visually distinguishing the species. Alternatively, accurate identification can be achieved using DNA barcoding. However, it is time-consuming and expensive. Secondly, understanding the niche of cryptic fishes, including diet and habitat requirements, is important in order to optimise ecosystem-based fisheries management strategies. However, based on the ecomorphology theory, the more similar the morphology is, the more similar the ecology and niche requirements are. Therefore, species-specific niche and partitioning patterns between cryptic species can be subtle and hard to detect. Thirdly, ecological studies are challenged by the complex life cycle of teleosts as niche requirements may differ for each life stage. Our understanding of juvenile fish ecology is particularly limited, possibly owing to difficulties of collecting samples of juvenile fish and identifying small-sized diet items. In order to overcome these challenges, I assessed the morphology and ecology of cryptic teleost species which have high value to commercial and recreational fishers in Australia.

Morphometric analyses on otoliths were conducted to validate the development of a robust, cost-effective species identification tool for nine teleost species from four genera (*Centroberyx*, *Lethrinus*, *Polyprion* and *Sillago*) that are morphologically alike within each genus (Chapter 2). The multivariate morphometric models provided very high correct species prediction rates (92.5-99.9%) for all genera. Size distribution of misclassified specimens was notably smaller than those of correctly classified specimens, indicating lower species predictive power for juveniles. Therefore, in the following chapter, I performed additional morphometric analyses on the cryptic juveniles of *Lutjanus erythropterus* and *L. malabaricus* using not only otolith, but also body morphometric variables (Chapter 3). The most parsimonious multivariate models achieved the correct species prediction at rates of 98.81% and 84.88% using body and otolith variables respectively. The findings from Chapters 2 and 3 highlighted the robustness of otolith and body morphometric approaches to discriminate between adult and juvenile, cryptic teleost species.

In order to understand diet requirements and niche partitioning patterns between the species and life stages of cryptic species, DNA metabarcoding dietary studies were performed on *L. erythropterus* and *L. malabaricus*. Predator-specific blocking primers were developed and polymerase chain reaction protocols were optimised in order to suppress the dominant predator

DNA (*Lutjanus* spp.) and amplify highly degraded prey-DNA during PCR (Chapter 4). A total of 37 prey taxa from six phyla were identified using the blocking primers and a series of taxa-specific and universal primers, revealing significant diet partitioning patterns between each species and their life stages (Chapter 5).

Spatial distribution range and essential fish habitats of *L. erythropterus* and *L. malabaricus* were assessed using a dataset comprising 19,784 individual Baited Remote Underwater Video systems collected from across Australia (Chapter 6). Using species distribution models, I identified the length-specific essential fish habitats of these species, indicating clear ontogenetic migration patterns from inshore to offshore mesophotic waters. This study also suggested differences in size distribution and schooling behaviours between the species. These findings are likely to be associated with the diet partitioning patterns between species and life stages identified in Chapter 5.

By combining the morphological and ecological data, I discussed evolutionary mechanisms and specialized adaptation required for the cryptic *Lutjanus* species to coexist within an ecosystem. Species-specific niche requirements may imply different susceptibility to fisheries and changing environment including habitat degradation, suggesting the importance of conducting species-specific fishery assessment and management for cryptic species. Length-specific distribution predictive maps provided key information to identify management strategies, such as no-take marine reserves, seasonal closures and restrictions of certain fishing gears (i.e. trawls), on nursery grounds to enhance the survival of vulnerable juveniles.

Statement of Contributions

Chapter 2: Takahashi, M., Wakefield, C. B., Saunders, B. J., Harvey, E. S., Newman, S. J. (in preparation) Testing the utility of otolith morphometric approaches to resolve cryptic species of tropical and temperate teleosts.

Author contributions: C.B.W and S.J.N designed the study and collected the samples. M.T. conducted data analyses and wrote the manuscript. All authors reviewed and commented on the manuscript.

Chapter 3: Takahashi, M., Wakefield, C. B., Newman, S. J., Hillcoat, K., Saunders, B. J., Harvey, E. S. (in preparation) Cryptic species discrimination for the juveniles of two lutjanids using body and otolith morphometry.

Author contributions: C.B.W and S.J.N designed the study. M.T, C.B.W, S.J.N, K.H collected the samples. M.T. conducted data analyses and wrote the manuscript. All authors reviewed and commented on the manuscript.

Chapter 4: Takahashi, M., Jarman, S., DiBattista, J. D., Bunce, M. (2020) Development of predator specific blocking primers for *Lutjanus erythropterus* and *L. malabaricus*; implication for DNA metabarcoding dietary studies on the fishery important red snappers. Supplementary information for: *Scientific Reports*, <https://doi.org/10.1038/s41598-020-60779-9>

Author contributions: M.T., J.D.D., S.J. and M.B. designed the study and developed the methods. M.T. performed experiments, bioinformatics and data analyses, and wrote the manuscript with the input from all authors.

Chapter 5: Takahashi, M., DiBattista, J. D., Jarman, S., Newman, S. J., Wakefield, C. B., Harvey, E. S., Bunce, M. (2020) Partitioning of diet between species and life history stages of sympatric and cryptic snappers (Lutjanidae) based on DNA metabarcoding. *Scientific Reports*. 10:4319, <https://doi.org/10.1038/s41598-020-60779-9>

Author contributions: M.T., E.S.H., M.B., S.J.N. and C.B.W. conceived and designed the study. M.T., J.D.D., S.J. and M.B. developed the methods. S.J.N. and C.B.W. collected the samples. M.T. performed experiments and bioinformatics. All authors discussed the results. M.T. and E.S.H. analysed data. M.T. wrote the manuscript with the input from all authors.

Chapter 6: Takahashi, M., Newman, S. J., Wakefield, C. B., Galaiduk, R., Langlois, T. J., Saunders, B. J., Harvey, E. S. (in preparation) The distribution and habitat preferences of two valuable sympatric snapper species.

Author contributions: M.T, E.S.H., T.J.L. and S.J.N. designed the study and collected samples. M.T. and R.G. performed data analyses. M.T. wrote the manuscript with the input from all authors.

I, as a co-author, endorse that the levels of contributions indicated above are appropriate.

Euan S. Harvey Signature:

Stephen J. Newman Signature:

Benjamin J. Saunders Signature:

Michael Bunce Signature:

Joseph D. DiBattista Signature:

Simon Jarman Signature:

Corey B. Wakefield Signature:

Tim J. Langlois Signature:

Ronen Galaiduk Signature:

Kyle Hillcoat Signature:

Acknowledgements

I acknowledge the traditional custodians of the land and sea country where this research was conducted and pay my sincere respects to the Elders past, present and emerging.

Every single PhD journey is different, and there is no such journey that is just about PhD. My PhD journey has been a big part of my life, in conjunction with motherhood and cancer. I could never go through either of them without all the supports I received from my supervisors, family and friends.

My primary supervisor, Euan Harvey, has provided me not only scientific guidance but also career and life advice. He helped me to create and proceed the PhD projects considering my family, health, work-life balance and post-PhD career. Thank you, Euan, for your support and the important academic and life lessons. I'd also like to thank my co-supervisors and co-authors for their support for lab work, analyses and writing - Steve Newman, Corey Wakefield, Ben Saunders, Mike Bunce, Joey DiBattista, Simon Jarman, Ronen Galaiduk and Kyle Hillcoat.

I'd like to thank my family in Japan for giving me full support and love every day of my life. Their kindness and hard-working ethics taught me how to be kind and resilient to proceed with any challenges I come across including my PhD. Thank you Jaume for your enormous love, kindness, patience and strength. You are the best partner, father, friend and PhD buddy in the whole world. Kaito, thank you for giving me so much happiness, joy, laughter, courage and strength on every single good and bad day, and also for not giving me much free time so that I was forced to be productive during the limited time given. Anita, Kathy, Kim, Zuzu and Ceci, our love for the ocean brought us together in Townsville when we were young and free. Although we are not so young and free anymore, it's been amazing to be reunited with you in Perth and share our paths together again. Thank you for your love, friendship, academic advice, and all the fun times together. Thank you for my friends (Kathy, Aidan, Manu, Francesco, Miki san, Ralf, Meg, Karl, Natasha, Owain, Mai, Ori, Anna, and many more) and their kids for looking after Kaito and playing with him. Without your help, I would be still writing my thesis for many more months.

Logistical support for this project was provided by Curtin University and the Department of Primary Industries and Regional Development, Government of Western Australia (DPIRD). Many thanks to all my friends and colleagues in TrEnD Lab and Fish Ecology Labs for your intellectual and technical help as well as your great companies and laughter inside/outside of office. For Chapter 2, I would like to thank all DPIRD staff for their help and assistance with

sample collections, measurements and processing. For Chapter 3, I acknowledge Kyle Hillcoat and Department of Agriculture and Fisheries in Queensland for collecting samples in QLD. For Chapter 4 & 5, I would like to send a special thanks to Matt Heydenrych, Katrina West, Matt Power, Kristen Fernandes, Alicia Grealy, Tina Berry, Megan Coghlan and Frederik Seersholm for teaching me about eDNA workflow and analyses. For Chapter 6, thank you Ronen for assisting me to learn modelling. Thank you, Zoe Richard, Natasha Hurley-Walker and Catherine Boisvert for your mentoring support and being my mother/scientist role model. It's been a steep, fun learning curve thanks to you all!

This PhD has been supposed by an Australian Postgraduate Award (APA) and Curtin University Postgraduate Scholarship (CUPS). Chapter 4 and 5 were funded by ACR Linkage Projects (LP16100839 and LP160101508). BRUVs data and metadata used in Chapter 6 were contributed via the online portal, GlobalArchive. I thank all the data providers who collected BRUVs data for other projects and supplied it to the GlobalArchive database. GlobalArchive was supported by the Australian Research Data Commons (ARDC) and synthesis work was supported through the ARDC's Marine Research Data Cloud project.

Table of Contents

Declaration	i	
Abstract	ii	
Statement of Contributions.....	iv	
Acknowledgements	vi	
Table of Contents	viii	
List of Figures	xii	
List of Tables.....	xvii	
Abbreviations	xxi	
Chapter 1	General introduction..... 1	
1.1	Background and rationale	1
1.1.1	Ecological theories and cryptic species.....	1
1.1.2	Diverse marine ecosystems and fishery management.....	2
1.1.3	Challenges and research needs.....	3
1.1.3.1	Identification of cryptic species.....	3
1.1.3.2	Needs for high resolution studies	3
1.1.3.3	Complex life cycle.....	4
1.2	Research questions and thesis structure	5
1.2.1	The utility of otolith morphometry for identifying cryptic species of tropical and temperate teleosts (Chapter 2).....	9
1.2.2	Cryptic species discrimination for the juveniles of two lutjanids using body and otolith morphometry (Chapter 3)	9
1.2.3	Development of predator specific blocking primers for <i>Lutjanus erythropterus</i> and <i>L. malabaricus</i> ; implications for DNA metabarcoding dietary studies on the fishery important red snappers (Chapter 4).....	9
1.2.4	Partitioning of diet between species and life history stages of sympatric and cryptic snappers (Lutjanidae) based on DNA metabarcoding (Chapter 5)	10
1.2.5	The distribution and habitat preferences of two sympatric snapper species on the northwest and northeast coasts of Australia (Chapter 6).....	10
1.2.6	General discussion (Chapter 7)	11
Chapter 2	The utility of otolith morphometry for identifying cryptic species of tropical and temperate teleosts	13
2.1	Abstract	13
2.2	Introduction	14

2.3	Materials and methods	17
2.3.1	Sample and data collection.....	17
2.3.2	Statistical analyses	18
2.4	Results	19
2.5	Discussion	28
Chapter 3	Cryptic species discrimination for the juveniles of two lutjanids using body and otolith morphometry.....	31
3.1	Abstract	31
3.2	Introduction	31
3.3	Materials and methods	33
3.3.1	Sample collection and genetic species identification.....	33
3.3.2	Morphometrics measurement.....	35
3.3.3	Statistical analyses	36
3.4	Results	37
3.4.1	Species distinction.....	37
3.4.1.1	Body morphometrics	37
3.4.1.2	Otolith morphometrics.....	38
3.4.1.3	Body and otolith combined	39
3.5	Discussion	45
Chapter 4	Development of predator specific blocking primers for <i>Lutjanus erythropterus</i> and <i>L. malabaricus</i> ; implication for DNA metabarcoding dietary studies on the fishery important red snappers.....	49
4.1	Abstract	49
4.2	Introduction	49
4.3	Materials and Methods.....	51
4.3.1	Blocking primer design.....	51
4.3.2	<i>In-silico</i> examination.....	52
4.3.3	<i>In-vitro</i> examinations	52
4.3.4	Bioinformatics.....	54
4.4	Results	54
4.5	Discussion	56
Chapter 5	Partitioning of diet between species and life history stages of sympatric and cryptic snappers (Lutjanidae) based on DNA metabarcoding.....	59
5.1	Abstract	59
5.2	Introduction	59
5.3	Materials and methods	61

5.3.1	Sample collection.....	61
5.3.2	Species identification of cryptic juveniles	64
5.3.3	Gastrointestinal tract content dissection.....	64
5.3.4	DNA extraction	65
5.3.5	Amplification and sequencing.....	65
5.3.6	Quality filtering of sequence reads and taxonomic assignment to prey taxa	67
5.3.7	Data analyses.....	68
5.4	Results	69
5.5	Discussion	75
5.6	Supplementary information.....	80
5.6.1	Assessment of sampling and sequencing depth	81
Chapter 6	The distribution and habitat preferences of two sympatric snapper species on the northwest and northeast coasts of Australia	89
6.1	Abstract	89
6.2	Introduction	90
6.3	Materials and methods	91
6.3.1	BRUVs sample and data collection.....	91
6.3.2	Species distribution modelling and predictive mapping	93
6.4	Results	96
6.4.1	Depth and latitudinal distribution patterns	96
6.4.2	MaxN records.....	99
6.4.3	Body length records	99
6.4.4	Presence/absence models	100
6.4.5	Body length models.....	104
6.4.6	Predictive maps of Presence/Absence and body length combined	104
6.5	Discussion	105
6.6	Supplementary materials.....	110
Chapter 7	General discussion	113
7.1	Major findings and significance of the thesis.....	115
7.1.1	Multivariate morphometric analysis is a robust tool to discriminate fishery important, cryptic species.....	115
7.1.2	Ecological insights of morphologically cryptic species.....	116
7.1.3	Ontogenetic shifts in niche.....	118
7.2	Future implications, management and conservation.....	118
7.3	Limitations of this thesis and future research directions.....	121

7.3.1	Spatial and temporal comparisons	121
7.3.2	Further studies on juvenile ecology	121
7.3.3	Dietary metabarcoding studies.....	122
7.3.4	Expansions to other taxa and monitoring studies.....	122
7.4	Thesis conclusion.....	123
Bibliography.....		125

List of Figures

Figure 1.1 Flow diagram outlining the background, rational and the structure of thesis.	6
Figure 2.1 Map of Western Australia indicating four bioregions and fishing areas where samples were collected. The map was sourced from Saunders <i>et al.</i> (2018).	17
Figure 2.2 Kernel density plots representing the distributions of fish length (mm) for each species and region.	22
Figure 2.3 Canonical Analysis of Principal Coordinates (CAP) ordination plots of otolith morphometrics data and fish length for each genus, using a euclidean distance similarity matrix. The overlay vectors are the multiple partial correlations of morphometric variables with the two canonical axes. The circle around the vectors indicates the correlation coefficient of 1. The closer the vector reaches to the circle, the higher the correlation coefficient is. CA, <i>C. australis</i> ; CG, <i>C. gerrardi</i> ; CL, <i>C.</i> <i>lineatus</i> ; LN, <i>L. nebulosus</i> ; LP, <i>L. punctulatus</i> ; PA, <i>P. americanus</i> ; PO, <i>P. oxygeneios</i> ; SB, <i>S. bassensis</i> ; SV, <i>S. vittate</i> ; FL, fish length; OL, otolith length; OW, otolith width; OT, otolith thickness; Owe, otolith weight.	23
Figure 2.4 Canonical Analysis of Principal Coordinates (CAP) ordination plots of otolith morphometrics data of nine study species, using a euclidean distance similarity matrix with different combinations of otolith morphometric variables (six scenarios) for each genus (A). The bar plots (B) indicate the CAP leave-one-out allocation success rates (%) for each scenario. Circled points in CAP plots are misclassified samples. Asterisk in the bar plots indicates the most parsimonious model of each genus, which achieved the highest allocation success rates with the least number of variables. The six scenarios are referred to in Table 2.2.	25
Figure 2.5 Boxplots (A) showing the medians of fish length (mm) (\pm 95% confidence interval) of correctly (blue) and incorrectly (red) assigned fish based on Canonical Analysis of Principal Coordinates (CAP) leave-one- allocation approach using the most parsimonious CAP model for each genus. The error bars indicate \pm 1.5 interquartile range. Scatter plots (B) of fish length showing misclassified samples indicated by the black circled points for each species.	26
Figure 2.6 Canonical Analysis of Principal Coordinates (CAP) ordination plot of otolith morphometrics data of nine study species for the ‘bag of unknown otoliths scenario’, using a euclidean Distance similarity matrix. The overlay vectors are the multiple partial correlations of morphometric variables with the two canonical axes. The circle around the vectors indicates the correlation coefficient of 1. The closer the vector reaches to the circle, the higher the correlation coefficient is. OL, otolith length; OW, otolith width; OT, otolith thickness; Owe, otolith weight.	27

- Figure 3.1 Location where samples of juvenile *Lutjanus erythropterus* (LE) and *L. malabaricus* (LM) were collected in the Pilbara (WA), Kimberley (WA) and central Queensland (QLD) regions of Australia. The numbers in boxes indicate the sample size of each species and region. 34
- Figure 3.2 Images of the juveniles and the distal aspect of left sagittal otoliths of *Lutjanus erythropterus* and *L. malabaricus*. The numbers in the images indicate the points of morphometric measurements; 1 – 2, jaw length; 1 – 3, jaw to operculum; 1 – 4, jaw to preoperculum; 1 – 5, jaw to eye; 6 – 7, eye to dorsal fin; 7 – 8, dorsal fin length; 9 – 10, body height; 1 – 11, fork length; 12 – 13, otolith length; 14 – 15, otolith width; 16, otolith thickness. 36
- Figure 3.3 Leave-one-out allocation success rates to the correct species (%) for the selected Canonical Analysis of Principal Coordinates (CAP) models using different combinations of body (left) and otolith (right) morphometric variables. Species (red) and species and region (blue) were used as factor(s) of groups in the CAP analyses. 39
- Figure 3.4 Canonical Analysis of Principal Coordinates (CAP) plots of body (left) and otolith (middle) morphometric arrangements of juvenile *L. erythropterus* (LE) and *L. malabaricus* (LM). The 1-dimensional plots (A) considered species as the factor for CAP analyses, and the 2-dimensional plots (B) considered species and regions as the factors for the analyses. The variables for each model were the most parsimonious models of each variable types (body (left) and otolith (middle)) and each CAP factor (species with/without region) (i.e. The body morphometric models were constructed using dorsal fin length, jaw length, and distance from jaw to eye). The CAP models with both body and otolith variables of each of the most parsimonious models were also assessed (right). The overlay vectors are the multiple partial correlations of morphometric variables with the two canonical axes. The circle around the vectors indicates the correlation coefficient of 1. The closer the vector reaches to the circle, the higher the correlation coefficient is. DF, dorsal fin; FL, fork length; OL, otolith length; OW, otolith width; OT, otolith thickness; Owe, otolith weight. 40
- Figure 4.1 Frequency histogram of the number of base pairs mismatched with *Lutjanus erythropterus* blocking primer (LEBP) (left) and *L. malabaricus* blocking primer (LMBP) (right), based on *in-silico* examination of 16S ribosomal RNA (rRNA) sequences. 55
- Figure 4.2 Mean C_T values (\pm SD, standard deviation) at different amounts of *Lutjanus malabaricus* blocking primer (LMBP) and annealing temperatures. The ratio on the x-axis refers to the ratio of LMBP to the Fish16S primer added into the PCR master mix. Letters above each bar imply statistically similar means for C_T values. 55
- Figure 4.3 Relative read abundance of prey (*Sardinops sagax*) and host (*Lutjanus erythropterus* and *L. malabaricus*) DNA with/without blocking primers. The ratio on the x-axis refers to the DNA ratio of prey to host in the template. Negative and positive symbols indicate mastermixes without and with blocking primer, respectively. SS, *S. sagax*; LE, *L. erythropterus*; LM, *L. malabaricus*; BP, blocking primer. 56

- Figure 5.1 Locations where juvenile and adult samples of *Lutjanus erythropterus* and *L. malabaricus* were collected in the Pilbara region of northwestern Australia (generated using ArcMap v10.3.1, <https://desktop.arcgis.com>). Areas open to commercial fish trawling (shaded) and the 50 m and 100 m depth contours (grey lines) are shown. 62
- Figure 5.2 Frequency-of-occurrence (FOO) (%) of prey taxa identified in the intestinal contents of juvenile and adult *Lutjanus erythropterus* (LE) and *L. malabaricus* (LM). Two to three letters at the end of the taxa names refers to general diet categories; Tel, teleost; Tun, tunicate; Mal, malacostracan crustacean; Cop, copepod; Cep, cephalopod; Pol, polychaete; Med, medusa; CJ, comb jelly. 71
- Figure 5.3 Canonical Analyses of Principal Coordinates (CAP) ordination plots of prey assemblage data from intestinal contents of adult and juvenile *Lutjanus erythropterus* (LE) and *L. malabaricus* (LM), using Jaccard coefficient matrix of presence and absence (PA) data. The overlaid vectors are the Pearson correlations of prey taxa with the two canonical axes, which had the correlation coefficient higher than 0.3. The circle in CAP indicated the correlation coefficient of 1. The closer the vector reaches to the circle, the higher the correlation coefficient is. The first three characters of the taxa names were displayed if the taxa were assigned to genus or higher levels. The first character of genus and three characters of species names are displayed if the taxa were assigned to the species level. Colour of the taxa labels indicate the functional categories..... 73
- Figure 6.1 Map of Australia indicating the location of BRUVs survey sites (yellow points). Close-up maps detail the northwest (left) and northeast (right) coasts that encompass all the BRUVs sites where *L. erythropterus* (top) and *L. malabaricus* (bottom) were sighted (red circles). The size of the red circles is directly related to the MaxN of each species. 92
- Figure 6.2 Heat maps of (A) the number of BRUVs deployed, and (B) the frequency of occurrence (FOO) (%) of *L. erythropterus* and *L. malabaricus* on the northwest (NW) (left) and northeast (NE) coasts (right) of Australia, at latitudes ranging from 10 to 30 °S and depths ranging from 0 to 350 m. Numbers in each grid also indicate the total number of BRUVs deployed (A) and FOO (B) within each depth and latitudinal range. ... 98
- Figure 6.3 Smoother estimates for the explanatory variables as obtained by boosted regression trees (BRT) for occurrence (A), and generalised additive mixed models (GAMMs) for body length (B) of *L. erythropterus* and *L. malabaricus* on the northwest coast of Australia. Marks in the plots represent the sampled data points. In the BRT, marks above the estimated lines represent the presence records, and marks below the lines represent the absence records. The datapoints of juveniles (under 150mm body length) were duplicated for *L. erythropterus* and *L. malabaricus* due to the inability of juvenile discrimination in BRUVs images. Std50, standard deviation of the local neighbourhood water depth of 50-grid cell kernel radius; SE, standard error. 102

Figure 6.4 Predictive maps of occurrence and body length of *L. erythropterus* and *L. malabaricus* on the northwest coast of Australia. Probability of occurrence (A) was predicted using the selected models of boosted regression trees, which was then converted to presence and absence (P/A) (B) based on the threshold (sensitivity = specificity) of 0.041 and 0.063 for *L. erythropterus* and *L. malabaricus* respectively. Body length (C) was predicted using the final models of the generalised additive mixed models. The predicted area covers the depth to 131 m, latitude between 13.3 and 25.5 °S, and longitude between 112.9 and 130.2 °E. 103

Figure 6.5 Predictive maps of the body length and occurrence combined for *L. erythropterus* (left) and *L. malabaricus* (right) on the northwest coast of Australia. Grey area indicates the area where absence of the species was predicted. The predicted area covers the depth up to 131 m, latitude between 13.3 and 25.5 °S, and longitude between 112.9 and 130.2 °E. 105

Figure 7.1 Flow diagram outlining the conclusions and future directions identified in this thesis. 114

Supplementary Figures

Figure S 5.1 The quality profiles of forward (A) and reverse (B) reads of paired-end sequences. Green line, orange line, and dashed orange lines represent the mean, median, and the 25th and 75th percentiles respectively. A grey-scale heat map represents the distribution of quality scores at each position, with dark colours corresponding to higher frequency. The mean quality scores gradually declined throughout the cycles for forward reads, whereas reverse reads experienced a steeper decline in quality scores approximately after the 100th cycle. 80

Figure S 5.2 Mean number of reads (A) and mean number of prey taxa (B) (+/- SD, standard deviation) obtained from the intestinal content of adult and juvenile *Lutjanus erythropterus* and *L. malabaricus*. Italics letters above the error bars imply statistically similar means for number of reads. 81

Figure S 5.3 Rarefaction curves of intestinal content samples from a universal (18SUni) and three sets of taxa specific primers (Fish16S, SCrust, and SCeph). The plateaus of the curves indicate the sufficient sequencing efforts to reveal the majority of the detected amplicon sequence variants (ASVs) (A) and prey taxa (B). SD, standard deviation. 82

Figure S 5.4 Species accumulation curves of amplicon sequence variants (ASVs) (A) and prey taxa (B) identified from the intestinal contents of adult and juvenile *Lutjanus erythropterus* (LE) and *L. malabaricus* (LM) with all primers combined. SD, standard deviation. 82

Figure S 6.1 Various measures of classification accuracy at different thresholds, based on boosted regression trees (BRT) for presence/absence of *L. erythropterus* (left) and *L. malabaricus* (right) on the northwest coast of Australia. For both species, higher sensitivity was achieved at sensitivity = specificity (red dotted line) compared to those at max

(sensitivity + specificity; dark green dotted line) and maximum Kappa (light green dotted line). Therefore, the threshold selection criterion of sensitivity = specificity was used in this study to ensure lower false negative rates and to minimise the chance of a management area leaving populations unprotected. 110

List of Tables

Table 1.1 Images and relevant information (common names, maximum size recorded, and distribution maps) of the study species. The distribution maps were generated using ArcMap v10.6 (https://desktop.arcgis.com) with the shapefile retrieved from Codes for Australian Aquatic Biota (CAAB) database (http://www.cmar.csiro.au/caab/) on October 16 2020. Occurrence points were mapped for <i>L. punctulatus</i> as a shapefile was not available (occurrence coordinates also retrieved from CAAB). The images of fish for <i>Lethrinus</i> spp. were sourced from Saunders <i>et al.</i> (2018), and <i>Sillago</i> , <i>Centroberyx</i> and <i>Polyprion</i> spp. were sourced from CSIRO Australian National Fish Collection.	7
Table 2.1 Images of fish and sagittal otoliths, common names, sampling regions and sample sizes (n) for the nine study species. Scale bars (white lines) on otolith images are 1 mm. GC, Gascoyne Coast; PN, Pilbara nearshore; PO, Pilbara offshore; WC, West Coast; SC, South Coast; SW, Southwest coast; Metro, adjacent to Perth metropolitan region. The images of fish for <i>Lethrinus</i> spp. were sourced from Saunders <i>et al.</i> (2018), and <i>Sillago</i> , <i>Centroberyx</i> and <i>Polyprion</i> spp. were sourced from CSIRO Australian National Fish Collection. Otolith photos were taken by Chris Dowling, Department of Primary Industries and Regional Development.	15
Table 2.2 Combinations of morphometric variables at different scenarios. FL, fish length; OL, otolith length; OW, otolith width; OT, otolith thickness; Owe, otolith weight.	19
Table 2.3 Descriptive statistics for fish length and otolith morphometric variables for the nine study species from Australia. All length measurements are in mm, and weight is in g. SE, standard error.	21
Table 2.4 Leave-one-out allocation success rates (%) of the Canonical Analysis of Principal Coordinates (CAP) using otolith morphometry and fish length data to distinguish the species (Spp) and region (Spp*Region) within each genus. GC, Gascoyne Coast; PN, Pilbara nearshore; PO, Pilbara offshore; WC, West Coast; SC, South Coast; SW, Southwest coast; Metro, adjacent to Perth metropolitan region.	24
Table 2.5 Leave-one-out allocation results of Canonical Analysis of Principal Coordinates (CAP) analyses using otolith morphometric measures of nine study species for the ‘bag of unknown otoliths scenario’. <i>C. aus</i> , <i>C. australis</i> ; <i>C. ger</i> , <i>C. gerrardi</i> ; <i>C. lin</i> , <i>C. lineatus</i> ; <i>L. neb</i> , <i>L. nebulosus</i> ; <i>L. pun</i> , <i>L. punctulatus</i> ; <i>P. ame</i> , <i>P. americanus</i> ; <i>P. oxy</i> , <i>P. oxygeneios</i> ; <i>S. bas</i> , <i>S. bassensis</i> ; <i>S. vit</i> , <i>S. vittata</i> ; % cor, correct allocation rate (%).	28
Table 3.1 Descriptive statistics for fork length measurements of <i>Lutjanus erythropterus</i> and <i>L. malabaricus</i> collected from Pilbara, Kimberley and Queensland (QLD). SE, standard error.	35

Table 3.2 Leave-one-out allocation success rates (%) to the correct species, and the combinations of body (A) and otolith (B) morphometric variables for the selected Canonical Analysis of Principal Coordinates (CAP) models using different combinations of morphometric variables. Species was considered as the factor of groups in the CAP analyses. The most parsimonious models were indicated in red, bold texts.	41
Table 3.3 Leave-one-out allocation success rates (%) to the correct species, and the combinations of body (A) and otolith (B) morphometric variables for the selected Canonical Analysis of Principal Coordinates (CAP) models using different combinations of morphometric variables. Species and regions were considered as the factors of groups in the CAP analyses. The most parsimonious models were indicated in red, bold texts.	42
Table 3.4 Leave-one-out allocation results using the most parsimonious Canonical Analysis of Principal Coordinates (CAP) models with body (A), otolith (B) and body and otolith (C) morphometric variables. Species was used as the factors for the CAP analyses. LE, <i>Lutjanus erythropterus</i> ; LM, <i>L. malabaricus</i> ; Ob, observed.	43
Table 3.5 Leave-one-out allocation results using the most parsimonious Canonical Analysis of Principal Coordinates (CAP) models with body (A), otolith (B) and body and otolith (C) morphometric variables. Species and regions were used as the factors for the CAP analyses. LE, <i>Lutjanus erythropterus</i> ; LM, <i>L. malabaricus</i> ; Pil, Pilbara; Kim, Kimberley; QLD, Queensland.	44
Table 4.1. The Fish16S primer and the host-specific blocking primer sequences (LEBP, <i>Lutjanus erythropterus</i> blocking primer; LMBP, <i>L. malabaricus</i> blocking primer). The first 10 base pairs of the blocking primers (bold and italic font) overlap with the 3' end of the forward Fish16S primer, followed by 15 base pairs of the host specific sequences. The C3 spacer at the 3' end is a modified DNA oligonucleotide, which inhibits annealing	52
Table 5.1 Number of juvenile and adult <i>Lutjanus erythropterus</i> (LE) and <i>L. malabaricus</i> (LM) for each category of sampling variables. Fullness of stomach was recorded as “full” when a prey item was observed in a stomach. Sampling details such as time and depth were not available for each adult specimen as trawl shot numbers were not recorded for individual fish. TL, total length.....	63
Table 5.2 List of primers targeting genes of potential prey items of <i>Lutjanus erythropterus</i> and <i>L. malabaricus</i> , and host-specific blocking primer (LEBP, <i>Lutjanus erythropterus</i> blocking primer; LMBP, <i>L. malabaricus</i> blocking primer). The first 10 base pairs of the blocking primers overlap with the 3' end of the forward Fish16S primer (bold and italic font), followed by 15 base pairs of the host specific sequences. The C3 spacer at the 3' end is a modified DNA oligonucleotide, which inhibits annealing. Minimum length of each primer is the threshold length used for quality filtering of sequences. T, annealing temperature; F, forward primer; R, reverse primer.	66

Table 5.3 The results of PERMANOVA (A) and pairwise-PERMANOVA (B) testing the differences in diet composition of juvenile and adult <i>Lutjanus erythropterus</i> (LE) and <i>L. malabaricus</i> (LM), using 9999 permutations. Fullness of stomach was incorporated into the analyses as a covariate to test its effect on diet composition. The tests were based on Jaccard coefficient matrix for presence and absence (PA) datasets.....	72
Table 6.1. Descriptions of the explanatory variables used for the boosted regression trees (BRT) and generalized additive mixed models (GAMMs)	94
Table 6.2 Summaries of BRUVs counts, MaxN and length of <i>L. erythropterus</i> and <i>L. malabaricus</i> sighted by BRUVs in northwest (NW) coast and northeast (NE) coast of Australia. Total number of BRUVs is the number of BRUVs deployed above 25 °S on each coast, regardless of the sighting of <i>L. erythropterus</i> and <i>L. malabaricus</i> . Range and mean of MaxN were generated excluding the absence records. Mean length was calculated without juveniles (under 150 mm). SD, standard deviation.....	99
Table 6.3 The summary of the final models and model validations of boosted regression trees (BRT) for presence/absence and generalised additive mixed models (GAMMs) for length of <i>L. erythropterus</i> and <i>L. malabaricus</i> on the northwest coast of Australia. The percentage values for the selected explanatory variables in BRT represent the percentage contributions to the models. Threshold dependent validation parameters, such as specificity and sensitivity, were the values at the threshold where specificity was equal to sensitivity. Normalised root mean square error (nRMSE) and adjusted R squared value (adj. R ²) were based on a linear regression between the observed values of the test dataset and values predicted without a null term. Asp, aspect; bathy, bathymetry; prof, profile; slp, slope; std50, standard deviation of the local neighbourhood water depth of 50-grid cell kernel radius; curv, curvature; rng30, maximum minus the minimum elevation in the local neighbourhood (local relief) of 30-grid cell kernel radius; AUC, area under curve.....	101

Supplementary Tables

Table S 5.1 Taxonomic assignment (A) as well as the results of PERMANOVA (B) and pairwise-PERMANOVA (C) using different percent identify match thresholds (0, 1 and 2%). The threshold defines the maximum difference between the percent identity matches of primary and non-primary reference sequences allowed in the lowest common ancestor (LCA) assignment algorithm. When the difference between the percent identity matches of primary and non-primary reference sequences was more than the threshold, the non-primary reference sequences were omitted prior to LCA assignment. PERMANOVA (B) and pairwise-PERMANOVA (C) examined the differences in diet composition of juvenile and adult <i>Lutjanus erythropterus</i> (LE) and <i>L. malabaricus</i> (LM), using 9999 permutations. Fullness of stomach was incorporated into the analyses as a covariate to test its effect on diet composition. The tests were based on Jaccard coefficient matrix for presence and absence (PA) datasets.....	83
---	----

Table S 5.2 The list of prey taxa as lowest common ancestors (LCA) and number of ASV, species, genus and family which were assigned to the LCA. % match indicates the range of % similarity between each ASV and the reference sequences of assigned taxa. Where LCA taxa level is genus or higher, the species list contains more than one species with a common ancestor. 85

Table S 5.3 The results of cross validation of diet composition observations in the canonical analyses (CAP) ordination, following to the leave-one-out approach. The values are the number of samples allocated into each of the classified groups. The juveniles of both *Lutjanus erythropterus* (LE) and *L. malabaricus* (LM) achieved higher allocation success rates (82%) versus adults. The allocation success rates of adults LE and LM were 45 % and 50 %, respectively, and the majority of the misclassified samples were allocated to LM Juvenile. 88

Table S 5.4 The results of distance based linear model (DistLM) to test the effects of sample variability on juvenile diet composition. Marginal test results (A) show the significance levels of each variable on diet compositions. BEST solution results (B) summarised the top five, most parsimonious combination of variables that best explained the juvenile diet composition based on the Akaike Information Criterion with finite sample sizes (AICc). The tests were based on a Jaccard coefficient matrix for presence and absence (PA) datasets. TL, total length (mm).88

Table S 6.1 A summary of candidate models to predict body length of *L. erythropterus* and *L. malabaricus*, with the delta Akaike Information Criterion corrected for finite sample sizes (AICc) of less than 2. The models in bold were selected due to the low AICc and least number of explanatory variables (most parsimonious). Normalised root mean square error (nRMSE) and adjusted R squared value (adj. R²) were based on a linear regression between the observed values of the test dataset and values predicted without a null term. Bathy, bathymetry; curv, curvature; sqrt.slp, square root-transformed slope; log.rng30, log-transformed, maximum minus the minimum elevation in the local neighbourhood (local relief) of 30-grid cell kernel radius. 111

Abbreviations

AICc	Akaike Information Criterion corrected for finite sample sizes
ANOVA	Analysis of Variance
ASV	Amplicon Sequence Variant
AUC	Area Under Curve
BLASTn	nucleotide Basic Local Alignment Search Tool
BRT	Boosted Regression Trees
BRUVs	Baited Remote Underwater Video systems
CAP	Canonical Analysis of Principal Coordinates
CV	Cross Validation
DistLM	Distance-based Linear Model
DNA	Deoxyribonucleic acid
DPIRD	Department of Primary Industries and Regional Development
EBFM	Ecosystem-Based Fisheries Management
eDNA	Environmental DNA
EFH	Essential Fish Habitat
FL	Fork Length
GAMs	Generalised Additive Models
GAMMs	Generalised Additive Mixed Models
GIT	Gastrointestinal Tracts
LCA	Lowest Common Ancestor
LEBP	<i>Lutjanus erythropterus</i> blocking primer
LMBP	<i>Lutjanus malabaricus</i> blocking primer
MaxN	The maximum number of fish observed in the field of view of the BRUVS at one time
MID	Multiplex identifier
NCBI	National Center for Biotechnology Information
NE	Northeast
nRMSE	Normalised Root Mean Square Error

NW	Northwest
PA	Presence / Absence
PCO	Principal Coordinates Analysis
PCR	Polymerase Chain Reaction
PERMANOVA	Permutational Multivariate Analysis of Variance
QLD	Queensland
qPCR	Quantitative PCR
RRA	Relative Read Abundance
RUVs	Remote Underwater Video systems
SD	Standard Deviation
SDM	Species Distribution Models
SE	Standard Error
TL	Total length
TrEnD	Trace and Environmental DNA
WA	Western Australia

Chapter 1 General introduction

1.1 Background and rationale

1.1.1 Ecological theories and cryptic species

The ecological principle of competitive exclusion was first presented by Charles Darwin in the nineteenth century (Darwin, 1859), and has evolved into the concept of “the ecological niche”. Complete competitors cannot coexist. However, niche partitioning is the fundamental process that allows species to coexist within the same ecosystem or habitat (Diamond, 1978; Gause, 1934; Hardin, 1960). Niche partitioning can drive ancestral populations to diverge phenotypically into distinct species. This process is known as ecological speciation (Rundle & Nosil, 2005; Schluter, 2000; Stroud & Losos, 2016).

Morphologically cryptic species (hereafter, cryptic species) are organisms that lack distinguishing morphological characters between them. Evolutionary mechanisms leading to morphological similarity vary on a species-by-species basis (see Fišer et al., 2018). Advancement in molecular delimitation methods has resulted in a significant acceleration in the identification of cryptic species (Bickford et al., 2007; Bucklin et al., 2011; Collins & Paskewitz, 1996; Palumbi, 1994). For example, on average, 2% of fish species examined in a large-scale DNA barcoding study have been revealed to be new cryptic teleost species (Bucklin et al., 2011). An example of such studies includes the Fishes of Australia, where 207 species were barcoded and 5 new cryptic species were discovered (Ward et al., 2005). Given this rate of new species detection, up to 600 cryptic fish species may be discovered in marine and freshwater systems through similar studies (Bucklin et al., 2011).

A number of detailed ecological studies on cryptic species have identified different ecological requirements along one or more dimensions such as food, time and space (Fišer et al., 2018). Such information can disentangle not only the ecology (i.e. evolutionary causality of speciation and mechanisms of coexistence), but also the susceptibility to environmental and biological factors across a range of cryptic species. This is likely to benefit biodiversity conservation and sustainable fisheries management initiatives (Bickford et al., 2007; Fišer et al., 2018).

1.1.2 Diverse marine ecosystems and fishery management

The number of species of marine fish is estimated to be approximately 15,000 globally (Vega & Wiens, 2012), with the diversity increasing closer to the equator (Manel et al., 2020; Sale, 1978). In such diverse marine ecosystems, there is often partitioning of resources (i.e. food and habitat) between sympatric and/or cryptic species (Haak et al., 2019; Longenecker, 2007; Nagelkerken et al., 2009; Prochazka, 1998). Niche partitioning within reef fish of the same species between the different life history stages is also a common strategy to minimise intra-specific competition (Dahlgren & Eggleston, 2000). Examples include life cycle migrations (i.e. from shallow to deep reefs as juveniles grow to adults) (Fry et al., 2009; Mumby, 2006; Nakamura et al., 2008; Williams & Russ, 1994) and ontogenetic dietary shifts (Rooker, 1995; Usmar, 2012; Wells et al., 2008). The corresponding patterns of habitat and diet partitioning between life history stages suggest that ontogenetic migration is based not only on finding a refuge from predation, but also for accessing food resources (Cocheret de la Morinière et al., 2003; Szedlmayer & Lee, 2004).

Fish communities provide fundamental ecosystem services, such as regulating the population dynamics of prey species and other sources of food and nutrient availability (Holmlund & Hammer, 1999), and maintaining ecosystem health (Elmqvist et al., 2003). Fish are also a vital source of food and livelihood to people, particularly in the fisheries sector that provides employment to 12.3 million full-time fishers, or part-time or full-time processors, and 16.7% of the animal protein consumed by the global population (FAO, 2014). In many parts of the world fish diversity, abundance, size structure and biomass are negatively impacted by anthropogenic factors, such as pollution, habitat degradation, fisheries and climate change (Duffy et al., 2016; Moberg & Folke, 1999; Tittensor et al., 2007, 2010). Effective management is crucial to sustain or recover fish populations and ecosystem functions (Hilborn et al., 2001; Moore et al., 2016; Worm et al., 2009).

For targeted fishes, fishery assessments based upon life history traits, reproduction patterns and stock structure are widely conducted to determine effective management strategies such as quotas (catch, effort), size regulations and seasonal closures (Methot & Wetzel, 2013; Newman et al., 2000, 2016). In addition to such management based on single-species models, ecosystem-based fisheries management (EBFM) is also strongly advocated and, in some cases, even mandated (Latour et al., 2003; NOAA, 1996). The objectives of EBFM include conserving biodiversity and ecosystem services, simultaneously optimising the yield of either single or multiple species, and long-term economic viability (Link, 2002). These can be achieved through various management approaches that include spatial closures and

prohibitions of destructive fishing methods (i.e. explosives, trawling) (Barnette, 2001). Identifying the distributional range, essential fish habitats (EFHs) and diet requirements of key species is a critical step for effective EBFM frameworks (Ciannelli et al., 2008; Moore et al., 2016; Thrush & Dayton, 2010). Given the complex inter- and intra-specific interactions of teleosts, it is important to understand different niche requirements and the susceptibility to various impacts for each species and life-history stage, and take them into account within EBFM strategies (Fišer et al., 2018; Piggott et al., 2020).

1.1.3 Challenges and research needs

1.1.3.1 Identification of cryptic species

Accurate identification of a species is fundamental in biology, ecology and conservation (Hey et al., 2003). While it is typically determined using morphological characteristics, identification of morphologically cryptic species often requires DNA barcoding (Fišer et al., 2018; Sievers et al., 2020), which necessitates a large amount of investigative time, is relatively expensive, and cannot be conducted in the field. Specimens for fishery assessments are commonly obtained from commercial fishers after being filleted in order to obtain size, age and reproductive information. Often the specimens are not fresh and have lost some of their phenotypic traits such as eye colour, body shape and body colouration. This contributes to the process of species identification being increasingly more difficult and inaccurate. For these reasons, biological and ecological studies, and fishery assessments of cryptic species can be confounded by incorrect identification. This can be problematic because vulnerability to fishery and environmental impacts are likely to vary between species due to the partitioning of niches required for coexistence. Therefore, a robust, simple identification tool is required to underpin species-specific biological, ecological and fishery assessments.

1.1.3.2 Needs for high resolution studies

The more similar the coexisting species are, the more intensively they compete (Nagelkerken et al., 2009; Prochazka, 1998; Razgour et al., 2011; Sale, 1974; Scriven et al., 2016; Wang et al., 2005). Furthermore, the more similar the morphology is, the more similar the ecology and niche requirements are. This ecomorphology theory describes the diet choice of teleosts being constrained and shaped by body morphology such as jaw structure, dentition and body size (Hulsey & León, 2005; Meyer, 1989; Wainwright & Richard, 1995). Based on this theory, niche partitioning is especially relevant among morphologically cryptic species, but the differentiation can be subtle and difficult to detect. For instance, high levels of dietary overlap between sympatric butterflyfishes (family Chaetodontidae) were identified using an *in-situ* feeding observation method and stable isotope analyses, whereas clear diet partitioning was

detected by visually examining their gut contents (Cox, 1994; Nagelkerken et al., 2009; Pratchett, 2005). These conflicting results suggest that some dietary analysis methods may lack the resolution needed to detect distinct, and sometimes subtle, differences in diet composition (Nagelkerken et al., 2009; Pompanon et al., 2012). Therefore, high resolution studies are required to understand the ecological interactions and niche requirements of cryptic species.

The metabarcoding approach has been increasingly applied in dietary studies due to its ability to detect highly digested prey items at high resolution (i.e. low taxonomic level) from gastrointestinal tracts or even from faecal samples (Johnson et al., 2021; Quéméré et al., 2021; Sousa et al., 2019). These advantages lend this method to a more comprehensive evaluation of dietary partitioning of sympatric, cryptic species at a much finer scale (Casey et al., 2019; Kume et al., 2021; Leray et al., 2019). However, an issue may arise in DNA-based diet studies when polymerase chain reaction (PCR) favours the amplification of the higher quality host (i.e. predator) DNA over partially digested prey DNA, and consequently the rare sequences of prey DNA may not be represented. This issue can be overcome by applying predator-specific blocking primers which suppress the amplification of predator DNA during PCR processing (Su et al., 2017; Vestheim & Jarman, 2008).

1.1.3.3 Complex life cycle

The life cycle of many reef fishes consists of a pelagic larval stage, followed by a demersal juvenile stage on nearshore habitats and an adult stage on deeper, high-relief or low-relief reefs (Dahlgren & Eggleston, 2000; Dance et al., 2021; Sievers et al., 2020). Owing to these complex life cycles, drivers of distribution, mortality rates and abundance of reef fish are expected to vary between life-history stages (Dahlgren & Eggleston, 2000; Galaiduk et al., 2018; Mumby, 2006; Nakamura et al., 2008; Williams & Russ, 1994). For instance, anthropogenic stressors such as coastal development and terrestrial run-off have more direct impacts on inshore nursery grounds than offshore adult habitats due to their closer proximity to coastal areas (Hamilton et al., 2017; Lowe et al., 2020). In addition, survival rates of juveniles are particularly susceptible to habitat degradation, as they require shelter from predators (Almany, 2004; Feary et al., 2007; Jones et al., 2004; Lindholm et al., 2001).

Essential fish habitat is defined as “*those waters and substrate necessary for fish to undertake spawning, breeding, feeding or growth to maturity*” (NOAA, 1996). This definition covers a species’ full life cycle, highlighting the complex life cycle of marine teleosts and the importance to define EFH for each life-history stage for effective EBFM strategies (Demartini et al., 2010; Lindholm et al., 2001; Vasconcelos et al., 2010). However, the majority of studies

on fishery important species focus on the adult life stage, possibly owing to difficulties of collecting juvenile samples, such as a lack of sampling sources from fishery catches and limited knowledge of their juvenile distributional range (Piggott et al., 2020; Wen et al., 2012). Furthermore, dietary studies on juveniles pose additional challenges in identifying small sized prey items. Consequently, our knowledge of the juvenile ecology of many species is limited, and as a result, increased efforts are required to fill this significant gap in knowledge.

1.2 Research questions and thesis structure

In order to overcome some of these challenges and address some of the research needs, this thesis is constructed with a primary research focus on “The morphology and ecology of fishery important, cryptic species” (Figure 1.1). The first two data chapters of the thesis (Chapter 2 and 3) were structured to investigate whether morphologically cryptic species could be discriminated using morphometric analyses. In chapter 2, I apply otolith morphometric analyses on nine morphologically cryptic teleost species from four families, while in Chapter 3, I use both otolith and body morphometric analyses to differentiate between cryptic juveniles of two sympatric *Lutjanus* species, *L. erythropterus* and *L. malabaricus* (Table 1.1). In Chapters 4, 5 and 6, I examine the ecology of these two sympatric, morphologically cryptic species, using metabarcoding dietary analyses and species distribution models (SDMs). In particular, my ecological questions for these chapters are 1) Is there diet partitioning between the different species and life stages? (Chapter 5), and 2) where are the length-specific EFHs for these species? (Chapter 6). All data chapters are written and formatted as stand-alone journal articles, and as a consequence there is some repetition in the introductions. They were written as collaborative articles with input from co-authors, and hence the plural personal pronoun of ‘we’ was used rather than ‘I’. Chapter 5 has been published in a peer reviewed journal along with Chapter 4 (development of blocking primers) in the supplementary materials. The significance and limitations of the research are synthesised in the general discussion (Chapter 7). Due to the use of similar references among chapters, references for all chapters are listed in one ‘Bibliography’ section at the end of this thesis. The specific research questions addressed in each chapter are outlined below.

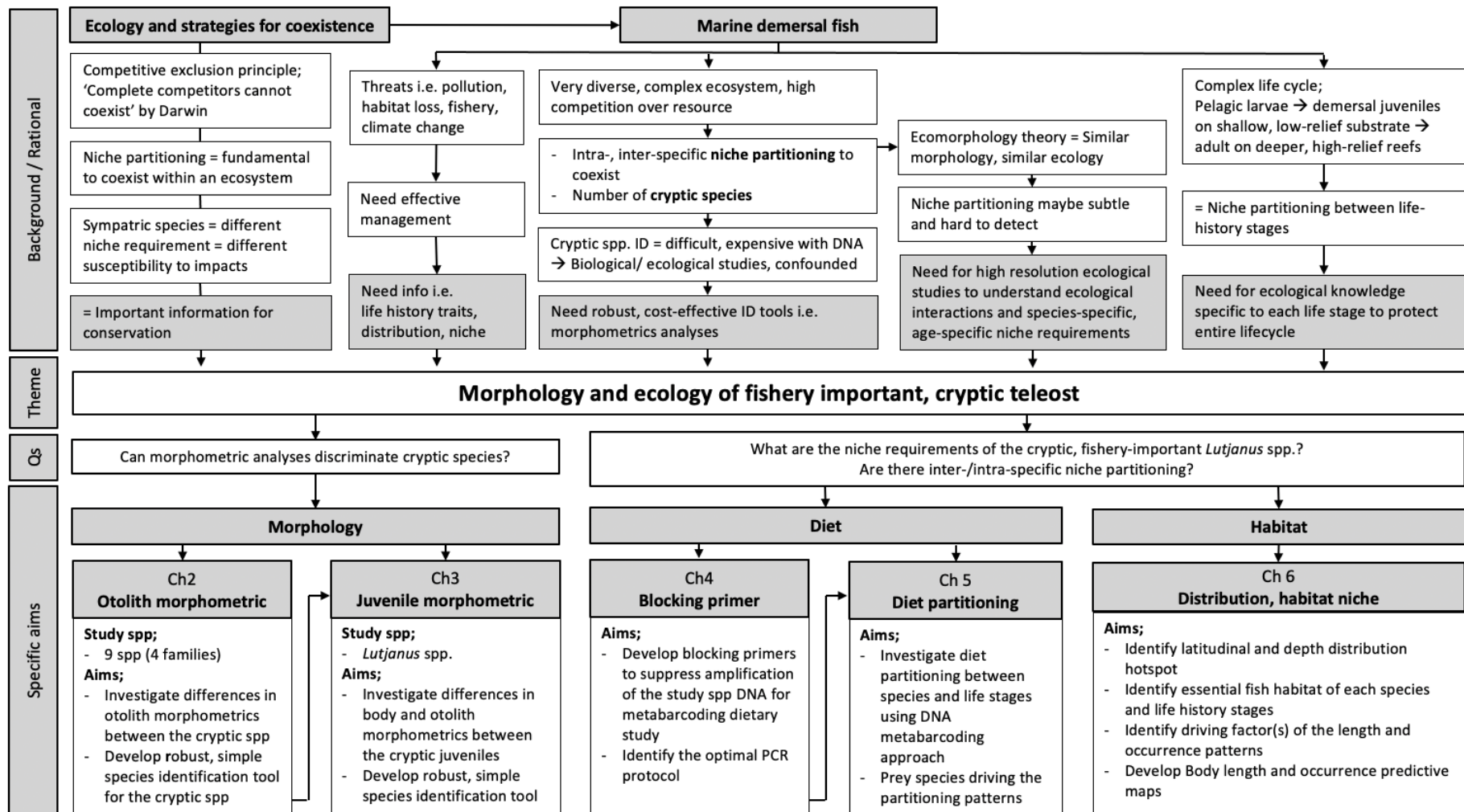


Figure 1.1 Flow diagram outlining the background, rational and the structure of thesis.

Table 1.1 Images and relevant information (common names, maximum size recorded, and distribution maps) of the study species. The distribution maps were generated using ArcMap v10.6 (<https://desktop.arcgis.com>) with the shapefile retrieved from Codes for Australian Aquatic Biota (CAAB) database (<http://www.cmar.csiro.au/caab/>) on October 16 2020. Occurrence points were mapped for *L. punctulatus* as a shapefile was not available (occurrence coordinates also retrieved from CAAB). The images of fish for *Lethrinus* spp. were sourced from Saunders *et al.* (2018), and *Sillago*, *Centroberyx* and *Polyprion* spp. were sourced from CSIRO Australian National Fish Collection.

Lethrinus nebulosus

- Spangled emperor, North west snapper
- 94cm TL*, 87cm TL**, 81mm FL***



Lethrinus punctulatus

- Bluespotted emperor, Lesser spangled emperor
- 38.4cm FL***



Sillago bassensis

- Southern school whiting
- 33cm SL**



Sillago vittata

- Western school whiting
- 30cm SL**



Centroberyx gerrardi

- Bight redfish, golden snapper, king snapper
- 46cm SL*, 66cm TL**



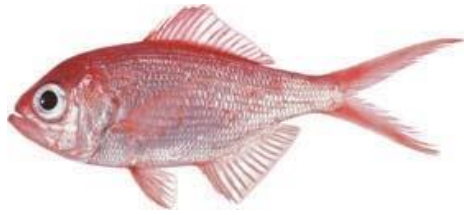
Centroberyx australis

- Yelloweye redfish, yelloweye red snapper
- 30cm SL*, 51cm TL**



Centroberyx lineatus

- Swallowtail, Swallowtail Nannygai
- 36cm SL*, 46cm TL**



Polyprion oxygeneios

- Hapuku, Blue cod, Deepwater rock cod
- 180cm TL*, 160cm TL**, 110cm TL***



Polyprion americanus

- Bass grouper
- 210cm TL*, **



Lutjanus erythropterus

- Crimson snapper, small-mouth nannygai
- 81.6cm FL**, 79cm FL***



Lutjanus malabaricus

- Saddletail snapper, large-mouth nannygai
- 100cm TL *, **, ***



* Retrieved on Oct 16 2020, from Fish of Australia (<https://fishesofaustralia.net.au/>) (Bray & Gomon, 2018)

** Retrieved on Oct 16 2020, from FishBase (www.fishbase.org) (Froese & Pauly, 2018)

*** Retrieved on Oct 16 2020, from Status of Australian Fish Stocks Reports (<https://fish.gov.au/report/>) (Stewardson et al., 2018).

1.2.1 The utility of otolith morphometry for identifying cryptic species of tropical and temperate teleosts (Chapter 2)

While DNA barcoding is used to distinguish many cryptic species, multivariate analyses using body or otolith morphometric data have proven to be a robust identification tool for cryptic teleost species (Ponton et al., 2013; Stransky & MacLellan, 2005; Tsoumani et al., 2013). This approach is considerably cheaper and quicker than DNA barcoding, and classification success rates can be as high as 95 - 100% (e.g. Wakefield et al., 2014; Zischke et al., 2016). In Chapter 2, I conducted otolith morphometric analyses on nine species from four families of teleosts (Lethrinidae, Sillaginidae, Berycidae and Polyprionidae) to develop robust, simple species discrimination tools.

This chapter has been formatted for submission to the peer-reviewed journal *Fisheries Research*.

1.2.2 Cryptic species discrimination for the juveniles of two lutjanids using body and otolith morphometry (Chapter 3)

In Chapter 3, morphometric analyses were carried out for the morphologically cryptic juveniles of *L. erythropterus* and *L. malabaricus*. Currently, these species can only be distinguished by DNA barcoding during the juvenile stage due to their cryptic features, which is time-consuming and costly. Based on the findings of Chapter 2, the species-specific predictive power of otolith morphometry alone for smaller fish was limited. As such, in this chapter I conducted the analyses using not only otolith morphometry, but also body morphometric variables.

This chapter has been formatted for submission to the peer-reviewed journal *Coral Reefs*.

1.2.3 Development of predator specific blocking primers for *Lutjanus erythropterus* and *L. malabaricus*; implications for DNA metabarcoding dietary studies on the fishery important red snappers (Chapter 4)

In this chapter I designed annealing inhibiting blocking primers specific for each host species (*L. erythropterus* and *L. malabaricus*) to suppress the amplification of their DNA. I tested the

efficacy of the blocking primers and identified the optimal PCR protocols through *in-silico* and *in-vitro* experiments. These blocking primers were applied in the following chapter.

This chapter has been published as supplementary material in the peer-reviewed journal *Scientific Reports*.

1.2.4 Partitioning of diet between species and life history stages of sympatric and cryptic snappers (Lutjanidae) based on DNA metabarcoding (Chapter 5)

In this chapter, I investigated the diet compositions of juvenile and adult *L. erythropterus* and *L. malabaricus*, and partitioning patterns between the species and their life stages, using a DNA metabarcoding approach. A range of universal and taxa-specific primers, including the Fish16S primer with the blocking primers developed in Chapter 4, were applied during PCR, to detect diverse prey taxa. This chapter contains extensive additional data, which have been provided as supplementary materials, and in particular a table with a full list of prey species identified.

This chapter has been published in the peer-reviewed journal *Scientific Reports*.

1.2.5 The distribution and habitat preferences of two sympatric snapper species on the northwest and northeast coasts of Australia (Chapter 6)

Spatial distribution ranges and hotspots of *L. erythropterus* and *L. malabaricus* across latitude and depth, and their length-specific essential habitats were investigated in this chapter. To do so, I used an extensive dataset, which consists of 19,784 Baited Remote Underwater Video systems (BRUVs) collected from across Australia and collated in the GlobalArchive database (globalarchive.org) (Harvey et al., 2021). Stereo-BRUVs allow accurate measurements of fish size, allowing me to carry out SDMs with presence/absence and fish length as the response variables in relation to bathymetry and various habitat descriptors. Based on the most parsimonious model for each species, I constructed length-specific spatial distribution predictive maps of the Western Australian coast for each species.

This chapter has been formatted for submission to the peer-reviewed journal *Coral Reefs*.

1.2.6 General discussion (Chapter 7)

In Chapter 7, I integrate and synthesize the research from the five data chapters. I critique the research, discuss the new knowledge and developments, and identify new questions and future research arising from this thesis.

Chapter 2 The utility of otolith morphometry for identifying cryptic species of tropical and temperate teleosts

2.1 Abstract

The cryptic morphology of fishes poses challenges to accurate species identification. This study assessed whether the morphometry of otoliths could be used as a method to distinguish closely related cryptic species. A total of nine fishes from four genera (*Centroberyx*, *Lethrinus*, *Polyprion* and *Sillago*) that are morphologically similar within each genus were compared and assessed. These species are highly valued by commercial and recreational fishers. Multivariate models that included combinations of morphometric variables (i.e. otolith length, width, thickness, weight and fish length) provided highly accurate species prediction rates ranging from 92.5 to 99.9% across all genera. For *Centroberyx*, *Polyprion* and *Sillago*, changes in species prediction accuracy rates were minimal (i.e. up to 3%) when different combinations of morphometric variables were used in the models. In contrast, fish length was a highly influential variable for discriminating between the two lethrinid species, with the prediction accuracy reducing by 7-25% when fish length was excluded. This is likely attributable to the larger size attained by *L. nebulosus* in comparison to *L. punctulatus*. For all genera, the exclusion of otolith weight from the multivariate analysis did not significantly decrease prediction accuracy. Simplifying data collection to only length-based otolith measurements would provide a more rapid and cost-effective method for discrimination and be more practical when sampling at sea where obtaining precise weight measurements of otoliths is typically unfeasible. Spatial variation in otolith morphometrics were evident for *C. gerrardi*, *L. punctulatus*, *P. oxygeneios* and *S. vittata*, which might be attributed to the differences in fish size distributions between the regions. The misclassified specimens within the cryptic species groups were notably smaller individuals, suggesting there is an ontogenetic divergence between otolith shape and somatic growth. Hence, further investigation of variations in morphological characteristics, other than otoliths, may be required for the discrimination of cryptic species at the juvenile stage. This study highlights the robustness of multivariate analysis of otolith morphometric data for discriminating closely related cryptic species.

2.2 Introduction

Morphologically cryptic species can be difficult to distinguish based on external features, despite being genetically distinct (Bickford et al., 2007; Collins & Paskewitz, 1996). The development of molecular based taxonomic approaches in association with traditional methods has allowed the separation of cryptic species (Bickford et al., 2007; Choat et al., 2012; Iwatsuki, 2013). This discrimination has facilitated a better understanding of species-specific biology and ecological niche patterns (i.e. Elliott, 1996; Takahashi et al., 2020). However, molecular approaches such as DNA barcoding are time-consuming, relatively expensive, and cannot be easily used in the field.

An alternative to adopting a molecular approach is multivariate analyses of morphometric data. This has already been demonstrated as a useful technique for distinguishing cryptic species in various fauna and flora, for example bats (Ashrafi et al., 2010), flies (Cazorla & Acosta, 2003), bivalves (Baker et al., 2003) and flowers (Fisher, 1936, 1938). In teleosts, multivariate analyses have been applied to body morphometry data, including hard parts of the body such as scales (Ponton et al., 2013; Tsoumani et al., 2013) and otoliths (Stransky & MacLellan, 2005; Tuset et al., 2006; Wakefield et al., 2014; Zischke et al., 2016). Otoliths are paired calcareous structures located in the inner ear of teleosts, serving the functions of measuring motion and detecting sound (Popper et al., 2005). Because daily or annual growth zones are deposited, otoliths can be used to derive age-based life history information on fish. Isotope analysis and otolith microchemistry can also provide information on movement and trophic ecology with the chemical signatures incorporated into the daily and annual increments in the otoliths (Campana, 2005; Newman et al., 2016). This information is useful for fisheries assessments. As a result, otoliths of targeted fishes or indicator species are routinely collected by fishery agencies for assessments (Begg et al., 2005; Newman et al., 2015; Williams et al., 2015). A multivariate analysis of otolith morphometry is considerably cheaper and quicker than the processing time required for DNA barcoding, and the classification success rates can be as high as 95 - 100% without the need to use the more costly DNA methods (i.e. Wakefield et al., 2014; Zischke et al., 2016). Therefore, this approach could potentially be a cost-effective method of discriminating between cryptic fishes.

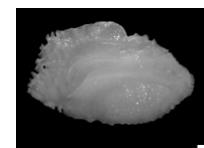
Biological samples of commercially important species are often provided from fishers to fishery agencies for either biological studies or stock assessments after the fish are filleted (e.g. as fish frames). These samples may lack freshness and body features such as colouration used for species identification may have faded or changed, posing an additional challenge to accurately discriminate cryptic species. As one example, *Centroberyx australis* is characterised by its yellow eyes, as described by the common name, yelloweye redbfish.

However, this species can be confused with other species, such as *C. gerrardi* and *C. lineatus*, as the eye colour of the filleted samples can fade by the time they reach scientific laboratories or after being frozen. To resolve this issue, we aimed to evaluate the reliability of using otolith morphometrics within a multivariate analysis to discriminate cryptic speciation. Nine species from four families were examined: *Lethrinus nebulosus* and *L. punctulatus* (Lethrinidae); *Sillago bassensis* and *S. vittata* (Sillaginidae), *Centroberyx gerrardi*, *C. australis* and *C. lineatus* (Berycidae); and *Polyprion oxygeneios* and *P. americanus* (Polyprionidae) (Table 2.1). All of these species are important to commercial and/or recreational fishers in Australia. Yet life history and ecological studies involving these cryptic congeners can be confounded due to difficulties in distinguishing between the species within each family. The species prediction accuracy of multivariate models with different combinations of otolith morphometric variables and fish length were examined. The combinations of variables were selected to represent fisheries relevant scenarios (e.g. otoliths damaged, no analytical balance available), and the most robust, simple, and parsimonious model was determined for each genus. For this study, we hypothesised that there would be significant differences in otolith morphometry between the cryptic species within each family, and that the multivariate otolith morphometric approach would potentially provide a rapid and reliable tool for species-specific identification.

Table 2.1 Images of fish and sagittal otoliths, common names, sampling regions and sample sizes (n) for the nine study species. Scale bars (white lines) on otolith images are 1 mm. GC, Gascoyne Coast; PN, Pilbara nearshore; PO, Pilbara offshore; WC, West Coast; SC, South Coast; SW, Southwest coast; Metro, adjacent to Perth metropolitan region. The images of fish for *Lethrinus* spp. were sourced from Saunders *et al.* (2018), and *Sillago*, *Centroberyx* and *Polyprion* spp. were sourced from CSIRO Australian National Fish Collection. Otolith photos were taken by Chris Dowling, Department of Primary Industries and Regional Development.

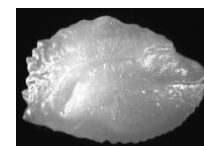
Lethrinus nebulosus

- Spangled emperor,
North west snapper
- GC (n=69), PN (n=31)



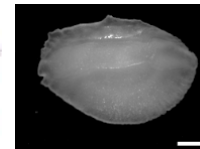
Lethrinus punctulatus

- Bluespotted emperor,
Lesser spangled emperor
- GC (n=2), PN (n=63),
PO (n=34)



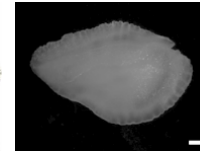
Sillago bassensis

- Southern school whiting
- WC (n=72), SC (n=50)



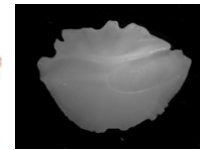
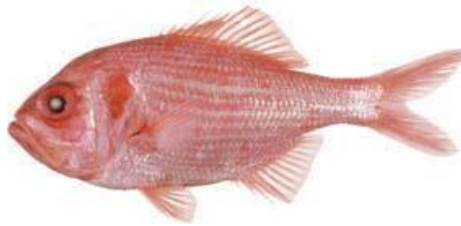
Sillago vittata

- Western school whiting
- GC (n=12), WC (n=113)



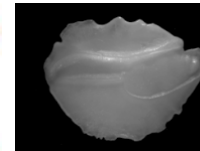
Centroberyx gerrardi

- Bright redfish, golden snapper, king snapper
- SC (n=8), SW (n=87)



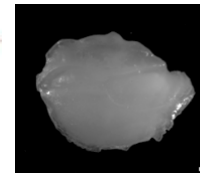
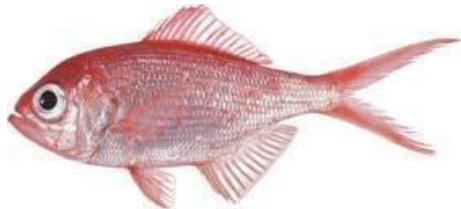
Centroberyx australis

- Yelloweye redfish, yelloweye red snapper
- SC (n=13), SW (n=39), Metro (n=8)



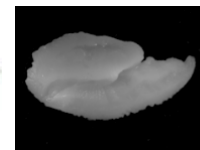
Centroberyx lineatus

- Swallowtail, Swallowtail Nannygai
- SC (n=69), SW (n=9), Metro (n=3)



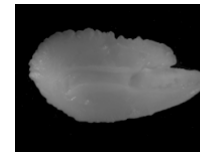
Polyprion oxygeneios

- Hapuku, Blue cod, Deepwater rock cod
- WC (n=88), SC (n=491)



Polyprion americanus

- Bass grouper
- WC (n=126), SC (n=13)



2.3 Materials and methods

2.3.1 Sample and data collection

Samples of nine teleost species (i.e. *Lethrinus nebulosus*, *L. punctulatus*, *Sillago bassensis*, *S. vittata*, *Centroberyx gerrardi*, *C. australis*, *C. lineatus*, *Polyprion oxygeneios* and *P. americanus*) were collected from commercial fishers that used a range of fishing gears (fish traps, fish trawls, lines) in Western Australia (Table 2.1 & Figure 2.1). Samples were also obtained from recreational fishers (using lines), primarily from donations of fish skeletons or frames (filleted fish bodies with heads, vertebrae and fins attached). Fish length (fork length for lethrinids and total length for all other species) was recorded to the nearest 1 mm. The sagittal otoliths were dissected from each fish, cleaned in water and stored dry. Morphometric measurements of each otolith were taken to the nearest 0.01 mm using digital callipers, and included the length from rostrum to postrostrum, the width at the widest point approximately perpendicular to the axis from rostrum to postrostrum, and the thickness across the primordium perpendicular to the sulcus acusticus. This was undertaken using one of the sagittal otoliths for each fish with the weight of the otolith being recorded to 0.0001 g using a calibrated balance with glass draft shields.

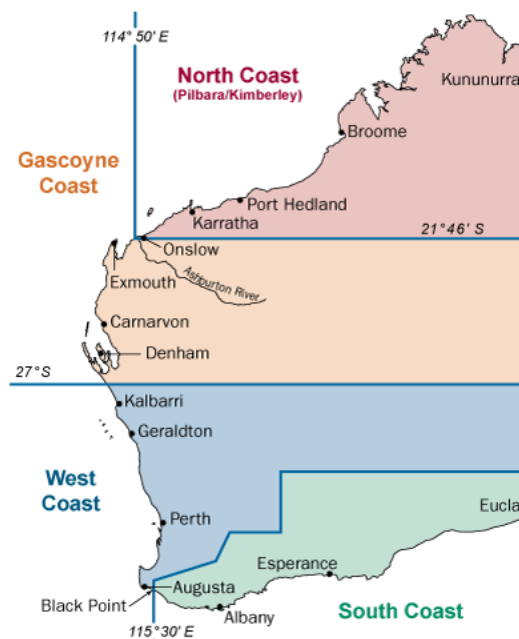


Figure 2.1 Map of Western Australia indicating four bioregions and fishing areas where samples were collected. The map was sourced from Saunders *et al.* (2018).

2.3.2 Statistical analyses

Multivariate data analyses were carried out to assess whether there was a significant difference in the otolith morphometric data between species, using the software PRIMER 7 (v. 7.0.13, <https://www.primer-e.com>) (Clarke et al., 2014). A euclidean distance similarity matrix of all otolith morphometric variables (length, width, thickness and weight) and fish length, was generated for each genus. The matrices were visualised using a Canonical Analysis of Principal Coordinates (CAP) ordination plot (Anderson & Willis, 2003), with species and regions as factors. While the aim of this study was to investigate variations in otolith morphometry between species, the factor “region” was also assessed in CAP considering that spatial variations in otolith shape are commonly used to determine stock structure of species (e.g. *Coryphaenoides rupestris* (Longmore et al., 2010), *Engraulis encrasicolus* (Jemaa et al., 2015), *Clupea harengus* (Libungan & Pálsson, 2015)). The choice of m (the number of Principal Coordinate (PCO) axes included in a CAP analysis) was based on the number of variables (i.e. $m = 5$ for the above dataset with five variables). The leave-one-out allocation success was used to determine the accuracy of species predictions. Multiple partial correlation of morphometric variables with the two canonical axes were assessed to understand the strength and direction of variables that contribute to species separation. No normalisation of the data is required in the CAP analysis, despite variables being measured using different scales, as the orthonormal PCO axes in CAP are automatically sphericised and are not scaled by their respective eigenvalues (Anderson et al., 2008). A normal distribution was ensured for each variable and no transformation was required.

The above analyses were repeated using different combinations of variables in order to assess the predictive power in each model in different practical scenarios (Table 2.2). The BiodiversityR package in R (v.2.12-1; Kindt, 2020) was used for these procedures to automate CAP and leave-one-out allocation assessments for each genus and scenario. For instance, Scenario 2 considers the situation where an analytical balance is not available and thus otolith weight cannot be acquired. Fish length is excluded in Scenario 3, 4 and 6 considering a case where the caudal fin is damaged or only fish heads or otoliths are available. Rostrums and/or postrostrums of otoliths can get chipped as part of capture (*ike jime*) or during dissection, which can prevent accurate otolith length and weight recording (i.e. Scenario 5, ‘Chipped otolith’).

Otolith morphometry can also be applied in dietary studies to identify the teleost prey taxa as otoliths are somewhat resistant to digestion and can be collected from gastrointestinal contents and faeces (Bowen, 2000; Gales, 1988; Škeljo & Ferri, 2012). Considering the situation where other body parts are too digested to identify them at either genus or family taxonomic levels

whereas otoliths remain undigested, a CAP analysis was performed with all nine species combined in a single dataset (hereafter, ‘a bag of unknown otolith scenario’). A euclidean distance similarity matrix of all otolith morphometric variables was generated. CAP analyses were performed, and leave-one-out allocation success rates were assessed as described above.

Table 2.2 Combinations of morphometric variables at different scenarios. FL, fish length; OL, otolith length; OW, otolith width; OT, otolith thickness; Owe, otolith weight.

Scenario	Used variables
Scenario 1. All 5 variables	FL, OL, OW, OT, Owe
Scenario 2. No weight	FL, OL, OW, OT
Scenario 3. FL missing	OL, OW, OT, Owe
Scenario 4. FL missing & No weight	OL, OW, OT
Scenario 5. Chipped otolith	FL, OW, OT
Scenario 6. FL missing & Chipped otolith	OW, OT

2.4 Results

A total of 1400 samples from nine species were collected across the four bioregions of Western Australia (Table 2.1 & Figure 2.1). Samples sizes comprised a wide length range for each species to ensure they were representative and adequate. A total of 236 of the samples were *Centroberyx* spp. with lengths ranging from 170 to 689 mm, 199 were *Lethrinus* spp. (169–715 mm), 718 were *Polyprion* spp. (521 – 1452 mm) and 247 were *Sillago* spp. (29 – 340 mm) (Table 2.3). The sample size of each species ranged from 60 to 125 for *Centroberyx*, *Lethrinus* and *Sillago*, and 139 and 579 for *P. americanus* and *P. oxygeneios* respectively (Table 2.3). Fish length distributions varied between regions within a species, particularly for *C. gerrardi*, *L. punctulatus*, *P. oxygeneios* and *S. vittata* (Figure 2.2).

Variations in otolith morphometrics were evident from the high degree of separation between species along the first CAP axes for all genera when all five morphometrics variables were used in the CAP analyses (Scenario 1; Figure 2.3 & Figure 2.4-A). The leave-one-out allocation rates to the correct species within each genus ranged from 91.46 to 99.86, with the highest success rate observed for *Polyprion* (99.86%), followed by *Centroberyx* (98.73%), *Sillago* (95.95%), and *Lethrinus* (91.46%) (Figure 2.4 -B). The separation of species within the genera *Centroberyx*, *Lethrinus* and *Polyprion* on the respective CAP plots was due primarily to the influence of the variables fish length and otolith length (as well as otolith width in *Centroberyx* and *Lethrinus*), indicated by the relatively long correlation vectors (Figure 2.3). The correlation coefficients of those variables ranged from 0.57 to 0.93, explaining 32.95 - 85.59% of the variations on the CAP plots. In contrast, the separation of species of *Sillago* was due to the influence of the variable otolith thickness and length (Figure

2.3). The variables fish length, otolith length and otolith thickness were the primary drivers of species separation in the CAP ordinations for each genus (Figure 2.3).

Regional variation in otolith morphometrics were apparent for some species by the separation of species-specific data in the CAP plots between locations (Figure 2.3). These species include *C. gerrardi* between the south and south-west coasts, *L. punctulatus* between the Pilbara nearshore and offshore areas and the Gascoyne Coast, *P. oxygeneios* between the west and south coasts, and *S. vittata* between the Gascoyne and west coasts (Figure 2.3). Regional allocation success rates ranged from 0 to 100% and were considerably lower than the species allocation success rates (80 - 100%) for all species (Table 2.4). This indicates that morphometric variations between species were more distinct than those between regions within each species.

The most parsimonious model for Scenario 1 (where all variables were included) was the genus *Centroberyx*, for Scenario 2 (no otolith weight) it was the genera *Lethrinus* and *Polyprion*, and for Scenario 4 (no fork length or otolith weight) it was the genus *Sillago* (Table 2.2 & Figure 2.4-B). Changes in the combinations of morphometric variables resulted in small fluctuations in the allocation success rates for *Centroberyx*, *Polyprion* and *Sillago*, ranging between 95.55 - 99.86% (Figure 2.4-B). Lower allocation success rates (85.93 – 86.43%) were obtained for the species of *Lethrinus* when fish length data was excluded from the analyses (Scenario 3 and 4; Table 2.2 & Figure 2.4-B), which decreased further to 67.84% when both otolith length and weight were also removed (Scenario 6; Table 2.2 & Figure 2.4-B). Across all genera, smaller fish were more often misclassified while larger fish were generally classified to the correct species (Figure 2.5).

The allocation success rates among species decreased in the ‘bag of unknown otoliths scenario’ where all nine species were analysed together in the one CAP analysis, ranging from 55.56 to 97.58% (Figure 2.6 & Table 2.5). The results were species-specific with over 90% of all *C. australis*, *C. lineatus* and *P. oxygeneios* specimens being assigned to the correct species, whereas *P. americanus* and *S. bassensis* had allocation success rates of 88 and 82% respectively and other species had allocation success rates below 75% (Table 2.5). Most of the misclassifications occurred within a genus, but some also occurred across genera, especially between *L. punctulatus*, *L. nebulosus* and *S. vittata* (Table 2.5). The *Polyprion* genera were readily separated on the CAP plot. This separation was primarily driven by the relatively longer otolith of *Polyprion* compared to other genera (Figure 2.6). Similarly, *C. gerrardi* were also distinct on the CAP plot, but their separation was due to the otolith width, indicating relatively larger values of this variable compared with the other species (Figure 2.6).

Table 2.3 Descriptive statistics for fish length and otolith morphometric variables for the nine study species from Australia. All length measurements are in mm, and weight is in g. SE, standard error.

	<i>C.australis</i>	<i>C.gerrardi</i>	<i>C.lineatus</i>	<i>L.nebulosus</i>	<i>L.punctulatus</i>	<i>P.americanus</i>	<i>P.oxygenios</i>	<i>S.bassensis</i>	<i>S.vittata</i>
Sample size	60	95	81	100	99	139	579	122	125
Fish length									
Mean (SE)	319.9 (6.68)	498.69 (11.63)	312.77 (8.76)	438.03 (15.11)	246.97 (5.04)	1053.7 (15.08)	760.41 (4.93)	195.48 (6.9)	186.86 (6.68)
Range	233 - 431	261 - 689	170 - 435	170 - 715	169 - 356	563 - 1452	521 - 1289	29 - 340	43 - 311
Otolith length									
Mean (SE)	14.43 (0.24)	20.75 (0.33)	12.36 (0.15)	12.33 (0.3)	8.85 (0.17)	23.38 (0.26)	14.18 (0.06)	7.28 (0.21)	7.86 (0.24)
Range	11.08 - 18.5	13.79 - 25.54	8.67 - 15.12	6.1 - 17.94	6.27 - 12.11	14.49 - 30.4	11.05 - 20.87	1.47 - 11.32	2.34 - 13.01
Otolith width									
Mean (SE)	9.95 (0.09)	12.97 (0.09)	8.7 (0.06)	7.48 (0.17)	6.04 (0.11)	11.35 (0.12)	6.89 (0.04)	4.57 (0.12)	4.65 (0.13)
Range	8.31 - 11.36	10.94 - 14.97	6.99 - 9.68	3.95 - 10.71	4.22 - 9.04	7.64 - 16.13	5.4 - 11.97	1.02 - 6.71	1.41 - 6.87
Otolith thickness									
Mean (SE)	2.87 (0.06)	4.1 (0.08)	2.99 (0.03)	2.13 (0.07)	1.63 (0.04)	3.4 (0.05)	2.25 (0.02)	2.13 (0.08)	1.22 (0.03)
Range	2.2 - 4.65	2.69 - 5.69	2.18 - 3.61	1.11 - 3.64	1.1 - 2.65	2.15 - 5.19	1.52 - 3.93	0.36 - 4.25	0.48 - 1.85
Otolith weight									
Mean (SE)	0.401 (0.018)	1.098 (0.042)	0.312 (0.007)	0.272 (0.018)	0.127 (0.007)	0.851 (0.027)	0.227 (0.004)	0.102 (0.007)	0.064 (0.004)
Range	0.219 - 0.952	0.441 - 1.983	0.148 - 0.452	0.032 - 0.797	0.042 - 0.349	0.201 - 1.772	0.096 - 0.866	0.001 - 0.324	0.002 - 0.209

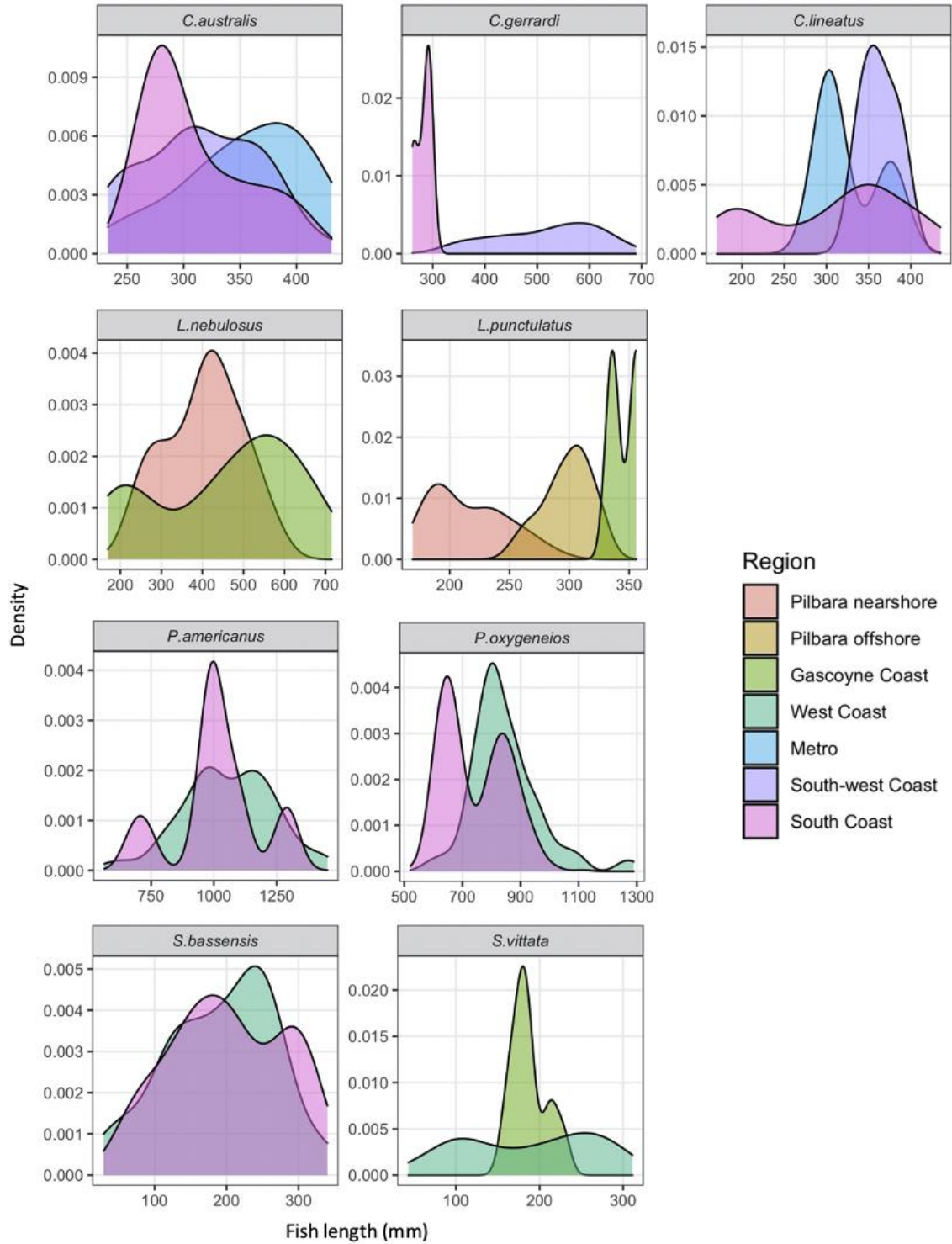


Figure 2.2 Kernel density plots representing the distributions of fish length (mm) for each species and region.

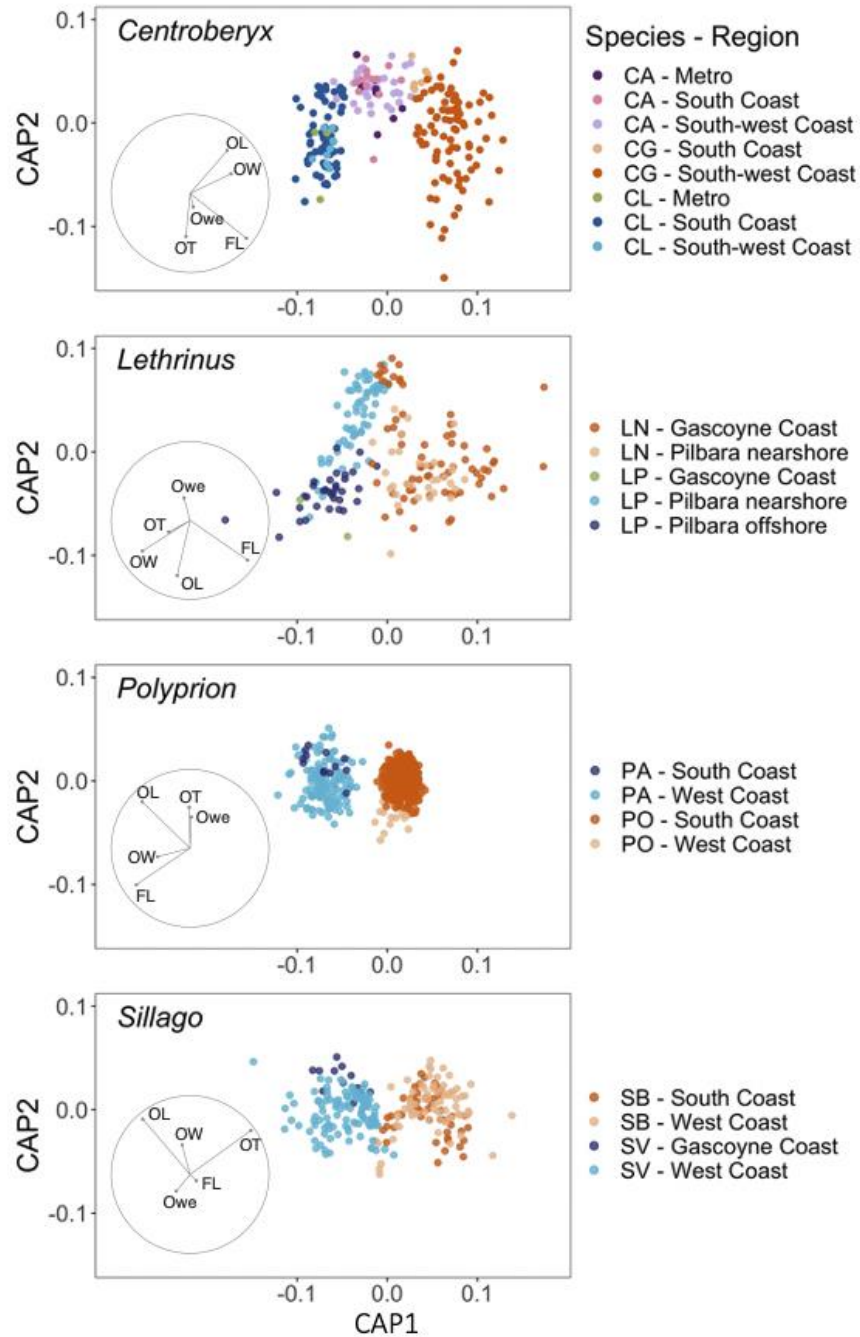


Figure 2.3 Canonical Analysis of Principal Coordinates (CAP) ordination plots of otolith morphometrics data and fish length for each genus, using a euclidean distance similarity matrix. The overlay vectors are the multiple partial correlations of morphometric variables with the two canonical axes. The circle around the vectors indicates the correlation coefficient of 1. The closer the vector reaches to the circle, the higher the correlation coefficient is. CA, *C. australis*; CG, *C. gerrardi*; CL, *C. lineatus*; LN, *L. nebulosus*; LP, *L. punctulatus*; PA, *P. americanus*; PO, *P. oxygeneios*; SB, *S. bassensis*; SV, *S. vittate*; FL, fish length; OL, otolith length; OW, otolith width; OT, otolith thickness; Owe, otolith weight.

Table 2.4 Leave-one-out allocation success rates (%) of the Canonical Analysis of Principal Coordinates (CAP) using otolith morphometry and fish length data to distinguish the species (Spp) and region (Spp*Region) within each genus. GC, Gascoyne Coast; PN, Pilbara nearshore; PO, Pilbara offshore; WC, West Coast; SC, South Coast; SW, Southwest coast; Metro, adjacent to Perth metropolitan region.

Species	Region	Total (n)	Misclassified (n)	% correct	
				Spp*Region	Spp
<i>C.australis</i>	Metro	8	0	50	96.67
	SC	13	1	38.46	
	SW	39	1	23.08	
<i>C.gerrardi</i>	SC	8	0	100	100
	SW	87	0	80.46	
<i>C.lineatus</i>	Metro	3	0	0	92.59
	SC	69	6	33.33	
	SW	9	0	44.44	
<i>L.nebulosus</i>	GC	69	17	37.68	80
	Pilbara nearshore	31	3	77.42	
<i>L.punctulatus</i>	GC	2	0	0	98.99
	Pilbara nearshore	63	0	84.13	
	Pilbara offshore	34	1	79.41	
<i>P.americanus</i>	SC	13	0	76.92	100
	WC	126	0	69.84	
<i>P.oxygeneios</i>	SC	491	0	76.17	100
	WC	88	0	69.32	
<i>S.bassensis</i>	SC	50	4	40	92.62
	WC	72	5	58.33	
<i>S.vittata</i>	GC	12	0	75	99.2
	WC	113	1	80.53	

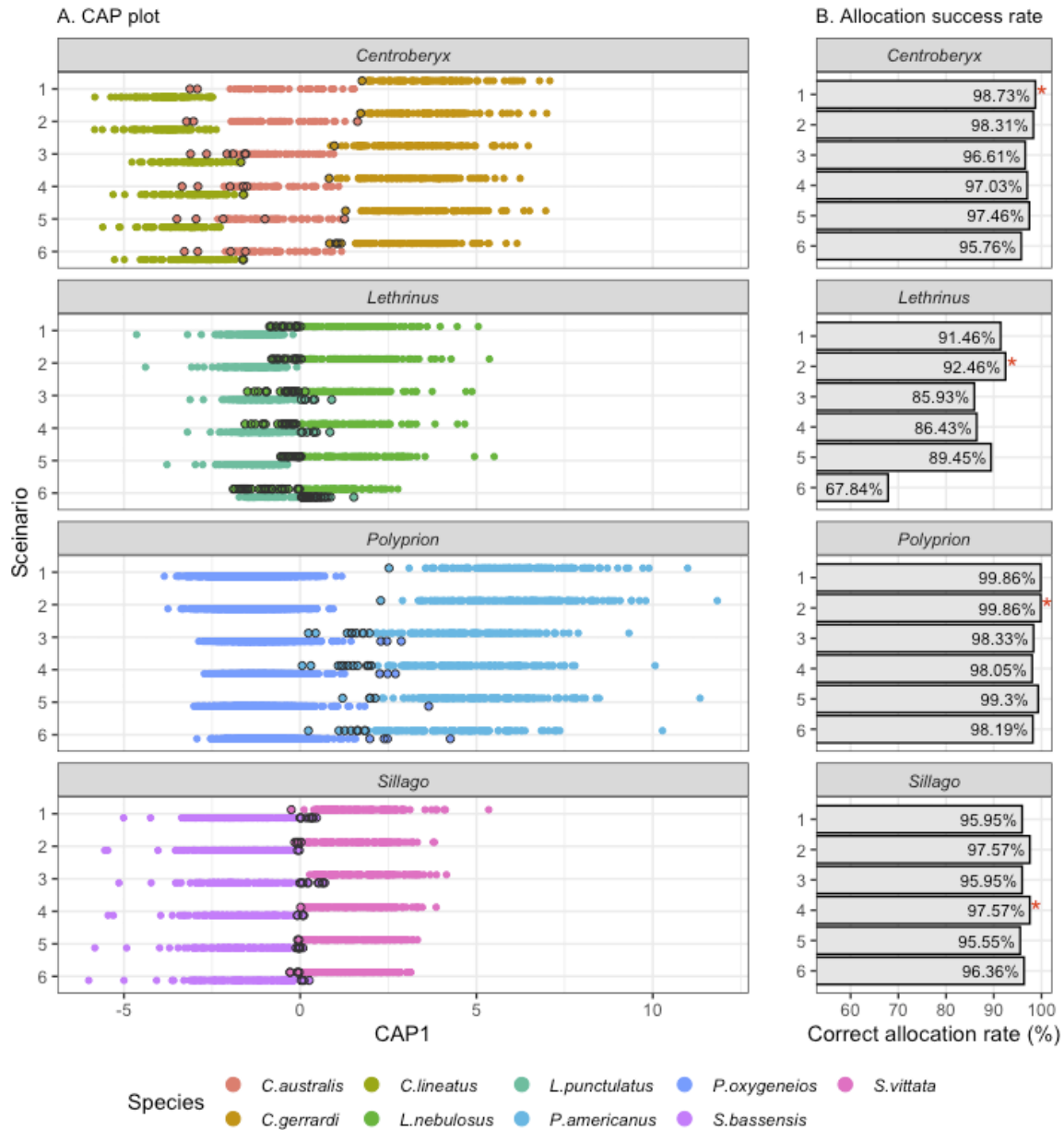


Figure 2.4 Canonical Analysis of Principal Coordinates (CAP) ordination plots of otolith morphometrics data of nine study species, using a euclidean distance similarity matrix with different combinations of otolith morphometric variables (six scenarios) for each genus (A). The bar plots (B) indicate the CAP leave-one-out allocation success rates (%) for each scenario. Circled points in CAP plots are misclassified samples. Asterisk in the bar plots indicates the most parsimonious model of each genus, which achieved the highest allocation success rates with the least number of variables. The six scenarios are referred to in Table 2.2.

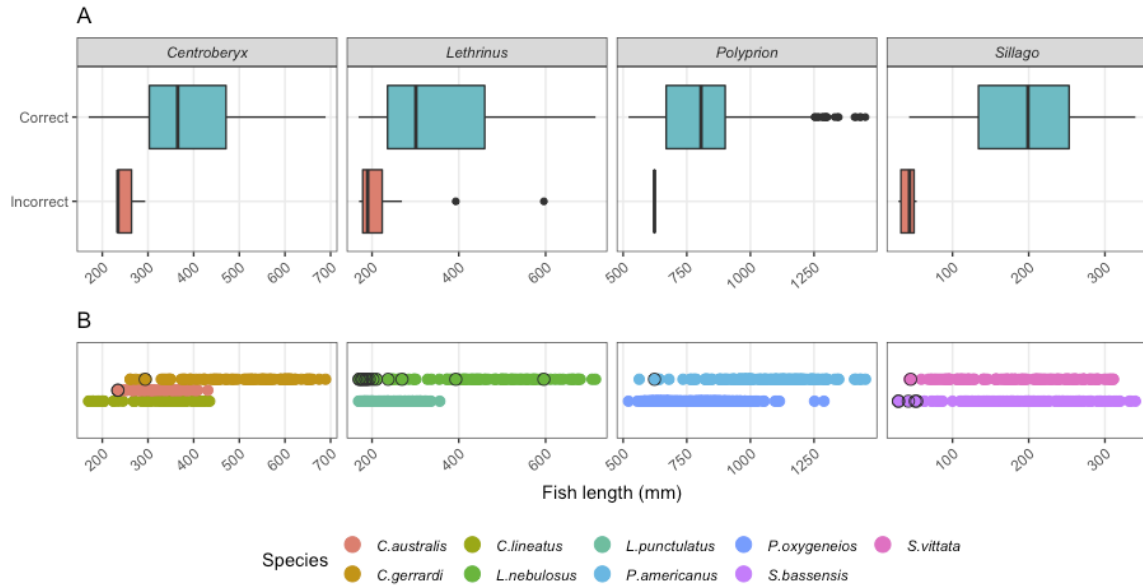


Figure 2.5 Boxplots (A) showing the medians of fish length (mm) (\pm 95% confidence interval) of correctly (blue) and incorrectly (red) assigned fish based on Canonical Analysis of Principal Coordinates (CAP) leave-one-allocation approach using the most parsimonious CAP model for each genus. The error bars indicate \pm 1.5 interquartile range. Scatter plots (B) of fish length showing misclassified samples indicated by the black circled points for each species.

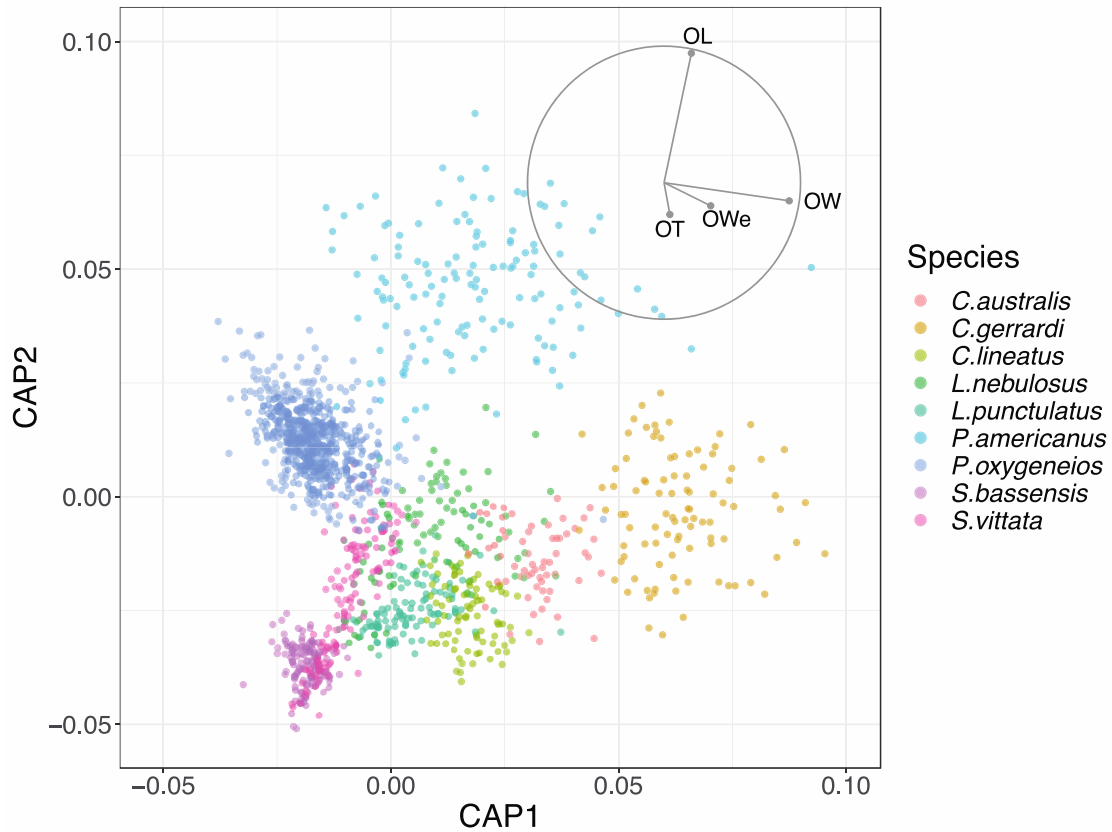


Figure 2.6 Canonical Analysis of Principal Coordinates (CAP) ordination plot of otolith morphometrics data of nine study species for the ‘bag of unknown otoliths scenario’, using a euclidean Distance similarity matrix. The overlay vectors are the multiple partial correlations of morphometric variables with the two canonical axes. The circle around the vectors indicates the correlation coefficient of 1. The closer the vector reaches to the circle, the higher the correlation coefficient is. OL, otolith length; OW, otolith width; OT, otolith thickness; Owe, otolith weight

Table 2.5 Leave-one-out allocation results of Canonical Analysis of Principal Coordinates (CAP) analyses using otolith morphometric measures of nine study species for the ‘bag of unknown otoliths scenario’. *C.aus*, *C. australis*; *C.ger*, *C. gerrardi*; *C.lin*, *C. lineatus*; *L.neb*, *L. nebulosus*; *L.pun*, *L. punctulatus*; *P.ame*, *P. americanus*; *P.oxy*, *P. oxygeneios*; *S.bas*, *S. bassensis*; *S.vit*, *S. vittata*; % cor, correct allocation rate (%).

		Classified group									Total	% cor
		<i>C.aus</i>	<i>C.ger</i>	<i>C.lin</i>	<i>L.neb</i>	<i>L.pun</i>	<i>P.ame</i>	<i>P.oxy</i>	<i>S.bas</i>	<i>S.vit</i>		
Original group	<i>C.aus</i>	55	0	5	0	0	0	0	0	0	60	91.67
	<i>C.ger</i>	24	71	0	0	0	0	0	0	0	95	74.74
	<i>C.lin</i>	3	0	78	0	0	0	0	0	0	81	96.30
	<i>L.neb</i>	10	0	3	61	6	0	1	1	18	100	61.00
	<i>L.pun</i>	1	0	2	19	55	0	0	0	22	99	55.56
	<i>P.ame</i>	0	4	0	1	0	122	12	0	0	139	87.77
	<i>P.oxy</i>	0	1	3	8	0	2	565	0	0	579	97.58
	<i>S.bas</i>	0	0	0	0	0	0	0	100	22	122	81.97
	<i>S.vit</i>	0	0	0	28	4	0	2	0	91	125	72.80

2.5 Discussion

A robust and reliable tool for species discrimination is required for fast and cost-effective identification of potentially cryptic species. This is particularly important for species targeted by commercial and recreational fishers to ensure accurate assessments of the stock status. Primarily there is a need to resolve any bias or confounding within sample collections that may lead to spurious assessment outcomes by virtue of the data possibly containing information from more than one species (Bickford et al., 2007). Our research identified significant variations in otolith morphometrics between each of the species, with very high species-specific accuracy in prediction rates from the multivariate models (between 92.46 and 99.66%). High accuracy rates have also been achieved across other species including *Scomberomorus* spp. (96%; Zischke et al., 2016), *Sebastes* spp. (88 - 97%; Stransky & MacLellan, 2005; Zhuang et al., 2015) and *Etelis* spp. (99 - 100%; Wakefield et al., 2014), using multivariate analytical approaches (i.e. linear or canonical discriminant analysis).

We also assessed the allocation success rates of multivariate morphometric models using different combinations of variables. These procedures allowed us to determine the applicability of this approach under different scenarios, as well as to identify the influential variables, and thus the most parsimonious models for each genus. For instance, the removal of otolith weight data from the models did not affect the species prediction accuracies for any genera, indicating that this

variable has little influence on the between-species variation in otolith morphometrics utilised in the most parsimonious models. Therefore, accurate species identification using otolith morphometrics can be achieved without the need for an analytical balance, which is more cost-effective as less time and equipment is needed to derive the data required. Potentially, this subset of measurement-based variables could be extracted in the field with a minimum of equipment and applied to a pre-set analytical routine, thus providing near real time resolution of any potential confounding individuals within sample collections.

Similarly, the removal of fish length and otolith length data still achieved a high discrimination accuracy for *Centroberyx*, *Polyprion* and *Sillago* spp. This finding is further supported by the results of Wakefield et al. (2014) that also identified the robustness of an otolith morphometric approach to discriminate cryptic *Etelis* snappers with, without fish length data. Such models without fish and/or otolith length data would be particularly useful when the caudal fin is damaged/missing, or the otoliths are chipped and/or either fish or otolith length data cannot be recorded. However, the species allocation success rates of *Lethrinus* spp. dropped from 92.46 to 85.93% when fish length was removed from the analyses, and further declined to 67.84% when otolith length and weight was also removed. This is possibly attributed to the large differences in the length distributions between the two species examined, i.e. *L. nebulosus* and *L. punctulatus*. These conflicting outcomes indicate that specific examination of influential variables and parsimonious models are required for each taxon.

Regional variations were evident in the CAP plots for *L. punctulatus*, *C. gerrardi*, *P. oxygeneios*, and *S. vittata*, which were less distinct compared to the differences between species. Previous studies have also revealed spatial variations in other teleost species (Jemaa et al., 2015; Longmore et al., 2010), which were likely due to the combination of restricted gene flow and environmental factors, including water temperature, dissolved oxygen and prey availability, influencing the growth and morphology of otoliths (Campana & Casselman, 1993; Thomas et al., 2014; Zhuang et al., 2015). However, the spatial variations revealed in this study may also be attributed to the fish size distributions. For instance, *L. punctulatus* from the Pilbara nearshore and offshore regions exhibited different otolith morphometric arrangements, as well as a smaller and larger body size range, respectively, which coincides with the common ontogenetic movement patterns of many reef fish species (Dahlgren & Eggleston, 2000). Other species with different size distributions between regions (*C. gerrardi*, *P. oxygeneios* and *S. vittata*) also displayed spatial variations in otolith morphology, whereas the remaining study species (*C. lineatus*, *C. australis*, *L. nebulosus*, *P. americanus* and *S. bassensis*) had relatively similar size distributions and otolith morphology

across regions within each species. In order to further examine species-specific otolith morphometric patterns within each region, there is a need to assess whether samples are representative of the available population (to avoid any sampling biases between putative populations), and furthermore to investigate if there is phylogenetic support for any potential population separation.

The size of misclassified specimens was notably smaller than those of correctly classified specimens across all genera. This is possibly due to the allometric accretion of otoliths relative to asymptotic somatic growth (Campana, 2005). Otolith morphometric data varies according to the length and presumably age of an individual, and thus the difference between species may become more evident as a species increases in length and age. This finding indicates that the otolith morphometric approach used herein as a species identification tool is less reliable for juveniles, requiring a careful interpretation of the size range of training data (the reference set of data used to construct a model) and test data (data from a new specimen). Cryptic body features are common during juvenile stages to derive a selective advantage for both coexistence and survival (Fišer et al., 2018; Sievers et al., 2020). While most fisheries assessments are conducted on adult fishes, further studies are required to identify more reliable and cost-effective species identification tools for the juveniles of fishery targeted species.

When applying this approach to dietary studies to identify teleost prey taxa using undigested otoliths in predators' stomachs ('bag of unknown otoliths scenario'), we assessed the species prediction accuracy using the CAP model with all nine study species combined. The accuracy rates were above 90% for *C. australis*, *C. lineatus* and *P. oxygenios*, whereas the rates dropped to 56 - 88% for other species. This indicates that otolith morphometric models can potentially be used to identify the species when the genus and/or family is unknown for some species. However, the expansion of CAP models with an extended range of taxa is required to further validate its utility in similar 'bag of unknown otoliths' situations.

In conclusion, otolith morphometric multivariate models successfully discriminated nine cryptic teleost species from four genera in Western Australia, with very high species-specific accuracy rates. This supports our hypothesis that the use of otolith morphometry is a useful method to discriminate between cryptic species. Given the importance of these species to fishers, the approaches described herein provide a direct, cost-effective application to facilitate accurate species identification to underpin species-specific assessments of stock status. However, further studies need to be undertaken to expand the general applicability of this approach to other species and/or juveniles to further assist species-specific biological assessments.

Chapter 3 Cryptic species discrimination for the juveniles of two lutjanids using body and otolith morphometry

3.1 Abstract

The sympatric red snappers, *Lutjanus erythropterus* and *L. malabaricus*, are targeted and retained by commercial and recreational fishers along the tropical northern coasts of Australia. Studies on the life history and ecology of these cryptic congeners are confounded by difficulties in distinguishing between juveniles of each species (i.e. < 200 mm fork length). This study aimed to validate a robust and cost-effective methodology to discriminate between *L. erythropterus* and *L. malabaricus* juveniles using body and/or otolith morphometric data in a multivariate analysis. Juvenile samples were collected from the northwest (n = 71) and northeast (n = 19) coasts of Australia, and species identification was confirmed using DNA barcoding. The most parsimonious multivariate models achieved accurate species prediction rates of 98.81% and 84.88% using body and otolith variables, respectively. The high level of discrimination between the cryptic juveniles of *L. erythropterus* and *L. malabaricus* highlights the robustness of this morphometric approach. Spatial variation in the otolith morphology of *L. malabaricus* between northwest and northeast coasts was also evident, indicating a need to collect more samples over a broader spatial scale to incorporate spatial variation across a species distribution for otolith morphometric models. The method we used could be applied more broadly to distinguish cryptic fishes from a range of sample collections, including archived otolith collections and potentially have a widespread utility in assessing species compositions from *in-situ* stereo-video body measurements.

3.2 Introduction

Lutjanus erythropterus (Bloch, 1790) and *L. malabaricus* (Schenider, 1801) are sympatric red snappers that are targeted by commercial, recreational and artisanal fishers throughout their distributions in the tropical and subtropical waters of the Indo-Pacific region (Allen, 1985; Blaber et al., 2005). In excess of 3,000 tonnes of these species are caught in Australia annually (Saunders et al., 2018), with their annual landed value in the order of \$ 20 million (Newman

2019, personal communications, 4 October). The high economic and social values of these species means that there is an investment in understanding their life history and ecology, with ongoing monitoring requirements to support stock assessments, and sustainable management (Fry & Milton, 2009; McPherson et al., 1992; Newman, 2002; Newman et al., 2000; O'Neill et al., 2011).

The accurate identification of a species is fundamental for monitoring and assessment programs, with species level identification usually being based on morphological characteristics (Hey et al., 2003). Adult *L. erythropterus* and *L. malabaricus* exhibit easily distinguished external morphology, particularly evident around the nape, mouth and caudal peduncle pigmentation, whereas juveniles are morphologically indistinguishable (i.e. cryptic). Based on ecomorphology theory, the more similar the morphology among closely related species, the more similar the ecology and niche requirements of the species under consideration (Meyer, 1989; Wainwright & Richard, 1995). Despite their morphological similarities, Takahashi et al. (2020) identified significant diet partitioning patterns between the species during the cryptic juvenile stage. Inter-specific reproductive strategies have also been observed, with each species exhibiting different spawning seasons and reproductive strategies (Fry et al., 2009; McPherson et al., 1992). These findings suggest that there are a range of specialised adaptations for cryptic, sympatric species to differentiate their niche and life history strategies in order to coexist within an ecosystem, highlighting the need for accurate species identification and the need for fishery assessments to be specific to each species.

Discrimination of the cryptic juveniles of *L. erythropterus* and *L. malabaricus* can be achieved using DNA barcoding (Elliott, 1996; Fry & Milton, 2009; Takahashi et al., 2020). However, ecological and biological knowledge of the juveniles is extremely limited, possibly owing to the shortcomings of molecular analyses (i.e. both high costs and long-time requirements for analysis) to discriminate between the species. Juvenile *L. erythropterus* and *L. malabaricus* have been found in the bycatch of commercial prawn trawl vessels (Fry et al., 2009; McPherson et al., 1992), however differentiation between these species cannot be ascertained directly in the field. There is a need to develop a robust, cost-effective identification tool to discriminate between the cryptic juveniles of *L. erythropterus* and *L. malabaricus*.

Previous studies have utilised multivariate morphometric approaches to discriminate cryptic species in a range of taxa, such as flowers (Fisher, 1936, 1938), snakes (Sanders et al., 2006), flies (Cazorla & Acosta, 2003) and bivalves (Baker et al., 2003). In fish biology, otolith morphometry has used multivariate analyses to identify species (Bani et al., 2013; Stransky & MacLellan, 2005; Wakefield et al., 2014; Zhuang et al., 2015) and stock structure (population subdivision) within a species (Jemaa et al., 2015; Longmore et al., 2010; Tracey et al., 2006).

Otoliths are paired calcareous structures in the inner ear of teleosts, which provide valuable information for biological and ecological studies, such as age, trophic ecology and population structure (Begg et al., 2005; Newman et al., 2015; Williams et al., 2015). While several studies have concluded that there is a high degree of inter-specific variation in the otolith morphometric data for cryptic adult teleosts (Stransky & MacLellan, 2005; Wakefield et al., 2014; Zhuang et al., 2015; Zischke et al., 2016), there is limited data and information for the separation of juveniles. Otolith morphometric analyses have been performed for *L. erythropterus* and *L. malabaricus* (Sadighzadeh et al., 2012), yet juvenile fish were not included in that study (minimum total fish length of 316 mm and 235 mm for *L. erythropterus* and *L. malabaricus*, respectively).

The aim of this research was to identify a robust, simple and cost-effective method to discriminate between *L. erythropterus* and *L. malabaricus* juveniles using body and/or otolith morphometric measurements as an alternative to DNA barcoding. Specifically, our objectives were to: 1) assess the differences in the body and/or otolith morphometric data between the species; 2) assess the allocation success rates of each prospective model; and 3) identify the most parsimonious model that can be replicated rapidly as an identification guide in the field or laboratory at a low cost.

3.3 Materials and methods

3.3.1 Sample collection and genetic species identification

A total of 90 juvenile fish were caught using prawn trawl nets from the Pilbara and Kimberley regions of Western Australia (WA), and from the coast of central Queensland (QLD), eastern Australia between 2014 and 2019 (Figure 3.1). Fin clips of each fish were collected and stored in 100 % ethanol to genetically identify each species. DNA from each fin clip was extracted and diluted to 1/10 with ultra-pure water. Polymerase chain reaction (PCR) was carried out using the FishBCH forward primer (5'-ACTTCYGGGTGRCCRAARAATCA -3') and the FishBCL reverse primer (5'-TCAACYAATCAYAAAGATATYGGCAC-3') to target 600 to 800 bp of the cytochrome c oxidase subunit I (COI) region, following the "HotSHOT" technique (Meeker et al., 2007). The choice of the target region and primers was based on the database availability and inter-specific diversity within the targeted amplicon for accurate species identification. The following PCR cycling program was used: (i) 94 °C for 4 minutes; (ii) 35 amplification cycles of 94 °C for 30 seconds, 50 °C for 30 seconds, 72 °C for 60 seconds; and (iii) a final extension step at 72 °C for 10 minutes. Successful amplification was tested by loading 4 µL of each amplicon onto a 2% agarose gel and analysing the gel image

under UV light with a Bio-Rad transilluminator and GelRed® nucleic acid staining dye (Molecular Probes). DNA was further diluted to 1/25 if no signature appeared on the gel image at the target size, re-amplified and visualised on a gel. A mixture of 10 µL of the amplicons, and 2 µL of exonuclease I and FastAP thermosensitive alkaline phosphatase (ExoFAP; USB, Cleveland, OH, USA) were combined and purified using the following cycling program: (i) 37 °C for 15 minutes; (ii) 80 °C for 15 minutes; and (iii) 4 °C for 10 minutes. The purified amplicons were shipped to Macrogen for Sanger Sequencing (Macrogen Facility, Seoul, Korea) in the forward direction only. A Basic Local Alignment Search Tool (BLASTn) query was carried out to assign each sequence to a species using the customised database of the National Center for Biotechnology Information (NCBI) GenBank nucleotide reference sequences (Benson et al., 2017) and the Western Australian fish database (Nester et al., 2020). All sequences were assigned to either *L. erythropterus* or *L. malabaricus* with over 99.5% fidelity.

After genetic identification it was found that a total of 26 *L. erythropterus* and 17 *L. malabaricus* were collected from the Pilbara region, 22 *L. erythropterus* and six *L. malabaricus* from the Kimberley region, and 19 *L. malabaricus* from central QLD (Table 3.1 & Figure 3.1). No *L. erythropterus* were collected from QLD. Fork length (FL) ranged from 60 to 200 mm across the samples. The smallest individual (60 mm) and smallest mean FL (98 mm ± 6.21 standard error) were observed in *L. erythropterus* from the Kimberley region, whereas the mean FL of other regions and/or species ranged from 126 to 167 mm (Table 3.1).

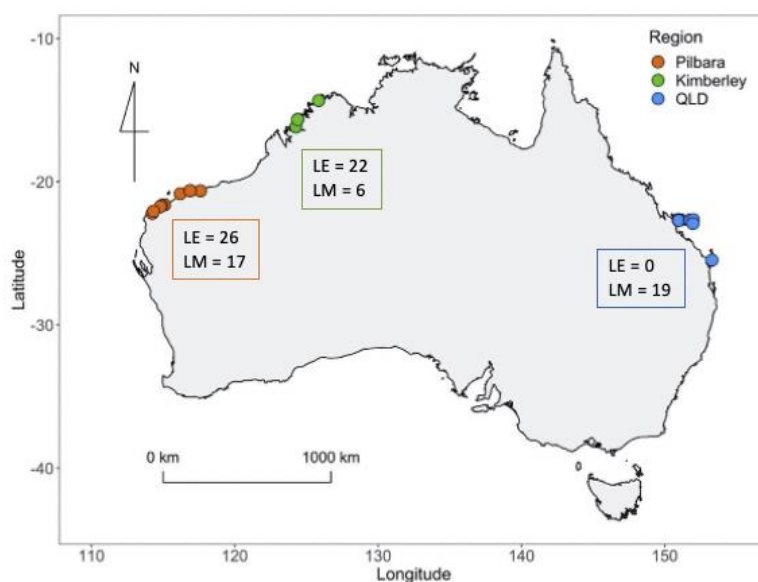


Figure 3.1 Location where samples of juvenile *Lutjanus erythropterus* (LE) and *L. malabaricus* (LM) were collected in the Pilbara (WA), Kimberley (WA) and central Queensland (QLD) regions of Australia. The numbers in boxes indicate the sample size of each species and region.

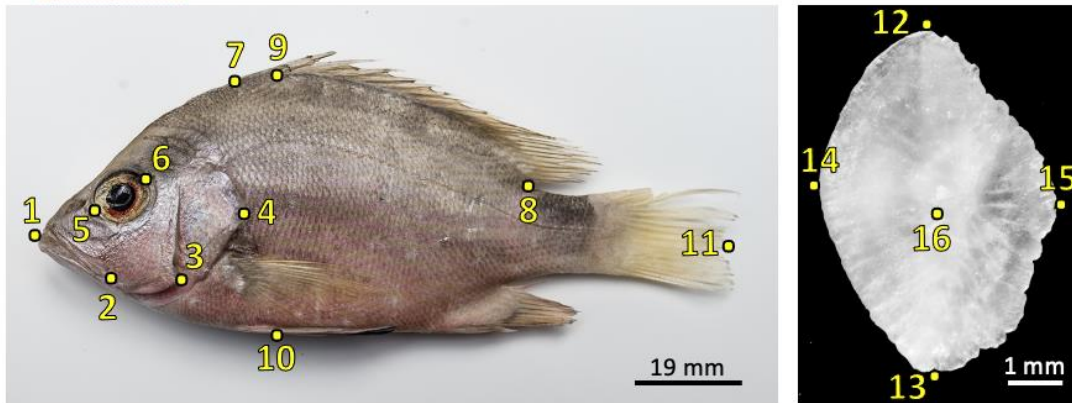
Table 3.1 Descriptive statistics for fork length measurements of *Lutjanus erythropterus* and *L. malabaricus* collected from Pilbara, Kimberley and Queensland (QLD). SE, standard error.

	n	Fork length (mm)	
		Range	Mean (SE)
<i>L. erythropterus</i>			
Pilbara	26	78.54 - 166.45	129.01 (4.53)
Kimberley	22	59.5 - 185.19	98.44 (6.21)
QLD	0	NA	NA
<i>L. malabaricus</i>			
Pilbara	17	103.7 - 198.65	129.82 (6.08)
Kimberley	6	136.66 - 200	167.44 (10.61)
QLD	19	94 - 179	126.47 (6.24)

3.3.2 Morphometrics measurement

Fork length (FL), jaw length, jaw to operculum, jaw to preoperculum, jaw to eye, eye to dorsal fin, dorsal fin length and body height were measured to the nearest 0.01 mm using digital callipers (Figure 3.2). Sagittal otoliths were dissected, cleaned in water and stored dry. Using digital callipers, otolith length (i.e. the length from the rostrum to the post-rostrum), otolith width (i.e. the width at the widest point approximately perpendicular to the length axis), and otolith thickness (i.e. the thickness of the otolith at the primordium perpendicular to the sulcus acusticus) from the left otolith (or right otolith if the left one was chipped or broken) of each fish were measured to the nearest 0.01 mm (Figure 3.2). The otolith weight - the weight of the otolith, was also measured to the nearest 0.001 mg using an analytical balance. Eye diameter was initially considered, however the variable was omitted due to its high variability depending on observers (i.e. observer bias) and the freshness of the specimen, as well as no improvement of the model with the variable in terms of species prediction accuracy.

L. erythropterus



L. malabaricus

Figure 3.2 Images of the juveniles and the distal aspect of left sagittal otoliths of *Lutjanus erythropterus* and *L. malabaricus*. The numbers in the images indicate the points of morphometric measurements; 1 – 2, jaw length, 1 – 3, jaw to operculum; 1 – 4, jaw to preoperculum; 1 – 5, jaw to eye; 6 – 7, eye to dorsal fin; 7 – 8, dorsal fin length; 9 – 10, body height; 1 – 11, fork length; 12 – 13, otolith length; 14 – 15, otolith width; 16, otolith thickness.

3.3.3 Statistical analyses

Multivariate analyses were carried out on the morphometric dataset of body and otolith measurements separately. Previously, a higher allocation success rate has been achieved with the fork length included in combination with otolith morphometric variables (Wakefield et al., 2014), so therefore we included fork length. A euclidean distance similarity matrix was constructed from each body morphometric and otolith dataset and a Canonical Analysis of Principal Coordinates (CAP) was carried out with species as *a priori* groups, and region and species as factors (Anderson & Willis, 2003). The dataset did not require transformation as the data were normally distributed. Additionally, there is no need to normalise data in the CAP analysis even when variables are measured using different units because the PCO axes in the CAP use orthonormal axes and are automatically sphericised and not scaled by their respective eigenvalues (Anderson et al., 2008). The leave-one-out approach was used to assess the

allocation success rates to the correct species and regions (Anderson & Willis, 2003). The number of PCO axes included in the CAP analyses (m) was defined as the number of variables in each test (Anderson & Willis, 2003).

In order to identify the most parsimonious model, the analyses described above were repeated for all combinations of the subset variables, with the number of variables ranging from two to seven for the body morphometric dataset, and from two to four for the otolith dataset. The most parsimonious model was considered to have the highest species prediction accuracy with lowest number of variables. Where possible, partial correlation vectors representing each morphometric variable were overlaid on ordinations to ascertain the strength and direction of their influence in separating the data clouds for each species. Trace and delta canonical test statistics were also obtained using 9999 permutations to assess the significant differences in body or otolith morphometric data between species and region. Finally, the CAP analyses were carried out with both body and otolith variables of the most parsimonious models combined, and the leave-one-out allocation success rates and test statistics were assessed. The model selections based on the leave-one-out allocation success rates were carried out using the CAPdiscrim function of the biodiversityR package in R (v. 2.12-1) (Kindt, 2020). The software PRIMER 7 (v. 7.0.13, <https://www.primer-e.com>) (Clarke et al., 2014) were used to plot the selected models and assess the multiple partial correlations of the morphometric variables and test statistics.

3.4 Results

3.4.1 Species distinction

3.4.1.1 Body morphometrics

The CAP models with all eight body measurement variables had a species prediction accuracy of 96.43% when species was used as a factor (Table 3.2-A), and 95.24% when species and regions were used as factors (Table 3.3-A & Figure 3.3). The highest allocation success rate (98.81%) was achieved by models where the number of variables were between three and seven (Figure 3.3), and only one *L. malabaricus* sample (110 mm FL) was misclassified as a *L. erythropterus* (Table 3.4-A & Table 3.5-A). The allocation success rates decreased from 98.81 to 96.43% when the number of variables were further reduced to two (Figure 3.3). Overall, the three-variable model (dorsal fin length, jaw to eye, and either jaw length or jaw to preoperculum) was the most parsimonious model for body morphometrics (Table 3.2-A & Table 3.3-A).

Significant differences in the body morphometrics between species were also identified by the clear separations of the clusters of each species along the first canonical axes (Figure 3.4-A & B) and significant values of test statistics using 9999 permutations ($p < 0.001$ for both trace and delta statistics). *Lutjanus malabaricus* had a relatively longer jaw length and a longer distance from the jaw to eye compared to *L. erythropterus*, based on the direction and length of their vectors (Figure 3.4-B). Dorsal fin length was highly correlated along the second canonical axis and was therefore more likely to be related to the size of the fish than differences between species (Figure 3.4-B). The overlapping clusters of data points for regions within a species suggest no regional variations in body morphometrics (Figure 3.4-B).

3.4.1.2 Otolith morphometrics

The allocation success rate of species from the most parsimonious otolith model was 84.88%, which contained five variables (fork length and all four otolith variables) with species and regions as factors (Table 3.3-B & Figure 3.3, $p < 0.001$ for trace and delta statistics). The lower species discrimination accuracy of the otolith morphometric model compared to those of the body morphometric model were evident from the leave-one-out allocation success rates (84.88% of the former as opposed to 98.81% of the latter) (Figure 3.3), as well as the observations of each species overlapping on the first canonical axis (Figure 3.4). The accuracy rate of otolith models further decreased when species was used as a factor (without a region factor), ranging between 74.42 and 79.07% (Figure 3.3 & Table 3.2-B). Fork length and otolith width were selected in all models with species as a factor, indicating they were significant predictor variables (Table 3.2-B).

Spatial variations in otolith morphometrics were evident by the observations of each group clustering together on the plot of the first two canonical axes, particularly for *L. malabaricus* between WA (Pilbara and Kimberley) and QLD (Figure 3.4-B). The highest allocation success rate to the correct species and region was achieved for the QLD *L. malabaricus* samples (87.5%) (Table 3.5-B), which also indicates significant spatial variation in the otolith morphometrics of *L. malabaricus* between WA and QLD. Otolith thickness was likely to be the influential factor separating the two populations of *L. malabaricus*, indicated by the correlation vectors on the CAP plot (Figure 3.4-B).

3.4.1.3 Body and otolith combined

When the selected variables of the most parsimonious body and otolith models were combined, the allocation success rate to species was 97.5% irrespective of whether the region factor was included in the analyses (Table 3.4-C, Table 3.5-C). The clear separation of the data clouds for each species was evident along the first canonical axis, driven by the jaw length and distance from the jaw to the eye (Figure 3.4-B). Spatial variations between the WA and QLD populations of *L. malabaricus* were evident along the second canonical axis, mainly driven by otolith thickness (Figure 3.4-B). Two samples were misclassified to the wrong species in both models with and without the factor 'region'. Those misclassified samples for the model with species as a factor were two *L. malabaricus* samples with FLs of 110 and 199 mm (Table 3.4-C). Those for the model with species and regions as factors were a *L. erythropterus* with a FL of 130 mm and a *L. malabaricus* with a FL of 110 mm (Table 3.5-C).

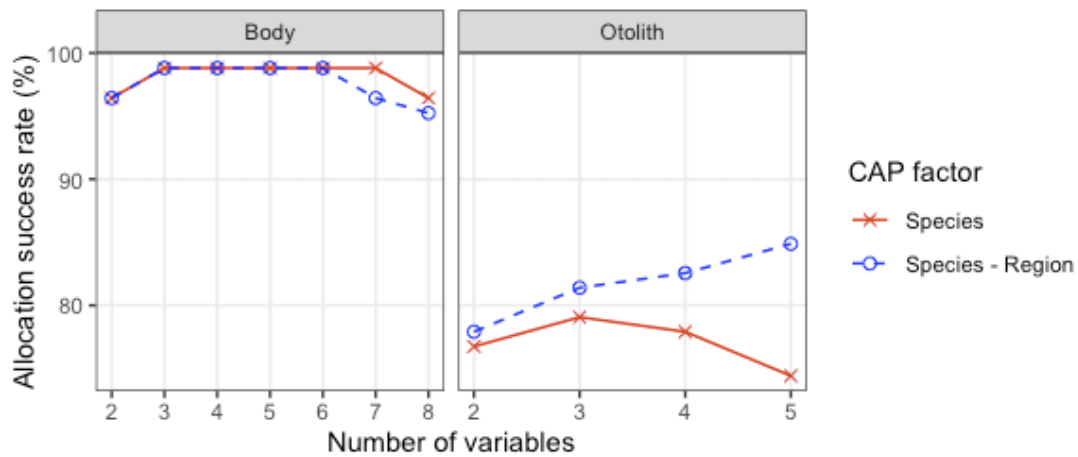


Figure 3.3 Leave-one-out allocation success rates to the correct species (%) for the selected Canonical Analysis of Principal Coordinates (CAP) models using different combinations of body (left) and otolith (right) morphometric variables. Species (red) and species and region (blue) were used as factor(s) of groups in the CAP analyses.

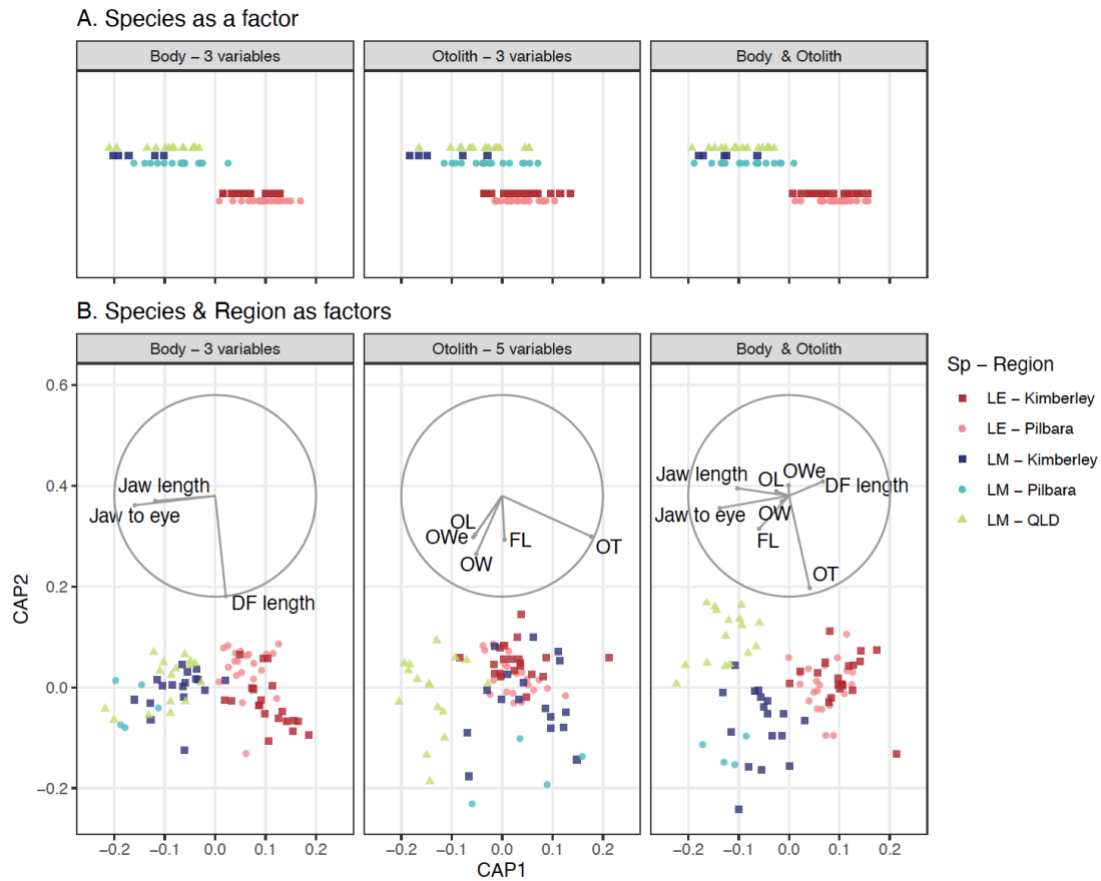


Figure 3.4 Canonical Analysis of Principal Coordinates (CAP) plots of body (left) and otolith (middle) morphometric arrangements of juvenile *L. erythropterus* (LE) and *L. malabaricus* (LM). The 1-dimensional plots (A) considered species as the factor for CAP analyses, and the 2-dimensional plots (B) considered species and regions as the factors for the analyses. The variables for each model were the most parsimonious models of each variable types (body (left) and otolith (middle)) and each CAP factor (species with/without region) (i.e. The body morphometric models were constructed using dorsal fin length, jaw length, and distance from jaw to eye). The CAP models with both body and otolith variables of each of the most parsimonious models were also assessed (right). The overlay vectors are the multiple partial correlations of morphometric variables with the two canonical axes. The circle around the vectors indicates the correlation coefficient of 1. The closer the vector reaches to the circle, the higher the correlation coefficient is. DF, dorsal fin; FL, fork length; OL, otolith length; OW, otolith width; OT, otolith thickness; Owe, otolith weight.

Table 3.2 Leave-one-out allocation success rates (%) to the correct species, and the combinations of body (A) and otolith (B) morphometric variables for the selected Canonical Analysis of Principal Coordinates (CAP) models using different combinations of morphometric variables. Species was considered as the factor of groups in the CAP analyses. The most parsimonious models were indicated in red, bold texts.

A. Body morphology – Species as a factor

No. of variables	Allocation success rates (%)	Fork length	Dorsal fin length	Jaw to eye	Jaw length	Jaw to preoperculum	Body height	Jaw to operculum	Jaw to dorsal fin
8	96.43	x	x	x	x	x	x	x	x
7	98.81	x	x	x	x	x		x	x
6	98.81		x	x	x	x	x	x	
		x	x	x	x	x			x
		x	x	x	x		x		x
5	98.81		x	x	x	x	x		
			x	x	x	x		x	
			x	x		x	x	x	
			x	x	x		x	x	
		x	x	x	x				x
		x	x	x	x	x			
		x	x	x	x		x		
4	98.81		x	x	x	x			
			x	x		x		x	
			x	x	x				x
			x	x	x			x	
			x	x		x	x		
			x	x	x		x		
		x	x	x	x				
3	98.81		x	x	x				
			x	x		x			
2	96.43		x	x					

B. Otolith morphology – Species as a factor

No. of variables	Allocation success rates (%)	Fork length	Length	Width	Thickness	Weight
5	74.42	x	x	x	x	x
4	77.91	x	x	x		x
3	79.07	x		x		x
2	76.74	x		x		

Table 3.3 Leave-one-out allocation success rates (%) to the correct species, and the combinations of body (A) and otolith (B) morphometric variables for the selected Canonical Analysis of Principal Coordinates (CAP) models using different combinations of morphometric variables. Species and regions were considered as the factors of groups in the CAP analyses. The most parsimonious models were indicated in red, bold texts.

A. Body morphology – Species and region as factors

No. of variables	Allocation success rates (%)	Fork length	Dorsal fin length	Jaw to eye	Jaw length	Jaw to preoperculum	Body height	Jaw to operculum	Jaw to dorsal fin
8	95.24	x	x	x	x	x	x	x	x
7	96.43	x	x	x	x	x	x	x	x
		x	x	x	x	x	x	x	x
		x	x	x	x	x	x	x	x
6	98.81	x	x	x	x	x	x	x	x
5	98.81		x	x	x	x		x	
			x	x		x	x	x	
			x	x	x		x	x	
		x	x	x	x	x			
		x	x	x	x		x		
			x	x	x			x	x
			x	x	x		x		x
4	98.81		x	x		x		x	
			x	x	x				x
			x	x	x	x			
			x	x	x			x	
		x	x	x	x		x		
3	98.81		x	x	x				
			x	x		x			
2	96.43		x	x					

B. Otolith morphology – Species and region as factors

No. of variables	Allocation success rates (%)	Fork length	Length	Width	Thickness	Weight
5	84.88	x	x	x	x	x
4	82.56	x	x	x	x	
3	81.40		x		x	x
		x			x	x
		x		x	x	
2	77.91				x	x

Table 3.4 Leave-one-out allocation results using the most parsimonious Canonical Analysis of Principal Coordinates (CAP) models with body (A), otolith (B) and body and otolith (C) morphometric variables. Species was used as the factors for the CAP analyses. LE, *Lutjanus erythropterus*; LM, *L. malabaricus*; Ob, observed.

A. Body – 3 variables

		Predicted		Correct %
		LE	LM	
Ob	LE	42	0	100
	LM	1	41	97.62

B. Otolith – 3 variables

		Predicted		Correct %
		LE	LM	
Ob	LE	41	7	85.42
	LM	11	27	71.05

C. Body & Otolith – 6 variables

		Predicted		Correct %
		LE	LM	
Ob	LE	42	0	100
	LM	2	36	94.74

Table 3.5 Leave-one-out allocation results using the most parsimonious Canonical Analysis of Principal Coordinates (CAP) models with body (A), otolith (B) and body and otolith (C) morphometric variables. Species and regions were used as the factors for the CAP analyses. LE, *Lutjanus erythropterus*; LM, *L. malabaricus*; Pil, Pilbara; Kim, Kimberley; QLD, Queensland.

A. Body – 3 variables

		Predicted						Correct %
		LE - Pil	LE - Kim	LE - Total	LM - Pil	LM - Kim	LM - QLD	
Observed	LE - Pil	12	8		0	0	0	60
	LE - Kim	4	18		0	0	0	81.82
	LE - Total			42				100
	LM - Pil	0	1		10	1	5	58.82
	LM - Kim	0	0		0	3	3	50
	LM - QLD	0	0		6	3	10	52.63
	LM - Total			1				41

B. Otolith – 5 variables

		Predicted						Correct %	
		LE - Pil	LE - Kim	LE - Total	LM - Pil	LM - Kim	LM - QLD		LM - Total
Observed	LE - Pil	21	4		1	0	0	80.77	
	LE - Kim	5	14		3	0	0	63.64	
	LE - Total			44				4	91.67
	LM - Pil	6	1		7	2	1	41.18	
	LM - Kim	0	0		2	3	0	60	
	LM - QLD	1	1		0	0	14	87.5	
	LM - Total			9				29	76.32

C. Body & Otolith – 8 variables

		Predicted						Correct %	
		LE - Pil	LE - Kim	LE - Total	LM - Pil	LM - Kim	LM - QLD		LM - Total
Observed	LE - Pil	13	6		1	0	0	65	
	LE - Kim	6	16		0	0	0	72.73	
	LE - Total			41				1	97.62
	LM - Pil	0	1		12	2	2	70.59	
	LM - Kim	0	0		4	1	0	20	
	LM - QLD	0	0		1	1	14	87.5	
	LM - Total			1				37	97.37

3.5 Discussion

Accurate identification of a fish is essential to underpin the study of its biology and ecology, which is needed for sustainable fisheries management. However, cryptic species pose challenges for these studies as they often require expensive and time-consuming molecular analyses for species identification. Our data suggested that multivariate models of body and otolith morphometric features can provide a robust and cost-effective alternative to molecular methods for discriminating the cryptic juveniles of *Lutjanus erythropterus* and *L. malabaricus*. Among the eight body morphometric variables recorded, the most parsimonious model contained just three variables (dorsal fin length, distance from the jaw to the eye, and either jaw length or distance from the jaw to the preoperculum) with a species classification accuracy of 98.81%. Despite the nearly total discrimination of the *L. erythropterus* and *L. malabaricus* juveniles with few body variables, visual identification is still not reliable. For example, the study conducted by Elliott (1996) determined that 68% of juvenile fish which were visually classified as *L. malabaricus* were genetically identified as *L. erythropterus*. This highlights the robustness of the multivariate morphometric approach described herein to discriminate these cryptic juveniles as an alternative to visual identification or the high cost and time-consuming molecular method.

Higher allocation success rates were achieved by the body morphometric model compared to the otolith morphometric model (98.81% of the former as opposed to 84.88% of the latter). The prediction rate of the otolith model was also lower than those of previous studies that examined otolith morphometrics to distinguish adult fishes (i.e. above 95%; Chapter 2; Wakefield et al., 2014; Zischke et al., 2016). The lower prediction rates in this study suggests that variations in otolith shape occur later in life, and the otolith morphometric approach may not be as effective for juveniles as it is for adults. A similar conclusion was reached in Chapter 2 of this thesis, where the average fish length of misclassified specimens was significantly smaller than those of the correctly classified specimens. The length range of fish in the current study was 60 to 200 mm FL. The otoliths of commercially important species are often routinely collected for fishery assessment purposes and related biological studies. While adult otolith models can be applied to discriminate among species from the archived collections, molecular approach using DNA from otoliths would provide more accurate discrimination among juveniles if body morphometrics were not recorded prior to dissection. Accurate species identification of the juveniles of *L. erythropterus* and *L. malabaricus* is particularly important where these species comprise part of the bycatch of significant fisheries. The juveniles of both species have been found in the bycatch of commercial prawn trawl vessels (Fry et al., 2009; McPherson et al., 1992). If the commercial prawn trawl fleets operate over broad areas, there

is a need for ongoing monitoring and assessment of nearshore exploitation levels to determine if any management mitigation measures are required in these fisheries.

Spatial variation in the otolith morphology of *L. malabaricus* was evident in the CAP plots, as well as by the improved species prediction accuracy when the region factor was taken into account in these models. Spatial subdivision among populations of individuals have been identified in a range of different teleost species (Elliott et al., 1995; Jemaa et al., 2015; Longmore et al., 2010). They are likely to be attributed to potentially restricted connectivity and limited movements. Spatial subdivision is likely to be influenced by a range of environmental factors, such as water temperature and dissolved oxygen, as well as diet components, which impact growth patterns of otoliths (Campana & Casselman, 1993; Thomas et al., 2014; Zhuang et al., 2015). Therefore, spatial variation in otolith morphology has been applied as a proxy for stock structure. Indeed, Elliott (1996) identified significant genetic heterogeneity of *L. malabaricus* between the populations sampled in the Pilbara region of WA, the Gulf of Carpentaria and the east coast of QLD, suggesting the presence of multiple stocks across northern Australia. Salini et al. (2006) identified shared stocks of *L. erythropterus* between the Gulf of Carpentaria and western Indonesia, however there have been no studies examining the potential for genetic stocks of *L. erythropterus* in the northwest and northeast coasts of Australia. No *L. erythropterus* samples were collected from QLD in this study, so a comparison of spatial variation between WA and QLD could not be undertaken. Further studies are required to collect more samples of both species over a broader spatial scale to incorporate spatial variation across a species distribution for otolith morphometric models.

In conclusion, this study successfully validated robust species identification models for the cryptic juveniles of *L. erythropterus* and *L. malabaricus* on the east and west coasts of Australia. The near total discrimination of these species highlighted the reliability of the body morphometric approach, a viable alternative to time-consuming and expensive molecular analyses. Morphometric analyses also hold a wide range of applications. For instance, given the very high species prediction accuracy of the models with as few as three body morphometric variables, species discrimination of these two cryptic juveniles has the potential to be applied to *in-situ* for stereo-video based studies (Cappo et al., 2003; Harvey & Shortis, 1995). Otolith morphometric models can also be applied to identify prey teleost species in dietary studies (Bowen, 2000; Gales, 1988; Škeljo & Ferri, 2012). Further, spatial comparisons of otolith morphometric datasets can potentially indicate stock structure or population subdivision, which is valuable information that can contribute to informing fisheries management arrangements. Our findings indicate that the spatial variation in the otolith morphometric data of *L. malabaricus* between the east and west coasts of Australia signifies population separation (i.e. no mixing). However, this needs to be investigated further. Data

and analyses described herein provide the basis for further studies to examine the stock structure of this species. No spatial variation was found in the body morphometric models, suggesting the application of this model is appropriate to a broad range of their distribution.

Chapter 4 Development of predator specific blocking primers for *Lutjanus erythropterus* and *L. malabaricus*; implication for DNA metabarcoding dietary studies on the fishery important red snappers

4.1 Abstract

DNA metabarcoding is being increasingly used in dietary studies due to its high sensitivity to detect digested prey at high taxonomic resolution (i.e. species level). However, prey DNA can be undetected when PCR favours the amplification of the higher quality predator DNA over partially digested prey DNA. Annealing inhibiting blocking primers were designed specifically for *Lutjanus erythropterus* and *L. malabaricus* to overcome this challenge. The blocking primers consist of the 3' end of the Fish16S forward primer and predator-specific sequences, which selectively binds to the target predator sequences, and a 3'-Spacer-C3-CPG at the 3' end to inhibit its amplification. *In-silico* examination determined that the number of mismatched bases between the blocking primers and potential prey sequences of 65 species (Family Apogonidae, Carangidae, Clupeidae, Gerreidae, Labridae, Leiognathidae, Mullidae and Terapontidae) ranged between one and eight. Given prey species could be co-blocked with as little as four mismatches, relative read abundance may be biased, and thus quantitative analyses are limited in the downstream bioinformatics. *In-vitro* examination determined the optimal annealing temperature (58 °C) and ratio of blocking primer to the Fish16S primer (10:1) in PCR reactions. The application of the blocking primers during PCR significantly suppressed the amplification of *L. erythropterus* and *L. malabaricus* DNA, and successfully detected prey fish sequences.

4.2 Introduction

The diet composition of fishery targeted species provides an understanding of their trophic links, niche requirement and ecosystem functions, which are important considerations for ecosystem-based management (Lynam et al., 2017; Plagányi et al., 2014). Traditional methods

used in dietary studies include *in-situ* feeding observation and visual identification of gut contents (Cox, 1994; Nagelkerken et al., 2009; Pratchett, 2005). DNA metabarcoding is being increasingly applied in the past decade due to its notable advantages, such as the ability to identify small and/or digested prey species at high taxonomic levels (Deagle et al., 2007; Siegenthaler et al., 2019; Sousa et al., 2019; Valentini et al., 2009). DNA metabarcoding simultaneously generates millions of copies of DNA sequences of digested prey from predators' gut contents or faeces, and matches them against barcode sequences in databases to reveal the taxa of consumed species (Razgour et al., 2011; Sousa et al., 2019). One of the major advantages is the high taxonomic resolution. Most prey items in predators' stomachs are partially digested and difficult to identify at low taxonomic levels (i.e. species and genus) using traditional gut content analysis, whereas metabarcoding is capable of detecting prey DNA and assigning them to species from low gastrointestinal tracts, or even from faecal samples (Berry et al., 2017; Casey et al., 2019). The technique is also advantageous to identifying very small prey items or soft bodied prey taxa which can be quickly digested and are difficult to identify visually (Jarman et al., 2013; McInnes et al., 2017). For these reasons, this method lends itself to more comprehensive evaluation of dietary studies at a much finer-scale (Casey et al., 2019; Leray et al., 2019).

In contrast, a challenge with DNA-based diet studies is when polymerase chain reactions (PCR) preferentially amplify non-target sequences, such as parasite, bacteria and host (i.e. predator) DNA, and subsequently prevent, or bias the sequences of prey DNA (Leray et al., 2013; Su et al., 2017; Vestheim & Jarman, 2008). For example, DNA templates of gastrointestinal samples often contain high-quality predator DNA. PCR miss the low-abundance sequences of degraded prey DNA in the early cycles and become dominated by predator DNA. Consequently, prey DNA sequences are not represented.

This issue can be resolved in some cases by applying taxa-specific primers for the targeting taxa, which do not bind to non-targeted, predator DNA (Harper et al., 2005; Jarman et al., 2004, 2006). However, taxa-specific primers cannot discriminate between them if target and non-target taxa are phylogenetically similar, or if a universal primer is required due to a large or unknown range of target species. In such cases, predator DNA can be subtracted by applying a predator-specific blocking primer along with a universal primer. One of the blocking primer types that was developed by Vestheim and Jarman (2008) is an annealing inhibiting blocker, which has been demonstrated to be effective at suppressing predator DNA during PCR. It consists of the 3' end of forward or reverse universal primer, followed by predator-specific sequences which selectively bind on predator DNA. The 3' end of the blocking primer contains a modified DNA oligonucleotide, such as 3'-Spacer-C3-CPG (C3 spacer), which creates

distance between an oligonucleotide and the conjugated modification, thus inhibits polymerases and exonucleases of the non-targeted predator DNA (Vestheim & Jarman, 2008). Annealing inhibiting blockers with C3 spacer have been applied in several metabarcoding dietary studies and successfully identified prey DNA sequences (Deagle et al., 2009; Leray et al., 2013; Vestheim et al., 2011).

As a part of the ecological component of this thesis, DNA metabarcoding analyses were carried out to investigate the diet composition of sympatric red snappers (*Lutjanus erythropterus* and *L. malabaricus*) which are important to fisheries across their distributional range in Indo-Pacific regions. The preliminary study was confronted by the DNA template issue, where the sequencing data contained only the predator sequences even when obvious prey fish tissue from other species was found in their stomachs. Therefore, we developed an annealing inhibiting blocker (hereafter, blocking primer) specific for each host species (*L. erythropterus* and *L. malabaricus*) and examined the efficacy and optimal PCR protocols through *in-silico* and *in-vitro* experiments.

4.3 Materials and Methods

4.3.1 Blocking primer design

Predator-specific blocking primers (*Lutjanus erythropterus* blocking primer (LEBP) and *L. malabaricus* blocking primer (LMBP)) were designed to suppress the amplification of DNA of *L. erythropterus* and *L. malabaricus*, respectively, and amplify prey fish DNA using the Fish16S primer. The Fish16S primer was used in this study to target teleost sequences at 16S rRNA mitochondrial gene region due to the richness of the reference database in the regions (Nester et al., 2020). LEBP and LMBP consisted of: 1) the 10 bases of the 3' end of Fish16S forward primer; 2) the 15 bases that were specific to each of the host sequences; and 3) a 3'-Spacer-C3-CPG at the 3' end (Table 4.1). The first 25 bases bind to the host sequences, and C3 CPG inhibits its elongation and thus amplification during a PCR. C3 SPG was chosen among various types of modifications to ensure the effectiveness in blocking as it is 100% synthesized and appears to be stable (i.e. no enzymatic impurities freeing the 3' hydroxyl group after synthesis) (Vestheim & Jarman, 2008).

Table 4.1. The Fish16S primer and the host-specific blocking primer sequences (LEBP, *Lutjanus erythropterus* blocking primer; LMBP, *L. malabaricus* blocking primer). The first 10 base pairs of the blocking primers (bold and italic font) overlap with the 3' end of the forward Fish16S primer, followed by 15 base pairs of the host specific sequences. The C3 spacer at the 3' end is a modified DNA oligonucleotide, which inhibits annealing

Primer	Primer sequence (5' – 3')	Reference
Fish16S (forward)	GACCCTATGGAG <i>CTTTAGAC</i>	Berry et al. (2017)
Fish16S (reverse)	CGCTGTTATCCCTADRGTA <i>ACT</i>	Deagle et al. (2007)
LEBP	<i>AGCTTTAGAC</i> ACCAAGGCAGACCAT / C3 /	This study
LMBP	<i>AGCTTTAGAC</i> ACCAAGGCAGAACAT / C3 /	This study

4.3.2 *In-silico* examination

In-silico examination of 16S ribosomal RNA (rRNA) sequences was conducted to validate that the blocking primers would only inhibit the amplification of host-DNA and not prey-DNA. The 15 base pairs of the designed blocking primers needed to be host-specific and different from prey sequences. A total of 65 species of fish (at the order- or family-level) were listed as potential prey in the diet of the two snapper species based on Salini et al. (1994). Eighty reference sequences of the 65 species were available from the Western Australian fish database (Nester et al., 2020). *Sardinops sagax* was also included in the potential prey list even though its sequence were not available from this in-house database because it is commonly used as a bait in the trap fisheries in Western Australia (Newman et al., 2011). For *S. sagax*, all the 40 available reference sequences from the NCBI reference database (downloaded 10 July 2017) were tested against the blocking primers. The software Geneious 10.2.3 was used for all alignments (Drummond et al., 2010).

4.3.3 *In-vitro* examinations

The first *in-vitro* pilot study was conducted to test the optimal annealing temperatures and concentration of the blocking primers. Firstly, DNA was extracted from the fin clips of two *L. malabaricus* using DNeasy Blood & Tissue Kits following the manufacturer's protocol (QIAGEN, CA, USA) to provide a high-quality template for downstream amplification. Quantitative PCR (qPCR) was carried out on these DNA extracts, using the three PCR mixtures containing different amounts of LMBP. Three different annealing temperatures (50, 54, and 58 °C) were also tested for each of the PCR mixtures, provided Berry et al. (2017) determined the optimal temperature for the Fish16S primer to be 54 °C. All PCR mixtures contained 2 µL of DNA extract and 23 µL of PCR mastermix, which consisted of 2 µL of 25mM MgCl₂ solution (Applied Biosystems, CA, USA), 2.5 µL of 10x Taq Gold buffer

(Applied Biosystems), 1 μL of 10mg/ml Bovine Serum Albumin (Fisher Biotec, WA, Australia), 1 μL each of forward and reverse the Fish16S primer (10 μM), 0.25 μL of 25mM dNTPs (Astral Scientific, NSW, Australia), 0.6 μL of 1/10,000 SYBR Green dye (Life Technologies, CA, USA), and 0.2 μL of Taq polymerase Gold (Applied Biosystems). Different amounts of LMBP were added to each of the PCR mixtures to test their efficacy; 1 μL of 100 μM LMBP (10 times higher than the Fish16S primer), 1 μL of 200 μM LMBP (20 times higher than the Fish16S primer), and no blocking primer. Ultrapure water was added to the PCR mixture to bring the reaction volume up to 23 μL per sample. qPCRs were performed in 25 μL reaction volumes containing 2 μL of DNA extract and 23 μL of PCR mastermix using a StepOnePlus Real-Time PCR System (Applied Biosystems), using the following cycling program: (i) 95 $^{\circ}\text{C}$ for 5 minutes, (ii) 45 amplification cycles of 95 $^{\circ}\text{C}$ for 30 seconds, (iii) three different annealing temperatures (50, 54, and 58 $^{\circ}\text{C}$) for 30 seconds, and (iv) 72 $^{\circ}\text{C}$ for 45 seconds, and (v) a final extension step at 72 $^{\circ}\text{C}$ for 10 minutes. Cycle threshold (C_t) values were recorded from the amplification curves and compared to assess the efficiency of the blocking primer. Two-way analysis of variance (ANOVA) was used to test the significance of the two factors (the amounts of LMBP added and annealing temperature) on the average C_t values using the software RStudio (v.1.0.143, <https://rstudio.com/>) (RStudio Team, 2016). Based on these results, downstream PCRs were carried out with the PCR reaction containing 10 times more blocking primer than the Fish16S primer (1 μL of 100 μM blocking primer to 1 μL of 10 μM the Fish16S primer in each PCR reaction), with an annealing temperature of 58 $^{\circ}\text{C}$.

The second *in-vitro* pilot study was carried out on the mock samples containing host- and prey-DNA mixed at different ratios. Firstly, qPCR was carried out with the DNA extracted from the fin clips of *L. erythropterus*, *L. malabaricus*, and *S. sagax* using the Fish16S primer without blocking primers. The relative concentrations of their DNA templates were estimated using their C_t values. DNA extracts were added to create the mock samples with different ratios of prey- to host-DNA (1:1, 1:100, 1:1000, and 10:1). The mock samples were amplified with and without blocking primers and sequenced each with unique six to eight base pair multiplex identifier (MID) tags in duplicate. Unique combinations of forward and reverse MID tags allowed us to assign sequences to a sample after metabarcoding the pooled samples. Single-end sequencing was performed for the pooled amplicons using an Illumina MiSeq platform in the Trace and Environmental DNA (TrEnD) Laboratory at Curtin University in Western Australia, following manufacturer's protocols. Version 2 reagent kit and either Standard or Nano flow cell were used for 300 – 500 cycles.

The fin clip of *L. erythropterus* and *L. malabaricus* for the above *in-vitro* examinations were obtained from the specimen collected for Chapter 5 from the Pilbara region of northwestern Australia using demersal trawls. *S. sagax* was sourced from a local recreational fishing shop sold as baits.

4.3.4 Bioinformatics

The sequencing output files were downloaded in FASTQ format, and assigned to samples by finding sample-specific MID tags and gene-specific primers using the DNABarcodes package in R (Buschmann, 2017). Sequencing adapter, MID tags, and 16SFish primers were annotated and trimmed. Sequences were dereplicated and singletons were removed, which were then assigned to the query sequences of either *L. erythropterus*, *L. malabaricus*, or *S. sagax* in the NCBI GenBank nucleotide reference databases and the Western Australian fish database (Nester et al., 2020), based on percentage similarities scores with a minimum of 98% identity matching.

4.4 Results

The results of the *in-silico* study showed that the number of base pairs mismatched with the blocking primers ranged between 1 and 8 (Figure 4.1). On average 3.3 ± 1.29 (SD) base pairs and 3.99 ± 1.23 base pairs mismatched with host-specific regions of LEBP and LMBP, respectively. None of the prey sequences matched the blocking primers with 100% fidelity.

The mean C_T values of *L. malabaricus* DNA template qPCR were significantly higher when LMBP was applied in the PCR mixture (two-way ANOVA; $F_{(2,17)} = 173.55$, $p < 0.001$) whereas there was no difference between the LMBP to Fish16S ratio of 10 to 1 and 20 to 1 (Figure 4.2). This indicates that LMBP effectively reduced the amplification of *L. malabaricus* DNA but adding extra LMBP did not improve the effectiveness. The annealing temperature had no significant effect on C_T values (two-way ANOVA ; $F_{(2,17)} = 4.39$, $p = 0.05$), and there was no significant interaction between the two factors (two-way ANOVA ; $F_{(4,17)} = 1.69$, $p = 0.24$) (Figure 4.2).

Both LEBP and LMBP effectively inhibited the amplification of host-DNA and increased the chance of detecting DNA of *S. sagax* when the prey-host DNA ratios were 1 to 1, 1 to 100, and 10 to 1 (Figure 4.3). When the *L. erythropterus* DNA was 1000 times higher than the *S. sagax* DNA, LEBP was no longer able to suppress the amplification of host-DNA to detect the prey DNA (Figure 4.3).

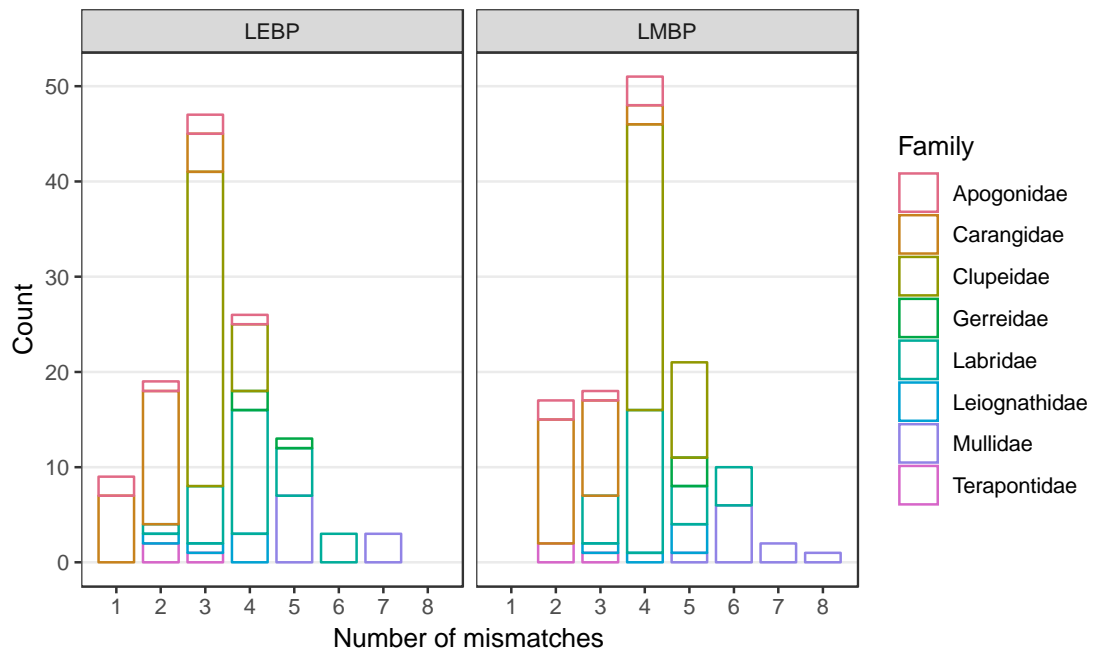


Figure 4.1 Frequency histogram of the number of base pairs mismatched with *Lutjanus erythropterus* blocking primer (LEBP) (left) and *L. malabaricus* blocking primer (LMBP) (right), based on *in-silico* examination of 16S ribosomal RNA (rRNA) sequences.

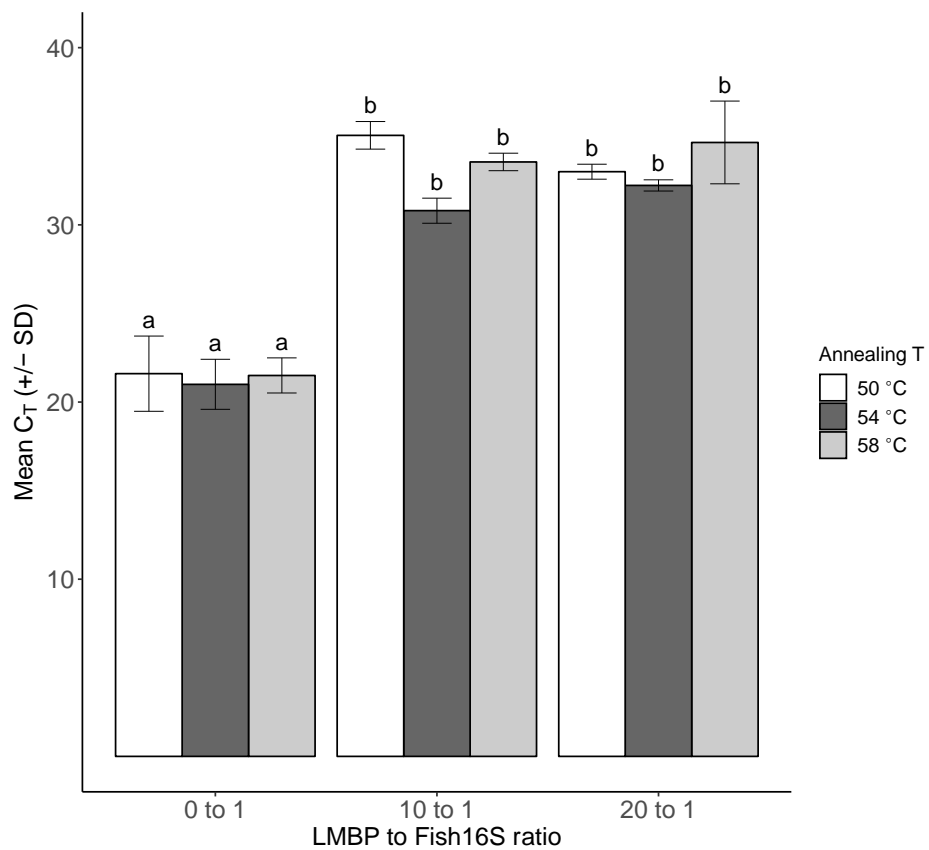


Figure 4.2 Mean C_T values (\pm SD, standard deviation) at different amounts of *Lutjanus malabaricus* blocking primer (LMBP) and annealing temperatures. The ratio on the x-axis refers to the ratio of LMBP to the Fish16S primer added into the PCR master mix. Letters above each bar imply statistically similar means for C_T values.

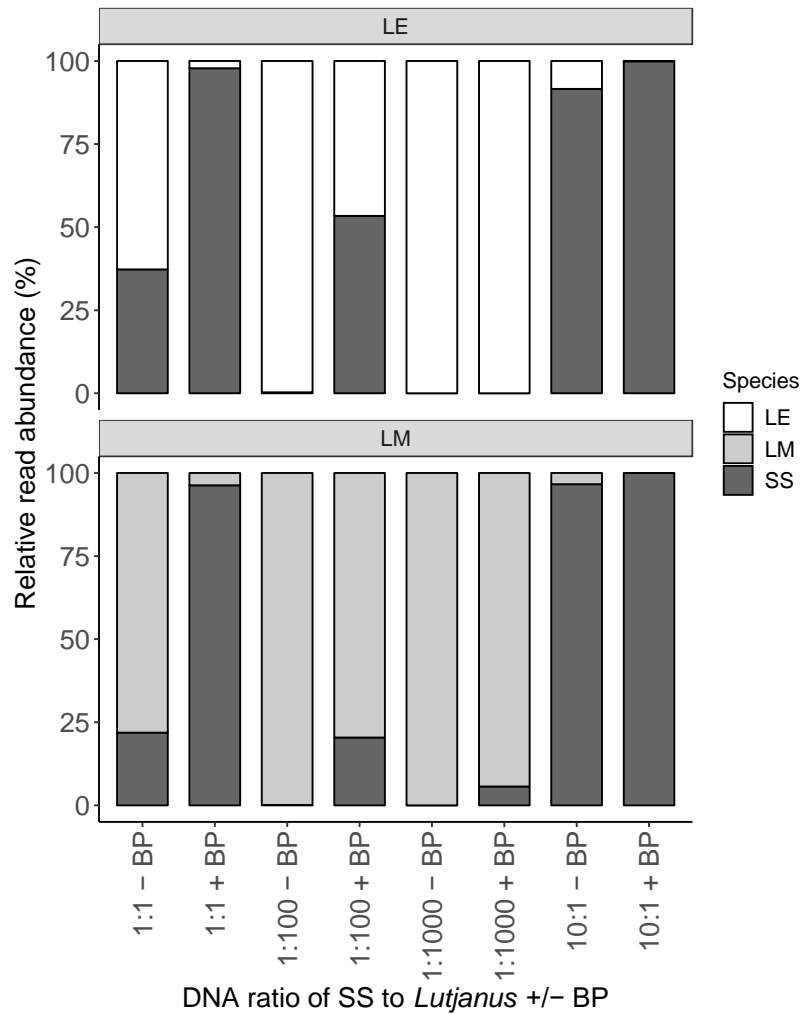


Figure 4.3 Relative read abundance of prey (*Sardinops sagax*) and host (*Lutjanus erythropterus* and *L. malabaricus*) DNA with/without blocking primers. The ratio on the x-axis refers to the DNA ratio of prey to host in the template. Negative and positive symbols indicate mastermixes without and with blocking primer, respectively. SS, *S. sagax*; LE, *L. erythropterus*; LM, *L. malabaricus*; BP, blocking primer.

4.5 Discussion

Metabarcoding is being increasingly applied as a tool to study diets in the past decade (Sousa et al., 2019). Application of blocking primers are necessary in some cases where higher quality predator DNA dominates PCR and masks degraded prey DNA. In this study, predator-specific annealing inhibiting blocking primers were developed specifically for *L. erythropterus* and *L. malabaricus*. The application of the blocking primers resulted in the increased C_T values and reduced relative read abundance (RRA) of predator sequences, which clearly indicated the effectiveness of the blocking primers to inhibit the amplification of the predator DNA during PCR.

Both *L. erythropterus* blocking primer (LEBP) and *L. malabaricus* blocking primer (LMBP) consisted of 10 base pairs which overlap with the 3' end of the forward the Fish16S primer, followed by 15 base pairs of the host specific sequences, and the C3 spacer at the 3' end. The optimal ratio of the blocking primer to the Fish16S primer was 10:1 as further increase in the ratio to 20:1 did not improve the efficacy to inhibit the amplification of predator DNA. This design and optimal ratio were comparable to those developed and applied in previous studies for other organisms, including krill (Vestheim & Jarman, 2008), seal (Deagle et al., 2009) and various species of teleost (Leray et al., 2013; Su et al., 2017), all of which also effectively blocked the predator sequences.

The *in-vitro* study did not identify the effect of annealing temperature on the blocking primers performance. Optimal annealing temperature is specific to each primer, depending on its length and compositions (Chen et al., 2003; Kämpke et al., 2001). For instance, higher the percentage of guanine-cytosine (GC) content is, higher the annealing temperature is. This is because the GC base pair is held by three hydrogen bonds, resulting in higher thermal stability, and thus requiring higher annealing temperature, compared to adenine-thymine (AT) base pair with two hydrogen bonds. The GC-contents of the Fish16S primer with and without a blocking primer were consistent at approximately 50%, whereas the number of bases had almost doubled with the blocking primer. Due to the increased length, a higher annealing temperature (i.e. 58 °C) is suggested to use when applying the blocking primer, compared to the optimal temperature for the Fish16S primer alone (54 °C; Berry et al., 2017).

The *in-silico* examination identified that the number of bases mismatched with BP ranged between 1 and 8, with the average of 3.3 and 3.99 base pairs for LEBP and LMBP respectively. These findings provide important considerations to be taken in the downstream bioinformatics, particularly in the aspect of quantitative analyses. None of the prey sequences matched the blocking primers with 100% fidelity, suggesting that the blocking primers should block the host-DNA and would not interfere with the amplification of target prey-DNA. However, Piñol et al. (2015) suggested that blocking primers could co-block prey species with as little as four mismatches during PCR reactions, suggesting a bias in prey sequence counts, and thus the limitation of a quantitative analysis. Studies using metabarcoding, including dietary studies, can interpret the relative read abundance (RRA) as a proxy for relative abundance of taxa based on positive correlations between RRA and independent measures of abundance (Deagle et al., 2019; Deagle & Tollit, 2007; Leray & Knowlton, 2015). On the other hand, presence/absence (PA) transformation of sequence reads is also commonly applied in eDNA studies due to the various sources of RRA bias, such as differences in template DNA abundance, marker choice, and the different states of digestion of prey material (Berry et al.,

2017; Deagle et al., 2019; Pompanon et al., 2012). Given these limitations, particularly driven by our blocking primers, it is likely that RRA will not be a reliable proxy for relative abundance, and thus PA data should be analysed when applying LEBP and LMBP.

In conclusion, the predator-specific blocking primers successfully suppressed the amplification of *L. erythropterus* and *L. malabaricus*. The findings suggest that 1) the optimal concentration of the blocking primers is 10-fold higher than the Fish16S primer, 2) the optimal annealing temperature is 58 °C, and 3) the final sequence data should be treated as an occurrence instead of RRA. While the optimal concentration was consistent with previous studies, it is essential to carry out such examinations each time when a new blocking primer is developed as optimal protocols and efficacy can vary between primers.

Chapter 5 Partitioning of diet between species and life history stages of sympatric and cryptic snappers (Lutjanidae) based on DNA metabarcoding

5.1 Abstract

Lutjanus erythropterus and *L. malabaricus* are sympatric, sister taxa that are important to fisheries throughout the Indo-Pacific. Their juveniles are morphologically indistinguishable (i.e. cryptic). A DNA metabarcoding dietary study was undertaken to assess the diet composition and partitioning between the juvenile and adult life history stages of these two lutjanids. Major prey taxa were comprised of teleosts and crustaceans for all groups except adult *L. erythropterus*, which instead consumed soft bodied invertebrates (e.g. tunicates, comb jellies and medusae) as well as teleosts, with crustaceans being notably absent. Diet composition was significantly different among life history stages and species, which may be associated with niche habitat partitioning or differences in mouth morphology within adult life stages. This study provides the first evidence of diet partitioning between cryptic juveniles of overlapping lutjanid species, thus providing new insights into the ecological interactions, habitat associations, and the specialised adaptations required for the coexistence of closely related species. This study has improved our understanding of the differential contributions of the juvenile and adult diets of these sympatric species within food webs. The diet partitioning reported in this study was only revealed by the taxonomic resolution provided by the DNA metabarcoding approach and highlights the potential utility of this method to refine the dietary components of reef fishes more generally.

5.2 Introduction

Reef fish communities are extraordinarily diverse (Sale, 1978), and there is often partitioning of resources, particularly for food and habitat, between sympatric reef fishes (Longenecker, 2007; Nagelkerken et al., 2009; Prochazka, 1998). This ecological process, called niche partitioning, is fundamental for the coexistence of species within an ecosystem (Gause, 1934). Niche partitioning is especially relevant among species of the same genus, which may include

cryptic and sympatric species, because the more similar the co-existing species are, the more intensively they presumably compete (Nagelkerken et al., 2009; Prochazka, 1998; Razgour et al., 2011). Niche partitioning within the same species is also a common strategy in reef fish in order to minimise intra-specific competition and can be associated with ontogenetic movements relative to life history stages. Indeed, the life cycle of many reef fishes consists of a pelagic larval stage, followed by a demersal juvenile stage on shallow, low-relief substrate (e.g. mangrove and seagrass nurseries), and an adult stage on deeper, high-relief reefs (Dahlgren & Eggleston, 2000; Fry et al., 2009). Ontogenetic dietary shifts were previously identified in a number of snapper species (family Lutjanidae) (Rooker, 1995; Usmar, 2012; Wells et al., 2008), suggesting that habitat partitioning between juvenile and adult fish was based not only on finding refuge from predation, but also for accessing food resources (Cochelet de la Morinière et al., 2003; Szedlmayer & Lee, 2004).

Lutjanus erythropterus (Bloch, 1790) and *L. malabaricus* (Bloch & Schneider, 1801) are sympatric snapper species that coexist in the tropical and subtropical Indo-Pacific region (Allen, 1985). They are sister taxa (Frédérich & Santini, 2017), and the juveniles are phenotypically cryptic (Fry et al., 2009). Both species support important commercial and recreational fisheries on tropical and subtropical coasts throughout their geographic distribution (Allen, 1985; Blaber et al., 2005). Diet compositions of fishery targeted species at all life history stages and their ecological interactions are important considerations for ecosystem-based fisheries management (Crowder & Norse, 2008; Thrush & Dayton, 2010). Due to their similarities in morphology, ecology, and the nature of their fisheries, they are often categorised as “red snappers” and are combined into a single species group within catch data in some parts of the world (Blaber et al., 2005; Leigh & O’Neill, 2016). Moreover, despite their importance to fisheries, little is known about their ecological interactions and niche partitioning (Blaber et al., 2005; Newman & Williams, 1996; Salini et al., 1994). Common dietary items visually identified from stomach contents in previous studies include crustaceans, teleosts and cephalopods (Brewer et al., 1991; Salini et al., 1994). Despite the length range of *L. erythropterus* and *L. malabaricus* examined in these dietary studies being from 38 to 570 mm, the diet partitioning between the species and life history stages has never been examined.

Understanding dietary partitioning between morphologically similar species, such as *L. erythropterus* and *L. malabaricus*, requires precise dietary analysis methods because these two predators are likely to be ecologically similar and exhibit subtle, if any, differentiation (Longenecker, 2007; Nagelkerken et al., 2009; Razgour et al., 2011). Previous studies identified high levels of dietary overlap between some of the coral-feeding, sympatric

butterflyfishes (family Chaetodontidae) using an *in-situ* feeding observation method (Cox, 1994; Pratchett, 2005). Niche overlap and coexistence are possible when the population sizes are not limited by the availability of shared resources. However, Nagelkerken et al. (2009) identified clear dietary partitioning between 21 species of butterflyfish by visually examining their gut contents, whereas other methods (*in-situ* feeding observations and stable isotope analyses) did not detect such partitioning. These conflicting results suggest that some dietary analysis methods may lack the resolution needed to detect distinct, and sometimes subtle, differences in diet (Nagelkerken et al., 2009; Pompanon et al., 2012). Species-level identification of prey items is now possible through the use of DNA metabarcoding (Deagle et al., 2007; Siegenthaler et al., 2019; Valentini et al., 2009). DNA metabarcoding simultaneously generates millions of copies of DNA sequences of digested prey from predators' gut contents or faeces, and matches them against barcode sequences in databases to reveal the taxa consumed species (Razgour et al., 2011; Sousa et al., 2019). This method lends itself to more comprehensive evaluation of dietary partitioning of sympatric, cryptic species at a much finer-scale (Casey et al., 2019; Leray et al., 2019).

In this study, we conducted metabarcoding-based dietary analyses to assess the diet composition of juvenile and adult *L. erythropterus* and *L. malabaricus*. We hypothesised that there would be significant dietary partitioning between species to reduce inter-specific competition. Dietary partitioning relating to developmental stage is also a reasonable explanation for coexistence by reducing intra-specific competition through ontogenetic habitat shifts, which have been previously observed in other lutjanid species (Cocheret de la Morinière et al., 2003; Rooker, 1995; Szedlmayer & Lee, 2004; Usmar, 2012; Wells et al., 2008). With the aid of DNA metabarcoding, we expected to identify a variety of prey taxa at lower taxonomic levels to test these hypotheses. Information on how diet varies between sister taxa and life history stages will improve our understanding of the ecological processes allowing them to coexist in marine ecosystems.

5.3 Materials and methods

5.3.1 Sample collection

Samples of juvenile and adult *L. erythropterus* and *L. malabaricus* were caught using demersal trawls from the Pilbara region of northwestern Australia (Figure 5.1, see trawl net configuration in Wakefield et al. (2007)). The use of this fishing method mitigated the potential for fish to consume bait during capture, which may confound natural diet compositions. In addition, to reduce potential biases that may be associated with temporal and spatial variations in diet composition, juveniles and adults were sampled from the same trawl catches. However,

considering juveniles and adults occupy different habitats for both species, the two life stages were sampled within as close a proximity as practical. Juvenile *L. erythropterus* and *L. malabaricus* (99 to 201 mm total length, TL) were sampled during a research survey from depths of 9-24 m within a nearshore marine embayment (i.e. Nicol Bay) in July and August 2017 (Table 5.1 & Figure 5.1). Concurrently, catches of adult *L. erythropterus* and *L. malabaricus* (482 to 795 mm TL) taken by commercial fishers using demersal fish trawls in 52-58 m depth and ~60 km directly offshore from where the juveniles were sampled (Table 5.1 & Figure 5.1), were labelled and kept separate from the rest of the catch before collection approximately three days later by research staff. All fish samples were frozen whole (-20 °C) prior to dissection under laboratory conditions to avoid potential contamination. The TL of each fish was measured to the nearest 1 mm.

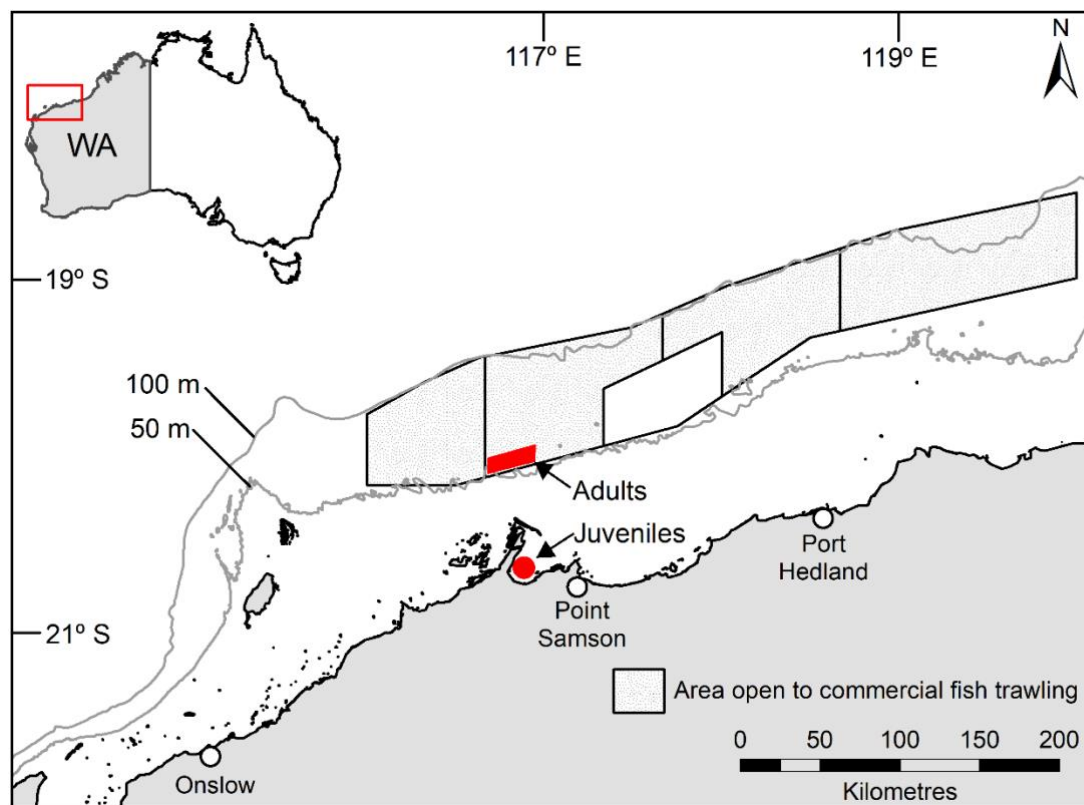


Figure 5.1 Locations where juvenile and adult samples of *Lutjanus erythropterus* and *L. malabaricus* were collected in the Pilbara region of northwestern Australia (generated using ArcMap v10.3.1, <https://desktop.arcgis.com>). Areas open to commercial fish trawling (shaded) and the 50 m and 100 m depth contours (grey lines) are shown.

Table 5.1 Number of juvenile and adult *Lutjanus erythropterus* (LE) and *L. malabaricus* (LM) for each category of sampling variables. Fullness of stomach was recorded as “full” when a prey item was observed in a stomach. Sampling details such as time and depth were not available for each adult specimen as trawl shot numbers were not recorded for individual fish. TL, total length.

Variables	Levels	Juvenile		Adult	
		LE (n=11)	LM (n=11)	LE (n=11)	LM (n=12)
Fullness of stomach	Empty	8	4	10	7
	Full	3	7	1	5
TL (mm)	50 - 100	1	0		
	100 - 150	9	8		
	150 - 200	1	2		
	200 - 250	0	1		
	450 - 500			3	
	500 - 550			8	
	550 - 600				1
	650 - 700				6
	700 - 750				1
	750 - 800				4
Date	14 Jul 2017	6	6		
	13 Aug 2017		1		
	18 Aug 2017	5	4	11	12
Time	00:01 - 03:00		1		
	06:01 - 09:00	1			
	09:01 - 12:00	1	2		
	15:01 - 18:00	3	3		
	18:01 - 21:00	6	2		
	21:01 - 24:00		3		
	03:30 - 22:40			11	12
Depth (m)	8.1 - 9	1			
	9.1 - 10		1		
	10.1 - 11		2		
	11.1 - 12	7	4		
	12.1 - 13	3	3		
	23.1 - 24		1		
	52 - 58			11	12

5.3.2 Species identification of cryptic juveniles

Considering juveniles of *L. erythropterus* and *L. malabaricus* are cryptic, fin clips were collected and stored in 99% ethanol to genetically identify the species via DNA barcoding. DNA of the tissues was extracted, diluted 1/10, and amplified following the “HotSHOT” technique described by Meeker et al. (2007). Polymerase chain reaction (PCR) was performed using FishBCH forward primer (5'-ACTTCYGGGTGRCCRAARAATCA -3') and FishBCL reverse primer (5'-TCAACYAATCAYAAAGATATYGGCAC-3') to target 600 to 800 bp of the cytochrome c oxidase subunit I (COI) region of the mitochondrial DNA. The PCR cycling program used was: (i) 94 °C for 4 minutes, (ii) 35 amplification cycles of 94 °C for 30 seconds, 50 °C for 30 seconds, and 72 °C for 60 seconds, and (iii) a final extension step at 72 °C for 10 minutes. Following amplification, 4 µL of amplicons were loaded onto a 2% agarose gel, and the gel image was analysed under UV light using a Bio-Rad transilluminator and GelRed nucleic acid staining dye (Molecular Probes) to ensure the successful amplification at the targeted size. DNA with no signature on the gel image was further diluted 1/25, re-amplified, and visualised on a gel. Two µL of exonuclease I and FastAP thermosensitive alkaline phosphatase were added to 10 µL of the PCR product and purified using the following thermocycler cycling program; (i) 37 °C for 15 minutes, (ii) 80 °C for 15 minutes, and (iii) 4 °C for 10 minutes. The purified amplicons were shipped to Macrogen for Sanger Sequencing (Macrogen Facility, Seoul, Korea) in the forward direction. Sequencing data were queried against the National Center for Biotechnology Information (NCBI) GenBank nucleotide reference database (Benson et al., 2017) and the Western Australian fish database (Nester et al., 2020) using the nucleotide Basic Local Alignment Search Tool (BLASTn) (Altschul et al., 1990). All sequences were assigned to either *L. erythropterus* or *L. malabaricus* based on percentage similarities scores.

5.3.3 Gastrointestinal tract content dissection

Juvenile and adult *L. erythropterus* and *L. malabaricus* (n = 13 for each species and life history stage) were thawed at room temperature prior to measurement and dissection. New, sterile surgical blades and gloves were used for each fish, and other dissection utensils were cleaned using bleach and ethanol and exposed to UV for a minimum of 20 minutes between each sample to minimise cross-contamination. Entire gastrointestinal tracts (GIT) were removed from host fish. Intestinal content was collected in a separate sample container. Intestinal contents were used instead of stomach contents in this study as non-prey tissues might have been ingested during trawl capture events. Fullness of stomach was recorded in binary format – “full” or “empty” if prey items were present or absent, respectively (Table 5.1).

5.3.4 DNA extraction

Each intestinal content sample of adult fish was homogenised using Omni Hard Tissue Tip homogeniser, and between 150 and 250 mg of homogenised content was subsampled into a 5 mL tube. Homogenising and subsampling steps were omitted for juvenile intestinal samples due to the low volume of material obtained from each juvenile fish. DNA from the GIT sample was extracted using QIAamp PowerFecal DNA Kits following the manufacturer's instructions. This extraction kit was used in this study as it was designed to effectively remove PCR inhibitors often present in gut content and faecal samples. DNA extraction controls consisting of the extraction reagents, but no samples were processed concurrently for each set of extractions.

5.3.5 Amplification and sequencing

DNA extracts of intestinal contents were amplified and sequenced separately for each sample. In order to determine the optimal dilution of DNA extracts specific to each sample and each primer, quantitative PCR (qPCR) was performed on the neat and 1/10 dilution of DNA extracts with a range of universal and taxa-specific primers (Table 5.2), and amplification efficiency and inhibition was examined by the C_T values and amplification curves. qPCR was performed following the PCR mixture formula and cycling program described in Berry et al. (2019), except for the PCR mixture containing the Fish16S primers. One μL of species-specific blocking primers developed in Chapter 4 (LMBP or LEBP, depending on the host species) (100 μM) was added into the PCR mixture containing the Fish16S primers to suppress the amplification of host DNA.

For metabarcoding using an Illumina MiSeq platform (V2 chemistry), fusion PCRs were then performed on DNA extracts (with appropriate DNA input determined by qPCR) for each fusion primer with MID tags – these PCRs followed the same reaction conditions and cycling program used in qPCR. To detect and minimise contamination, undiluted extraction controls, as well as the PCR controls containing the PCR mixture with no DNA extracts were also amplified with the MID tags of each primer during the fusion PCR. Each sample was run in duplicate with the same MID tag to mitigate PCR stochasticity and ensure a sufficient concentration of amplicons was available for library pooling and quantitation. DNA library preparation and sequencing were performed, following the technique described in Berry et al. (2019). All the laboratory procedures were carried out in the Trace and Environmental DNA (TrEnD) Laboratory at Curtin University in Western Australia.

Table 5.2 List of primers targeting genes of potential prey items of *Lutjanus erythropterus* and *L. malabaricus*, and host-specific blocking primer (LEBP, *Lutjanus erythropterus* blocking primer; LMBP, *L. malabaricus* blocking primer). The first 10 base pairs of the blocking primers overlap with the 3' end of the forward Fish16S primer (bold and italic font), followed by 15 base pairs of the host specific sequences. The C3 spacer at the 3' end is a modified DNA oligonucleotide, which inhibits annealing. Minimum length of each primer is the threshold length used for quality filtering of sequences. T, annealing temperature; F, forward primer; R, reverse primer.

Primer name	Primer sequence (5' - 3')	Target taxa	Target gene	T (°C)	Product size (bp)	Minimum length (bp)	Reference
18SUni (F)	GCCAGTAGTCATATGCTTGTCT	Universal	18S	52	350-420	200	Pochon et al. (2013)
18SUni (R)	GCCTGCTGCCTTCCTT						Pochon et al. (2013)
SCeph (F)	GCTRGAATGAATGGTTTGAC	Cephalopods	16S	50	90-110	50	Peters et al. (2014)
SCeph (R)	TCAWTAGGGTCTTCTCGTCC						Peters et al. (2014)
SCrust (F)	GGGACGATAAGACCCTATA	Crustaceans	16S	51	140-190	100	Berry et al. (2017)
SCrust (R)	ATTACGCTGTTATCCCTAAAG						Berry et al. (2017)
Fish16S (F)	GACCCTATGG <i>AGCTTTAGAC</i>	Teleosts	16S	58	200	100	Berry et al. (2017)
Fish16S (R)	CGCTGTTATCCCTADRGTAACT						Deagle et al. (2007)
LMBP	<i>AGCTTTAGACACCAAGGCAGACCAT</i> / C3 / <i>L. malabaricus</i>		16S	58	N/A	N/A	Chapter 4
LEBP	<i>AGCTTTAGACACCAAGGCAGAACAT</i> / C3 / <i>L. erythropterus</i>						Chapter 4

5.3.6 Quality filtering of sequence reads and taxonomic assignment to prey taxa

The sequencing output files were downloaded in FASTQ format, and assigned to samples by finding sample-specific MID tags and gene-specific primers using the DNABarcodes package in R (Buschmann, 2017). Sequencing adapter, MID tags, and gene-specific primers were annotated and trimmed. Quality filtering was run on the trimmed sequences using DADA2 R package (Callahan et al., 2016) with the following criteria: 1) removal of reads shorter than primer-specific minimum length thresholds (Table 5.2), and 2) removal of reads with the number of expected errors more than 1 for single-end reads and the forward reads of paired-end sequences, and 2 for reverse reads of paired-end sequences. Higher maximum number of expected errors (maxEE; less stringent cut-off) was allowed for reverse reads of paired-end sequences because the quality of reverse reads is generally poorer than those of forward reads in Illumina paired-end sequencing technology (Bolger et al., 2014; Wangenstein & Turon, 2017). Indeed, the quality profile plots produced in the DADA2 pipeline demonstrated that our reverse reads had lower quality scores towards the end of the cycles compared to forward reads (Figure S 5.1). Filtered sequences were dereplicated and singletons and chimeric sequences were removed. Paired end sequences were merged with the minimum overlap of 20 bases. Denoised, exact sequence variants constructed using this protocol are called amplicon sequence variants (ASVs) (Callahan et al., 2017). ASV tables were created for each primer (Callahan et al., 2017), and a BLASTn search was carried out against the NCBI GenBank nucleotide reference databases and the Western Australian fish database (Nester et al., 2020) to assign ASVs to taxa (Benson et al., 2017), allowing 100% coverage matching and a minimum of 95% identity matching.

The reference sequences with the highest identity matching to query sequences were called primary reference sequences. When the difference between the percent identity matches of primary and non-primary reference sequences was more than a set similarity threshold, the non-primary reference sequences were omitted. In other words, the threshold defined the maximum difference between the percent identity matches of primary and non-primary reference sequences allowed in the lowest common ancestor (LCA) assignment algorithm. The threshold of 0, 1 and 2% were used initially to examine how the threshold selection would affect the results of our study. 0% threshold provided the highest proportion of taxonomic assignments, whereas 1 and 2% thresholds provided equivalent taxonomic assignments (Table S 5.1-A). The statistical significance of diet partitioning patterns remained unchanged with different thresholds (Table S 5.1-B & C). Following these comparisons, the 1% threshold was selected primarily because it reduced potential artefact taxa and was no different to the 2%

threshold assignments. When there was more than one species assigned to an ASV, the taxonomic level was dropped to lower levels (i.e. genus, family) in order to assign the LCA. For instance, if one unique ASV was assigned to multiple species from the same genus, it was assigned to the genus of those species. If the assigned species were from different genera but the same family, the taxonomic assignment was dropped to the family level. When the taxonomic level of LCA was Class or above, the ASV was removed. The LCA assignment was performed using the script developed by Mousavi et al. (2021).

Terrestrial fauna, flora and fungi (e.g. human, flowering plants) were considered to be environmental contaminants and removed from the list of the assigned taxa. The following marine taxa were also assumed to be non-prey items and removed from the list of prey taxa; parasitic organisms commonly found on fish, algae, dinoflagellates, ciliates, unicellular flagellate eukaryotes, and the host species. Three ASVs were detected from extraction controls using the 18SUni primers. Two of them (both assigned to *Penaeus vannamei*) were only detected from one control sample and not from any of the intestine samples, whereas one ASV (assigned to family Pomacanthidae using LCA) was detected in all five extraction controls as well as all intestine samples using the 18SUni primer, accordingly, the ASV was removed from the prey item list.

5.3.7 Data analyses

The number of samples and sequencing depth were examined to inspect whether our sampling and sequencing efforts were sufficient to capture the majority of their potential prey taxa (see Supplementary 5.6.1 ‘Assessment of sampling and sequencing depth’, Figure S 5.2, Figure S 5.3 and Figure S 5.4). The mean number of reads and prey taxa obtained from each life history stage and species were compared using analysis of variance (ANOVA).

Studies using metabarcoding, including dietary studies, can interpret the relative read abundance (RRA) as a proxy for relative abundance of taxa based on positive correlations between RRA and independent measures of abundance (Deagle et al., 2019; Deagle & Tollit, 2007; Leray & Knowlton, 2015). On the other hand, presence/absence (PA) transformation of sequence reads is also commonly applied in eDNA studies due to the various sources of RRA bias, such as differences in template DNA abundance, marker choice, and the different states of digestion of prey material (Berry et al., 2017; Deagle et al., 2019; Pompanon et al., 2012). RRA data generated with universal primers, including the 18SUni primer used in this study, are particularly biased due to the mismatches in the primer binding regions and amplification of diverse multi-template mixtures including non-target species, such as unicellular eukaryotes (Elbrecht & Leese, 2015; Piñol et al., 2015). Furthermore, Piñol et al. (2015) suggested that

blocking primers could co-block non-target species with as little as four mismatches during PCR reactions, suggesting the limitation of a quantitative analysis. Given these limitations in quantitative approaches, we carried out multivariate analyses using PA data only, while further study using RRA might be possible using other primers and a more controlled experimental design. Jaccard coefficient matrices were constructed from the LCA table with PA datasets (Clarke et al., 2014). The difference in the diet compositions between the species and life history stages were statistically tested using two-way permutational multivariate analysis of variance (PERMANOVA) with 9999 permutations, followed by pairwise PERMANOVA due to a significant interaction term. Fullness of the stomach was incorporated in PERMANOVA as a covariate to test whether the diet composition was affected by the timing of recent feeding events and fish sampling. The similarity matrices were visualised using Canonical Analysis of Principal Coordinates (CAP) ordination plot (Anderson & Willis, 2003). Allocation success rates on CAP plots were estimated using the “leave-one-out” approach. Trace and delta canonical test statistics were also obtained using 9999 permutations in order to support the results of PERMANOVA. Distance-based linear model (DistLM) analysis was undertaken in order to test the interaction effects between sample variability and diet composition of juvenile fish. The factors tested in DistLM included species and TL, and various sampling factors such as time, date and depth of sampling (Table 5.1). Detailed sampling information is not available for adult fish samples as trawl shot numbers were not recorded for individual fish, thus DistLM was not carried out for the adult fish samples. BEST routine and Akaike Information Criterion values for finite sample sizes (AICc) were used to select the most parsimonious combination of variables that best explained the diet data (Clarke et al., 2014). The above multivariate analyses were conducted using the software PRIMER 7 (v. 7.0.13, <https://www.primer-e.com/>) (Clarke et al., 2014). All figures were produced using RStudio (v.1.0.143, <https://rstudio.com/>) (RStudio Team, 2016).

5.4 Results

A total of 9,389,741 reads were obtained from 45 intestinal samples of juvenile and adult *L. erythropterus* and *L. malabaricus* using four metabarcoding primers selected to profile prey items. A total of 7,166,024 reads (accounting for 76% of the total reads) remained after quality filtering. These reads were dereplicated to a total of 1,244 ASVs; 863 ASVs were assigned to taxa, and 179 ASVs were considered as potential primary prey items, which consisted of 37 unique prey taxa (Figure 5.2 & Table S 5.2).

The number of sequence reads varied between samples, ranging from 3,385 to 301,747 reads. The mean number of reads obtained from each life history stage and species were significantly

different (ANOVA: $F_{3,41} = 11.6$, $p < 0.001$), juvenile *L. erythropterus* had a significantly higher number of reads than all other groups (Figure S 5.2-A). The mean number of prey taxa were not significantly different between the groups, ranging from 2.18 (± 0.87 SD) to 3.67 (± 2.23 SD) (ANOVA: $F_{3,41} = 1.31$, $p = 0.28$) (Figure S 5.2-B). There was no correlation between the number of reads and the prey taxa assigned (Pearson's correlation: $t_{43} = 0.13$, $p = 0.90$). These non-significant results cumulatively indicate that the sequencing effort did not affect the number of prey taxa identified from the intestinal content despite some differences in read depth. This finding was also supported by rarefaction curves, where most curves plateaued between 1000 and 5000 reads, suggesting that sequencing depth was sufficient for our samples to detect the average number of ASV and prey items within a primer (Figure S 5.3). Therefore, no rarefaction or sequence subsampling was applied to our dataset for further analyses. By contrast, species accumulation curves did not reach a plateau with the number of samples collected for this study, indicating that more prey taxa might have been identified with more sample replicates (Figure S 5.4).

Species level assignment was achieved for 57% of the prey taxa, whereas 43% were dropped from species to higher taxonomic levels using the LCA assignment algorithm; 19%, 16%, and 8% at genus, family, and order levels respectively (Table S 5.1-A). Up to three species from the same genus were assigned to each ASV with the LCA taxa level of genus (Table S 5.2). When LCA taxa levels are family and order, up to 10 and 30 species, respectively, were assigned to the ASV(s) (Table S 5.2). ASVs with the LCA of Decapoda (order) were assigned to the total of 30 species from 14 families, with the percentage similarities ranging between 96.68 and 100% (Table S 5.2). The prey taxa consisted of 6 phyla (Chordata, Arthropoda, Cnidaria, Ctenophora, Annelida and Mollusca), and they were further categorised into eight general diet categories; (i) teleosts, (ii) malacostracan crustaceans, which includes crabs, prawns, mantis shrimps and mysid shrimps, (iii) copepods, (iv) medusa including hydrozoa and scyphozoa that have a free-swimming medusa stage at one point of their life cycle, (v) tunicates, (vi) comb jellies, (vii) polychaetes, and (viii) cephalopods. The majority of the prey taxa were from the groups of teleost and malacostraca (most of which are from the order Decapoda), accounting for 27% and 45% of the total taxa found, respectively (Figure 5.2). Two of the 37 assigned taxa (accounting for 5% of the total taxa detected) were shared across all the four groups all of which were teleosts; Pomacanthidae and *Labrus bergylta* (Figure 5.2). Pomacanthidae, the angelfish family, was the most common prey taxa across both species and life stages with high occurrence rates (Figure 5.2). Pomacanthidae was the lowest common ancestor (LCA) of 10 species, indicating that multiple species of Pomacanthidae might have been consumed (Table S 5.2). Importantly, 27 out of the 37 assigned taxa (accounting for 73%) were not shared and occurred in only one of the four groups (Figure 5.2).

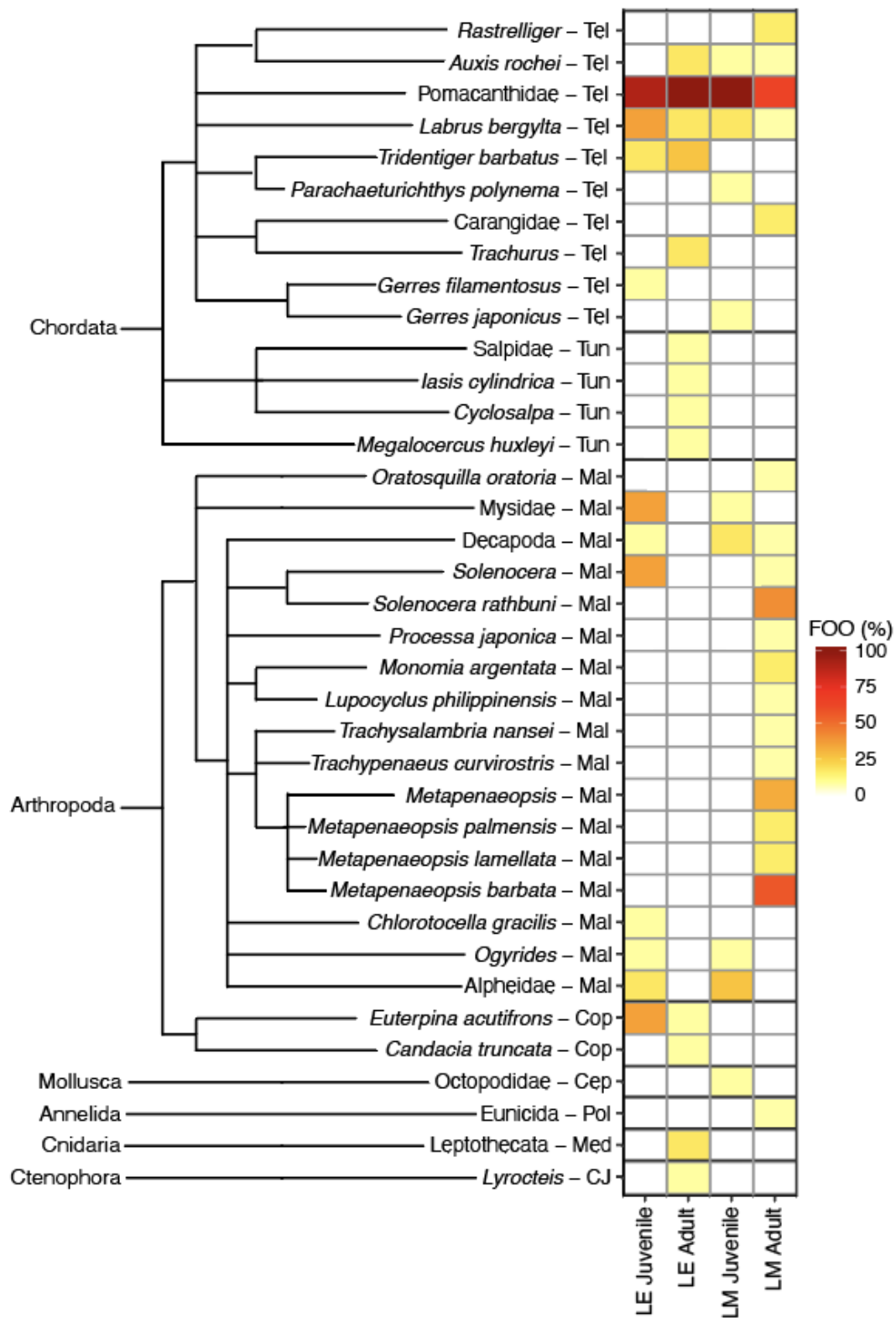


Figure 5.2 Frequency-of-occurrence (FOO) (%) of prey taxa identified in the intestinal contents of juvenile and adult *Lutjanus erythropterus* (LE) and *L. malabaricus* (LM). Two to three letters at the end of the taxa names refers to general diet categories; Tel, teleost; Tun, tunicate; Mal, malacostracan crustacean; Cop, copepod; Cep, cephalopod; Pol, polychaete; Med, medusa; CJ, comb jelly.

Diet compositions were significantly different between the species and their life history stages (PERMANOVA: $p < 0.01$ and < 0.001 respectively, Table 5.3-A). The effect of stomach fullness on diet composition was not significant (PERMANOVA: $p = 0.12$, Table 5.3-A). The interaction between the two factors was significant, indicating that the partitioning patterns were not consistent within each factor (PERMANOVA: $p < 0.01$, Table 5.3 – A). Pairwise PERMANOVA identified the significant inter-specific dietary partitioning within each of the life history stages ($p < 0.05$ within juvenile, $p < 0.05$ within adult; Table 5.3-B) and significant intra-specific partitioning within each of the species ($p < 0.05$ within *L. erythropterus*, $p < 0.01$ within *L. malabaricus*; Table 5.3-B).

Table 5.3 The results of PERMANOVA (A) and pairwise-PERMANOVA (B) testing the differences in diet composition of juvenile and adult *Lutjanus erythropterus* (LE) and *L. malabaricus* (LM), using 9999 permutations. Fullness of stomach was incorporated into the analyses as a covariate to test its effect on diet composition. The tests were based on Jaccard coefficient matrix for presence and absence (PA) datasets.

A. PERMANOVA

	df	SS	F Model	p
Species	1	6416	2.40	<0.01
Life stage	1	7667	2.87	<0.001
Fullness of stomach	1	3820	1.43	0.12
Sp x Life stage	1	8071	3.02	<0.01
Residuals	40	106770		

B. Pairwise-PERMANOVA

		df	t	p
Inter-specific	Within Juvenile	19	1.50	<0.05
	Within Adult	20	1.43	<0.05
Intra-specific	Within LE	19	1.43	<0.05
	Within LM	20	1.99	<0.01

The two canonical test statistics also identified the significant differences in the diet compositions among the four groups ($p < 0.001$ and < 0.01 for trace and delta statistics, respectively, with 9999 permutations), supporting the results of PERMANOVA. The squared canonical correlations of the first and second canonical axes were 0.82 and 0.73. The CAP

analysis included 12 PCO axes ($m = 12$), which achieved the maximum proportion of correct allocations (64%). Leave-one-out allocation success rate ranged from 45% to 82%; The juveniles of both *Lutjanus erythropterus* and *L. malabaricus* achieved higher allocation success rates (82%) compared to adults (45 % and 50 % for *Lutjanus erythropterus* and *L. malabaricus* respectively) (Table S 5.3). The majority of the misclassified samples were allocated to juvenile *L. malabaricus*. The partitioning of diet compositions among the four groups was also evidenced by the observations of each group clustering together on the plot of the first two canonical axes (Figure 5.3).

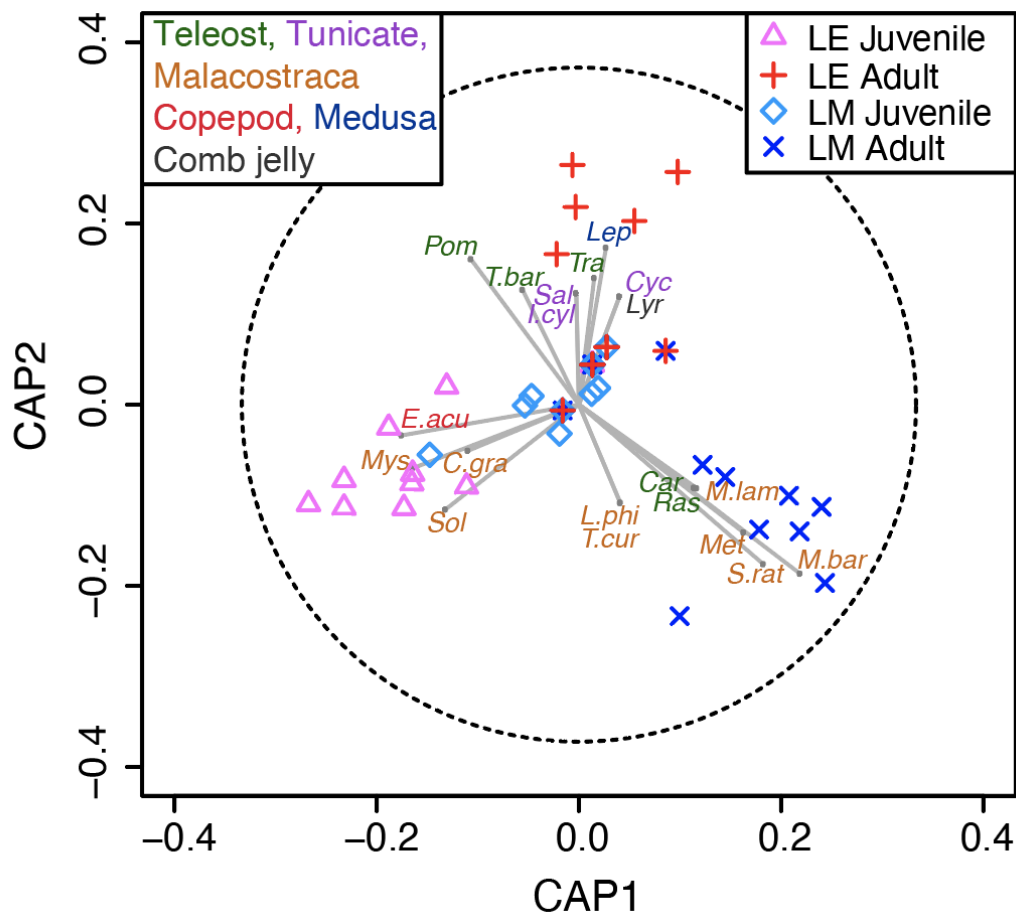


Figure 5.3 Canonical Analyses of Principal Coordinates (CAP) ordination plots of prey assemblage data from intestinal contents of adult and juvenile *Lutjanus erythropterus* (LE) and *L. malabaricus* (LM), using Jaccard coefficient matrix of presence and absence (PA) data. The overlaid vectors are the Pearson correlations of prey taxa with the two canonical axes, which had the correlation coefficient higher than 0.3. The circle in CAP indicated the correlation coefficient of 1. The closer the vector reaches to the circle, the higher the correlation coefficient is. The first three characters of the taxa names were displayed if the taxa were assigned to genus or higher levels. The first character of genus and three characters of species names are displayed if the taxa were assigned to the species level. Colour of the taxa labels indicate the functional categories.

DistLM identified significant effects of species on juvenile diet composition, whereas other sampling variables such as TL, depth, time, and date of sampling were not significant as interaction effects (Table S 5.4-A). This finding indicates that the inter-specific dietary partitioning patterns are unlikely to be confounded by other sampling variables. BEST analyses identified that the most parsimonious model describing the diet composition was the model with species as a single variable, which supports the DistLM marginal test results (Table S 5.4 – B).

Diet composition of adult *L. malabaricus* was unique from those of other 3 groups, mainly characterised by the following three factors. Firstly, prey richness was the highest with the total number of prey taxa at 19, whereas those of other groups were between 10 and 13. Secondly, their diet was strongly characterised by a high richness and frequency-of-occurrence of malacostracan taxa (Figure 5.2). Thirteen of the 19 prey taxa of adult *L. malabaricus* was malacostracans (accounting for 68%) and all of them except for Decapoda (an order including shrimps and crabs) and *Solenocera* (a genus of prawns) were not shared with the other groups (Figure 5.2). Significant influences of malacostracan crustaceans on the partitioning of adult *L. malabaricus* were also indicated by a number of correlation vectors of malacostracan taxa pointing towards the cluster of adult *L. malabaricus* on CAP plot (Figure 5.3). These taxa include *Metapenaeopsis barbata*, *Metapenaeopsis lamellata*, *Metapenaeopsis* and *Solenocera rathbuni*. frequency-of-occurrence of *S. rathbuni* and *M. barbata* were particularly high, ranging from 42 to 58% (Figure 5.2). Thirdly, the patterns of occurrence of teleost taxa were unique from those of the other three groups. For instance, Pomacanthidae was the most common teleost taxa across all the groups, but the frequency-of-occurrence were relatively low in adult *L. malabaricus* (67%) compared to those of other three groups (between 91 and 100%) (Figure 5.2). In contrast, Carangidae (except *Trachurus*) and *Rastrelliger* were found with 17% frequency-of-occurrence in adult *L. malabaricus* whereas they were not found in other groups (Figure 5.2).

Contrary to the diet of adult *L. malabaricus*, which was dominated by malacostracans, no malacostracans was detected in the intestinal content of adult *L. erythropterus* (Figure 5.2). Diet composition of adult *L. erythropterus* was characterised by teleosts and soft bodied taxa including tunicates, medusa and comb jellies (Figure 5.3). A total of 38% of the prey taxa for adult *L. erythropterus* were teleosts, two of which (Pomacanthidae, *Tridentiger barbatus*) had particularly high occurrence rates (100 and 27% respectively; Figure 5.2).

Juveniles' diet was dominated by teleosts and malacostracans for both *L. erythropterus* and *L. malabaricus*, similar to those of adult *L. malabaricus* (Figure 5.2). Eleven and 10 prey taxa were identified from juvenile *L. erythropterus* and *L. malabaricus*, respectively. For juvenile

L. erythropterus, 36 and 55% of their diet taxa were teleosts and malacostracans respectively, accounting for 91% of their total taxa identified. The following taxa had relatively high frequency-of-occurrence (Figure 5.2) and strong correlations with canonical axis 1 pointing towards the cluster of juvenile *L. erythropterus* observations (Figure 5.3), indicating the high contribution of the partitioning of their diet: *Euterpina acutifrons*, *Chlorotocella graciles*, *Solenocera* and Mysidae. These taxa were either not found or found with a low frequency-of-occurrence in juvenile *L. malabaricus*. For juvenile *L. malabaricus*, 50 and 40% were teleosts and malacostracans respectively. Prey taxa which were unique to *L. malabaricus* juveniles include *Parachaeturichthys polynema*, *Gerres japonicus* and Octopodidae. The frequency-of-occurrence of these taxa were relatively low (9%) (Figure 5.2) thus they were not correlated along CAP axes (Figure 5.3).

5.5 Discussion

Information on dietary partitioning of sympatric and highly valued fisheries species is fundamental to understanding the ecological processes that support their coexistence. High resolution methods are required to assess dietary partitioning of sympatric, cryptic species, such as *L. erythropterus* and *L. malabaricus*, because they are likely to exhibit subtle differentiation due to their ecological similarity (Nagelkerken et al., 2009; Razgour et al., 2011). Dietary studies on juvenile fish have also been particularly challenging due to the relatively low abundance, a limited seasonal window for sample collection corresponding to the recruitment seasons, and difficulty in identifying small-sized prey items using traditional methods (i.e. morphological identification of gut contents). This study was the first molecular based dietary study on juveniles and adults of sympatric, cryptic fish, which revealed clear dietary partitioning patterns between the species and life history stages.

The major prey categories of adult *L. malabaricus* were teleosts and malacostracan crustaceans which includes crabs, prawns, mantis shrimps and mysid shrimps, whereas no malacostracans were identified in the diet of adult *L. erythropterus*. In contrast, the common prey items of adult *L. erythropterus* were teleosts (specifically pomacanthids, jack mackerel and gobies), in combination with a variety of prey from minor dietary categories, including medusae, tunicates and comb jellies. These findings are supported by those of Salini et al. (1994) who also identified a variety of crustaceans from the stomach content of *L. malabaricus*, but not from those of *L. erythropterus*. One of the major factors which constrain and shape diet choice is body morphology such as jaw structure, dentition and body size (Wainwright & Richard, 1995). This ecomorphology theory may assist in explaining the diet specialization of adult *L. erythropterus* and *L. malabaricus* observed in this study, as these species exhibit notable

differences in jaw morphology. *Lutjanus malabaricus* has a longer jaw on average than *L. erythropterus*. One of the common names of *L. malabaricus* and *L. erythropterus* are large-mouth and small-mouth nannygai, respectively which reflect this diagnostic characteristic. In general, length of fish jaws correlates with the volume of their oral cavity and, consequently, the force of suction (Wainwright & Richard, 1995) and diversity of prey that they can successfully feed on (Kwak et al., 2015). The larger mouth of *L. malabaricus* may have increased its feeding capacity, allowing it to prey on a variety of malacostracan crustaceans as observed in the current and previous studies (Salini et al., 1994). In contrast, *L. erythropterus*, with a smaller mouth, may have shifted their choice to other prey categories such as medusae, comb jellies and tunicates, which are much slower swimmers and have softer bodies compared to crustaceans. *Lutjanus malabaricus* possesses a larger mean and maximum body length compared to *L. erythropterus*, which is consistent with previous studies (Fry et al., 2009; Salini et al., 1994) and may have played a role as another ecomorphological factor to differentiate the diet patterns.

Habitat associations also play a role in differentiating diet patterns. For example, *L. malabaricus* is considered a true demersal species. In contrast, *in-situ* observations from underwater video indicate that *L. erythropterus* is benthopelagic (S. Newman, C. Wakefield personal observations). This vertical habitat partitioning concurs with the composition of their prey. The major prey categories of adult *L. malabaricus* were malacostracan crustaceans, which are benthic or epibenthic, and prey categories of adult *L. erythropterus* were composed predominantly of teleosts, medusa, tunicates and comb jellies, some of which generally occupy the water column. These patterns reinforce the idea that diet composition is strongly linked to habitat utilisation, and moreover, diet patterns reflect fine scale partitioning of habitat mosaics between sympatric species.

Another example of the link between habitat association and diet partitioning is the ontogenetic shifts in diet, which was observed in the present studies as well as previous studies on reef fish (Cocheret de la Morinière et al., 2003; Rooker, 1995; Usmar, 2012; Wells et al., 2008). Juveniles of many coral reef fish, including *L. erythropterus* and *L. malabaricus*, occur in shallow, low-relief habitat such as soft sediments and seagrass beds, whereas adults are found on deeper coral reefs (Dahlgren & Eggleston, 2000; Fry et al., 2009). These commonly observed ontogenetic shifts in reef fish diet suggest that life history partitioning is a strategy to provide refuge from predation but also the segregating of resources to minimise intra-specific competition.

While there are previous studies on diet partitioning between life history stages within a species (Cocheret De La Morinière et al., 2003; Szedlmayer & Lee, 2004; Usmar, 2012) or

sympatric fish at the adult stage (Leray & Knowlton, 2015; Nagelkerken et al., 2009), studies on niche partitioning between juvenile fish of closely related species (i.e. sympatric, cryptic, same genus or family) are extremely rare. Examples include a morphological gut content analysis of *Lutjanus* spp. (i.e. snapper) by Pimentel and Joyeux (2010) and a stable isotope analysis of otoliths of *Albula* spp. (i.e. bonefish) by Haak et al. (2019). Although both studies identified significant differences in the measured parameters (diet composition and $\delta_{13}\text{C}$) between species, diet partitioning of the juvenile stage remained unclear. Pimentel and Joyeux (2010) reported that their results might have been confounded by other interspecific variations such as length of juvenile fish. Moreover, the stable isotope measured by Haak et al. (2019) was not a direct measure of diet composition. Our metabarcoding analyses accounted for other variables that might influence diet, such as the length of the fish, fullness of stomachs, time, date and depth of sampling events. The findings indicated that the diet differentiations within the juvenile stage were solely shaped by the individual species and not by other factors examined, providing the first evidence of diet partitioning between cryptic juveniles of lutjanid species. However, although their diet partitioning was statistically significant, there is still a large proportion of variance unexplained. In addition, this differentiation in diet was not as distinctive as those observed within the adult stage, particularly at the level of the general prey category. Contrary to the clear differences in morphology and habitat separation within the adult stage, juveniles of *L. erythropterus* and *L. malabaricus* are visually cryptic and fine scale habitat differentiation has not previously been studied. Further studies are required to better understand niche partitioning mechanisms in juvenile stages of reef fish.

While the interspecific diet compositions of juveniles were analysed with potential confounding factors considered, such analyses were not possible for adult samples due to the lack of detailed sampling information. Furthermore, the sampling period for juveniles spanned over a month, whereas adult samples were collected on one day thus the adults' prey compositions identified in this study represented the "meal" of the day rather than the general diet composition of the species. Given that the interspecific diet partitioning patterns of cryptic juveniles were solely influenced by species and not by other factors including sampling dates, it is likely that the diet partitioning between the morphologically distinctive adults were also shaped by the individual species and not confounding factors. However, further studies with larger sample sizes, an extended sampling period and detailed sampling information across wider geographic ranges are required to resolve this uncertainty.

In the past decade there have been a growing number of studies to assess diets of diverse fauna using DNA metabarcoding approaches due the various advantages associated with this technique. One of the main advantages is the unprecedented level of resolution in prey taxa

detection (Casey et al., 2019; Leray & Knowlton, 2015). Previous dietary studies on predatory fish using traditional morphological methods achieved high levels of resolution for penaeid (prawn) identification whereas few or no prey teleosts (fish) were identified at species and genus levels (Salini et al., 1990; Usmar, 2012). In this study, 57% of the prey taxa identified was to species and 19% to genus. For teleosts in particular, 60% of the 10 teleost taxa were identified at species level. Taxonomic levels were dropped from species to genus or even further when multiple species were assigned to one sequence through the LCA assignment algorithm. This is likely to be the result of a lack of comprehensive reference databases, suggesting that improvement to reference databases can further increase the resolution of prey detection via metabarcoding.

Another notable advantage is the high sensitivity of detection of digested prey items. Most traditional dietary studies using morphological identification approaches only investigate prey items in stomach content (Salini et al., 1994; Usmar, 2012; Wells et al., 2008) as they are less digested compared to those from intestine and faecal samples. However, stomach contents provide snapshots of prey composition based on items that are ingested immediately before being captured, especially for predators with a high digestion rate. In contrast, metabarcoding techniques are capable of identifying highly digested prey taxa, in some cases, from lower gastrointestinal tracts or even from faecal samples (Berry et al., 2017; Deagle et al., 2010). Due to this high level of sensitivity to the detection of highly digested prey, we were able to identify diverse prey taxa from intestinal contents even from individuals with empty stomachs. Furthermore, the fullness of a stomach and sampling time were not significant in the analyses and as such were not influential factors. This study also detected DNA sequences of soft body prey taxa such as comb jellies, tunicates and medusae, possibly due to the increased sensitivity of this method as tissues of soft-bodied taxa can be quickly digested and are difficult to identify visually (Jarman et al., 2013; McInnes et al., 2017). Such advantages and the associated outcomes identified in this study suggest that metabarcoding is a promising tool for dietary studies, particularly to analyse partitioning between closely associated species where fine-scale resolution is required.

Along with the advantages provided by DNA metabarcoding, there are also limitations associated with this technique. A common challenge encountered in molecular based dietary analyses is to extract and amplify prey-DNA since host-DNA is frequently amplified and often masks highly degraded prey-DNA (Su et al., 2017; Vestheim & Jarman, 2008). We were able to overcome these challenges and successfully sequenced prey-DNA by applying host-specific blocking primers which were designed and tested in Chapter 4. Applying the same logic, highly abundant prey DNA may mask the amplification of rare prey sequences during PCR

and make them harder to detect. Another metabarcoding shortcoming is the limited applications for quantitative analyses. For instance, the weight of prey items are often recorded in traditional dietary studies (Brewer et al., 1991; Salini et al., 1994; Wells et al., 2008), however, the utility of relative read abundance (RRA) from metabarcoding data as a proxy for relative abundance of prey taxa is still under debate (Deagle et al., 2010, 2019; Deagle & Tollit, 2007; Leray & Knowlton, 2015). RRA was explored in this study but ultimately deemed to have too many potential flaws – notably, RRA can be particularly biased when blocking primers or universal primers are applied (Piñol et al., 2015), which was the case in our study. Size of the prey item is another piece of information that cannot be confirmed using a metabarcoding approach. Dietary studies using traditional morphological approaches also often reveal how the size of prey items can increase, as the size of the consumer grows from a juvenile to an adult (Cocheret de la Morinière et al., 2003; Usmar, 2012). This is not feasible with metabarcoding data. The prey taxa detected in this study could be from any life history stage including larvae and eggs. Lack of comprehensive DNA databases can lead to the misidentification of prey taxa and/or reduced taxonomic resolution via LCA assignment algorithm. Other sources of metabarcoding limitations include PCR bias (Deagle et al., 2013), missing prey identification due to a lack of its sequence in reference databases (Leray et al., 2012), and the detection of secondary prey (the prey of a prey) (Sheppard et al., 2005).

In conclusion, high resolution dietary studies of sympatric species provide a tool to better understand not only trophic links, but also ecological and evolutionary processes, behaviour, essential habitat associations, and ultimately management strategies. Our dietary studies with metabarcoding approach identified significant differences in diet composition of juvenile and adult *L. erythropterus* and *L. malabaricus*. Firstly, given that our study species are phylogenetically, morphologically and ecologically closely allied forms, our findings provide us with new insights on the specialised adaptations required for the coexistence of closely related species. This study provides the first evidence of diet partitioning between cryptic juveniles of different snapper species. Secondly, this study provides an increased understanding of the dietary preferences of both adults and juveniles of important fishery species. Combined with the close association between diet and habitat, the different diet compositions may imply differential vulnerability to a changing environment. For instance, *L. malabaricus* adults, whose primary diets consisted of benthic malacostracan crustaceans, may be more susceptible to habitat degradation than *L. erythropterus* adults, who predominantly feed on diet items presumably suspended in the water column. Finally, our study highlights the robustness of DNA metabarcoding to detect fine-scale differences in diet between sympatric species, including the detection of soft bodied prey. While this study examined two sympatric species in both juvenile and adult forms, it also facilitates a wider ‘whole of

ecosystem' view of how these species (and their prey) coexist within the wider trophic network. Ultimately, these data may enable more informed fisheries management decisions regarding spatial management arrangements and also how these species may respond to future climatic perturbations. Furthermore, the selection of a range of fish taxa that profile a wide diversity of the ecosystem (via their diet) may form the basis of a monitoring program that extends beyond just fish into whole ecosystem responses.

5.6 Supplementary information

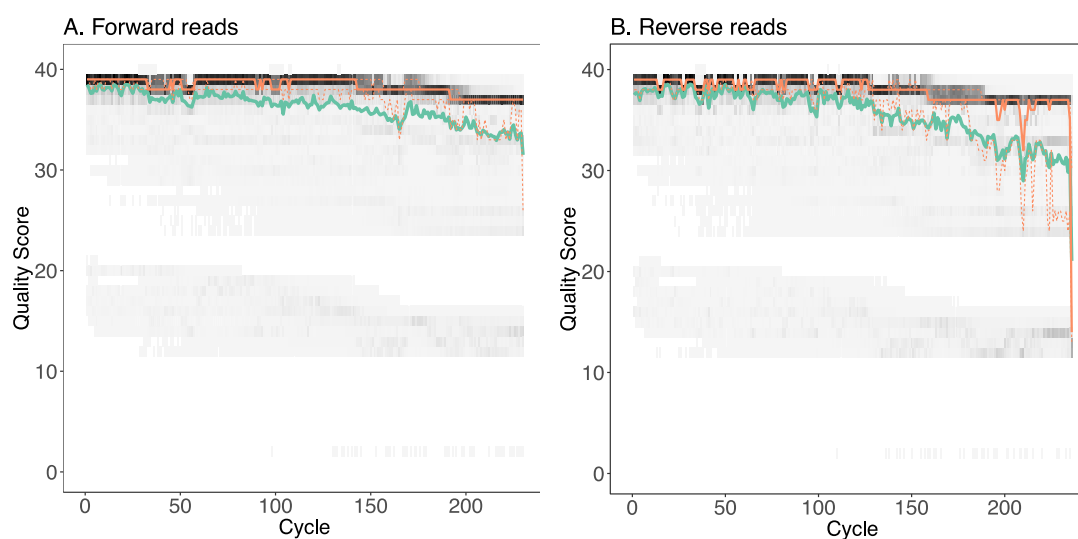


Figure S 5.1 The quality profiles of forward (A) and reverse (B) reads of paired-end sequences. Green line, orange line, and dashed orange lines represent the mean, median, and the 25th and 75th percentiles respectively. A grey-scale heat map represents the distribution of quality scores at each position, with dark colours corresponding to higher frequency. The mean quality scores gradually declined throughout the cycles for forward reads, whereas reverse reads experienced a steeper decline in quality scores approximately after the 100th cycle.

5.6.1 Assessment of sampling and sequencing depth

The relationship between number of reads and prey taxa was examined using Pearson correlation to inspect whether the number of prey taxa detected was affected by sequencing depth. Analysis of variance (ANOVA) was also carried out to test the differences in mean number of reads and prey taxa detected between each group. The assumption of the samples coming from a normal distribution was tested and the number of prey taxa were transformed using a square-root transformation to meet the assumption. Rarefaction curves were plotted describing the diet of each species and life history stage. Random subsampling of sequences was conducted 1000 times at every 1000 reads for each sample, following the approach explained by Colwell (2013), and the total number of ASV and prey taxa detected by subsampling were averaged within the samples of the same group (species and life history stage). Species accumulation curves were plotted to assess whether the number of samples were sufficient to capture the majority of their potential prey taxa consumed by each species and life history stage. The software RStudio (v.1.0.143, <https://rstudio.com/>) was used to carry out statistical analyses and subsampling, and produce plots (RStudio Team, 2016).

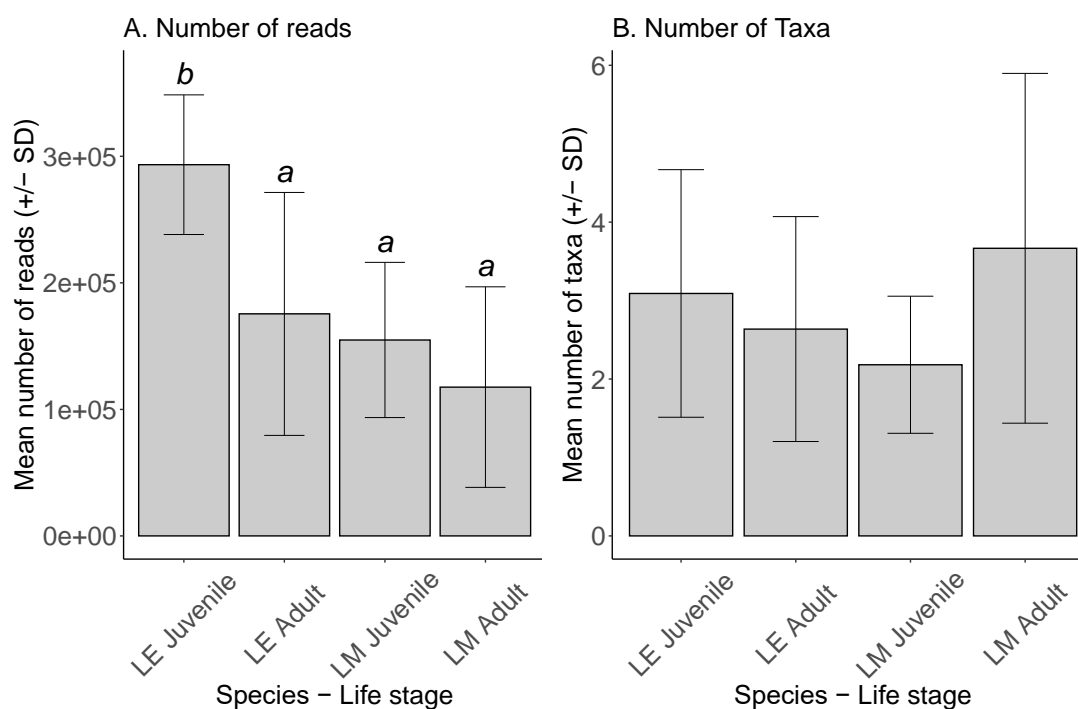


Figure S 5.2 Mean number of reads (A) and mean number of prey taxa (B) (+/- SD, standard deviation) obtained from the intestinal content of adult and juvenile *Lutjanus erythropterus* and *L. malabaricus*. Italics letters above the error bars imply statistically similar means for number of reads.

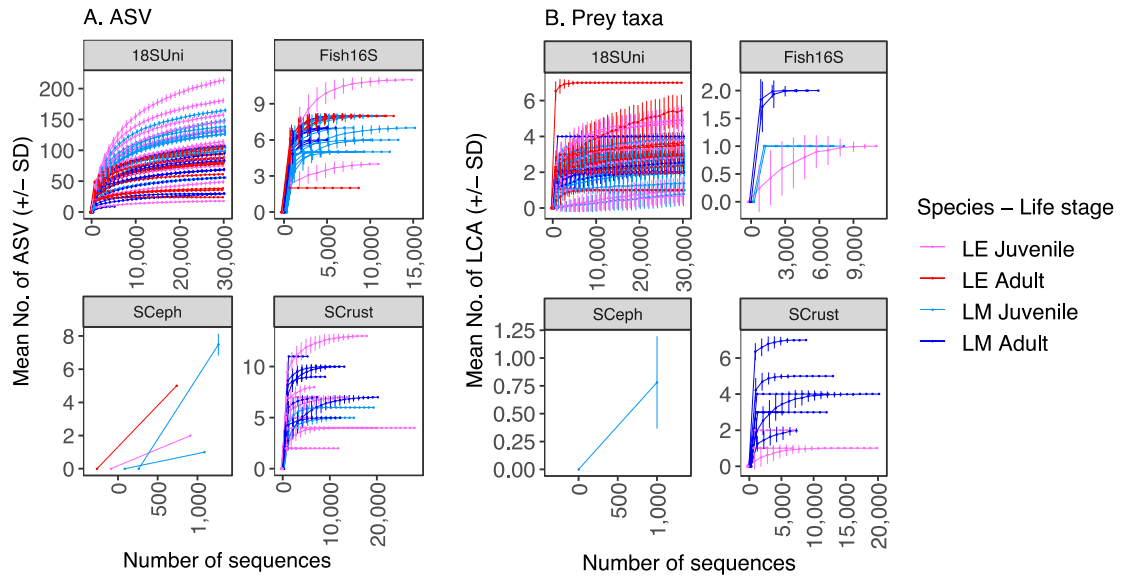


Figure S 5.3 Rarefaction curves of intestinal content samples from a universal (18SUni) and three sets of taxa specific primers (Fish16S, SCrust, and SCeph). The plateaus of the curves indicate the sufficient sequencing efforts to reveal the majority of the detected amplicon sequence variants (ASVs) (A) and prey taxa (B). SD, standard deviation.

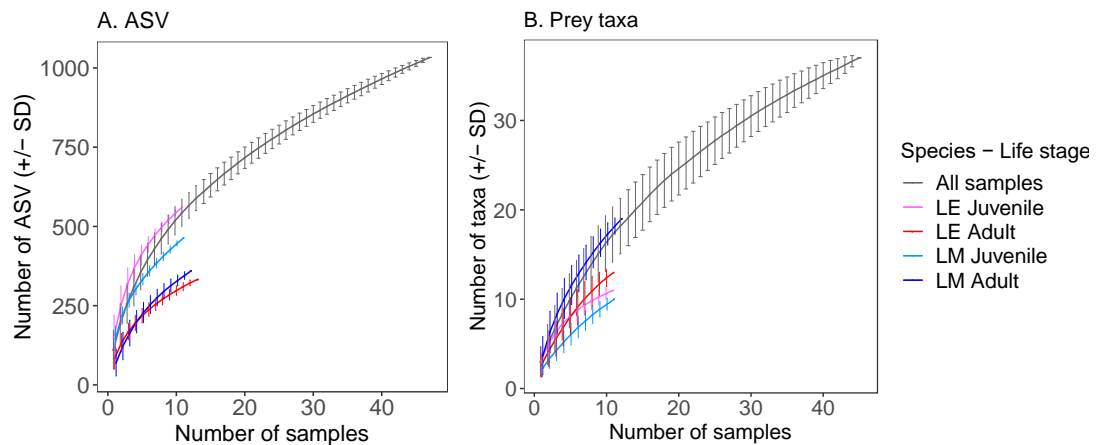


Figure S 5.4 Species accumulation curves of amplicon sequence variants (ASVs) (A) and prey taxa (B) identified from the intestinal contents of adult and juvenile *Lutjanus erythropterus* (LE) and *L. malabaricus* (LM) with all primers combined. SD, standard deviation.

Table S 5.1 Taxonomic assignment (A) as well as the results of PERMANOVA (B) and pairwise-PERMANOVA (C) using different percent identify match thresholds (0, 1 and 2%). The threshold defines the maximum difference between the percent identity matches of primary and non-primary reference sequences allowed in the lowest common ancestor (LCA) assignment algorithm. When the difference between the percent identity matches of primary and non-primary reference sequences was more than the threshold, the non-primary reference sequences were omitted prior to LCA assignment. PERMANOVA (B) and pairwise-PERMANOVA (C) examined the differences in diet composition of juvenile and adult *Lutjanus erythropterus* (LE) and *L. malabaricus* (LM), using 9999 permutations. Fullness of stomach was incorporated into the analyses as a covariate to test its effect on diet composition. The tests were based on Jaccard coefficient matrix for presence and absence (PA) datasets.

A. Taxonomic assignment

Threshold (%)	Number of prey taxa				
	Total	Species level	Genus level	Family level	Order level
0	51	35 (69%)	10 (19%)	4 (8%)	2 (4%)
1	37	21 (57%)	7 (19%)	6 (16%)	3 (8%)
2	37	20 (54%)	8 (22%)	6 (16%)	2 (8%)

B. PERMANOVA

	Threshold (%)	df	SS	F Model	p
Species	0	1	8943	3.14	<0.001
	1	1	6416	2.40	<0.01
	2	1	6314	2.36	<0.01
Life stage	0	1	7715	2.71	<0.01
	1	1	7667	2.87	<0.001
	2	1	7880	2.95	<0.001
Fullness of stomach	0	1	4566	1.60	0.064
	1	1	3820	1.43	0.116
	2	1	3803	1.42	0.122
Species x Life stage	0	1	7954	2.79	<0.01
	1	1	8071	3.02	<0.01
	2	1	8213	3.08	<0.01
Residuals	0	40	113960		
	1	40	106770		
	2	40	106800		

C. Pairwise-PERMANOVA

		Threshold (%)	df	t	p
Inter-specific	Within Juvenile	0	19	1.59	<0.01
		1	19	1.50	<0.05
		2	19	1.50	<0.05
	Within Adult	0	20	1.61	<0.01
		1	20	1.43	<0.05
		2	20	1.40	<0.05
Intra-specific	Within LE	0	19	1.51	<0.05
		1	19	1.43	<0.05
		2	19	1.43	<0.05
	Within LM	0	20	1.83	<0.01
		1	20	1.99	<0.01
		2	20	2.02	<0.01

Table S 5.2 The list of prey taxa as lowest common ancestors (LCA) and number of ASV, species, genus and family which were assigned to the LCA. % match indicates the range of % similarity between each ASV and the reference sequences of assigned taxa. Where LCA taxa level is genus or higher, the species list contains more than one species with a common ancestor.

LCA	LCA level	Primer	No. ASV	No. species	No. genus	No. family	% match	Species list
<i>Rastrelliger</i>	genus	Fish16S	1	2	1	1	99.52 ~ 100	<i>Rastrelliger kanagurta</i> / <i>R. brachysoma</i>
<i>Auxis rochei</i>	species	18SUni	4	1	1	1	98.25 ~ 100	<i>Auxis rochei</i>
Pomacanthidae	family	18SUni	104	10	4	1	95.04 ~ 98.25	<i>Apolemichthys griffisi</i> / <i>Centropyge flavissima</i> / <i>Holacanthus tricolor</i> / <i>Centropyge eibli</i> / <i>C. venusta</i> / <i>C. aurantia</i> / <i>Paracentropyge multifasciata</i> / <i>Holacanthus ciliaris</i> / <i>H. passer</i> / <i>H. africanus</i>
<i>Labrus bergylta</i>	species	18SUni	4	1	1	1	95.75 ~ 98	<i>Labrus bergylta</i>
<i>Tridentiger barbatus</i>	species	18SUni	1	1	1	1	95.01	<i>Tridentiger barbatus</i>
<i>Parachaeturichthys polynema</i>	species	Fish16S	1	1	1	1	97.49	<i>Parachaeturichthys polynema</i>
Carangidae	family	Fish16S	1	2	2	1	100	<i>Decapterus maruadsi</i> / <i>Trachurus novaezelandiae</i>
<i>Trachurus</i>	genus	18SUni	1	2	1	1	95.24	<i>Trachurus mediterraneus</i> / <i>T. trachurus</i>
<i>Gerres filamentosus</i>	species	Fish16S	1	1	1	1	98.04	<i>Gerres filamentosus</i>
<i>Gerres japonicus</i>	species	Fish16S	1	1	1	1	97.17	<i>Gerres japonicus</i>
Salpidae	family	18SUni	2	5	3	1	95.29 ~ 96.34	<i>Ritteriella retracta</i> / <i>Iasis cylindrica</i> / <i>Salpa fusiformis</i> / <i>S. thompsoni</i> / <i>S. maxima</i>
<i>Iasis cylindrica</i>	species	18SUni	1	1	1	1	100	<i>Iasis cylindrica</i>
<i>Cyclosalpa</i>	genus	18SUni	1	3	1	1	99.22 ~ 100	<i>Cyclosalpa sewelli</i> / <i>C. polae</i> / <i>C. affinis</i>
<i>Megalocercus huxleyi</i>	species	18SUni	1	1	1	1	99.47	<i>Megalocercus huxleyi</i>

<i>Oratosquilla oratoria</i>	species	SCrust	1	1	1	1	95.43	<i>Oratosquilla oratoria</i>
Mysidae	family	18SUni	1	5	4	1	95.65 ~ 96.42	<i>Boreomysis arctica</i> / <i>B. tridens</i> / <i>Mysidella typica</i> / <i>Dactylerythrops bidigitata</i> / <i>Rhopalophthalmus sp.</i>
Decapoda	order	18SUni	14	30	25	14	96.68 ~ 100	<i>Daldorfia horrida</i> / <i>Pachygrapsus fakaravensis</i> / <i>Eriphia smithii</i> / <i>E. sebana</i> / <i>E. verrucosa</i> / <i>Portunus trituberculatus</i> / <i>Otmaroxanthus balboai</i> / <i>Pseudocarcinus gigas</i> / <i>Panopeus herbstii</i> / <i>Platyxanthus orbignyi</i> / <i>Pilumnus floridanus</i> / <i>Menippe nodifrons</i> / <i>M. mercenaria</i> / <i>M. adina</i> / <i>Lobopilumnus agassizii</i> / <i>Callinectes sapidus</i> / <i>Carpilius maculatus</i> / <i>Frevillea barbata</i> / <i>Maja crispata</i> / <i>M. brachydactyla</i> / <i>Zaops ostreum</i> / <i>Tritodynamia horvathi</i> / <i>Eriocheir sinensis</i> / <i>Homalaspis plana</i> / <i>Hypothalassia armata</i> / <i>Hexapanopeus angustifrons</i> / <i>Eupilumnus laciniatus</i> / <i>Eriphides hispida</i> / <i>Charybdis japonica</i> / <i>Ozius rugulosus</i>
<i>Solenocera</i>	genus	SCrust	1	2	1	1	95.35	<i>Solenocera crassicornis</i> / <i>S. pectinata</i>
<i>Solenocera rathbuni</i>	species	SCrust	1	1	1	1	98.26	<i>Solenocera rathbuni</i>
<i>Processa japonica</i>	species	SCrust	1	1	1	1	95.91	<i>Processa japonica</i>
<i>Monomia argentata</i>	species	SCrust	1	1	1	1	100	<i>Monomia argentata</i>
<i>Lupocyclus philippinensis</i>	species	SCrust	1	1	1	1	98.28	<i>Lupocyclus philippinensis</i>
<i>Trachysalambria nansei</i>	species	SCrust	1	1	1	1	100	<i>Trachysalambria nansei</i>

<i>Trachypenaeus curvirostris</i>	species	SCrust	1	1	1	1	95.35	<i>Trachypenaeus curvirostris</i>
<i>Metapenaeopsis</i>	genus	SCrust	1	2	1	1	95.93	<i>Metapenaeopsis barbata</i> / <i>M. acclivis</i>
<i>Metapenaeopsis palmensis</i>	species	SCrust	1	1	1	1	98.26	<i>Metapenaeopsis palmensis</i>
<i>Metapenaeopsis lamellata</i>	species	SCrust	1	1	1	1	97.67	<i>Metapenaeopsis lamellata</i>
<i>Metapenaeopsis barbata</i>	species	SCrust	5	1	1	1	95.32 ~ 98.83	<i>Metapenaeopsis barbata</i>
<i>Chlorotocella gracilis</i>	species	SCrust	1	1	1	1	98.13	<i>Chlorotocella gracilis</i>
<i>Ogyrides</i>	genus	18SUni	1	1	1	1	96.72	<i>Ogyrides sp.</i>
Alpheidae	family	18SUni	5	4	2	1	97.47 ~ 98.23	<i>Alpheus packardii</i> / <i>A. lobidens</i> / <i>Alpheidae sp.</i>
<i>Euterpina acutifrons</i>	species	18SUni	2	1	1	1	99.74 ~ 100	<i>Euterpina acutifrons</i>
<i>Candacia truncata</i>	species	18SUni	8	1	1	1	99.47 ~ 100	<i>Candacia truncata</i>
Octopodidae	family	SCeph	1	3	2	1	95.83	<i>Cistopus taiwanicus</i> / <i>Octopus fusiformis</i> / <i>Octopus sp</i>
Eunicida	order	18SUni	4	2	2	2	99.22 ~ 99.74	<i>Chloeia flava</i> / <i>Archinome rosacea</i>
Leptothecata	order	18SUni	1	4	3	3	98.20 ~ 98.72	<i>Octophialucium indicum</i> / <i>Blackfordia virginica</i> / <i>Aequorea victoria</i> / <i>A. aequorea</i>
<i>Lyrocteis</i>	genus	18SUni	1	1	1	1	100	<i>Lyrocteis sp.</i>

Table S 5.3 The results of cross validation of diet composition observations in the canonical analyses (CAP) ordination, following to the leave-one-out approach. The values are the number of samples allocated into each of the classified groups. The juveniles of both *Lutjanus erythropterus* (LE) and *L. malabaricus* (LM) achieved higher allocation success rates (82%) versus adults. The allocation success rates of adults LE and LM were 45 % and 50 %, respectively, and the majority of the misclassified samples were allocated to LM Juvenile.

		Classified group				Total	% correct
		LE Juvenile	LE Adult	LM Juvenile	LM Adult		
Original group	LE Juvenile	9	0	2	0	11	82
	LE Adult	0	5	5	1	11	45
	LM Juvenile	2	0	9	0	11	82
	LM Adult	0	1	5	6	12	50

Table S 5.4 The results of distance based linear model (DistLM) to test the effects of sample variability on juvenile diet composition. Marginal test results (A) show the significance levels of each variable on diet compositions. BEST solution results (B) summarised the top five, most parsimonious combination of variables that best explained the juvenile diet composition based on the Akaike Information Criterion with finite sample sizes (AICc). The tests were based on a Jaccard coefficient matrix for presence and absence (PA) datasets. TL, total length (mm).

A. Marginal tests

Variables	df	F	p
Species	2	2.11	<0.05
TL	2	0.46	0.91
Depth	2	0.17	0.99
Time	6	1.08	0.25
Date	3	0.81	0.61

B. BEST solutions

AICc	R ²	Selected variables
174.07	0.096	Species
175.41	0.039	date
175.78	0.023	TL
175.81	0.13	Species, date
176.1	0.008	depth

Chapter 6 The distribution and habitat preferences of two sympatric snapper species on the northwest and northeast coasts of Australia

6.1 Abstract

Fish populations vary in abundance and size composition across their distribution in relation to the availability and type of habitat that is accessible. In many cases knowledge of the essential fish habitats for many fish species is limited, particularly for specific life history stages (i.e. juveniles) and/or in remote areas (i.e. deep water). This study investigated the distribution patterns and hotspots of two red snapper species, *Lutjanus erythropterus* and *L. malabaricus*, across latitude and depth in Australia. The length-specific distribution of these species in relation to bathymetry and a range of habitat descriptors was also explored in Western Australia. All analyses were based on data from 19,784 Baited Remote Underwater Video system samples collected from across Australia. Given most of the fish length data were from the northwest coast of Australia, we were only able to develop species distribution models and length-specific continuous predictive maps for Western Australian populations. A total of 698 *L. erythropterus* and 511 *L. malabaricus* were recorded across Australia at depths ranging from 4 to 129 m, with the southernmost sighting at 24 °S. Both the frequency of occurrence and body length were significantly influenced by bathymetry. Other influential explanatory variables that characterised occurrence included slope, direction of slope, and the standard deviation of water depth within a 50-grid cell kernel radius (1.56 km²). Length-specific predictive maps indicated clear ontogenetic movement to deeper waters as fish increase in size and presumably age, providing valuable information to identify priority management areas to effectively protect specific life stages. This study highlights the potential utility of Species Distribution Models and length-specific predictive maps in combination with extensive datasets to derive essential fish habitats for fish species, particularly for those fishes of high socio-economic value.

6.2 Introduction

Fish populations vary in abundance and size composition across their range of distribution in relation to the structure and availability of habitat (Bellwood et al., 2004; Jones et al., 2004; Williamson et al., 2014). Spatial management arrangements in the marine environment benefit from elucidating and describing species-habitat relationships (Conover et al., 2000; Moore et al., 2016). Identifying essential fish habitat (EFH) is important to optimise conservation and fishery management actions such as the design and location of no-take marine reserves, temporal fishing closures and gear restrictions, or as a consideration in environmental impact assessments. For many fishes, knowledge about EFH at different life stages (i.e. nursery habitats for juvenile life stages) is limited, or absent, particularly in remote areas or deep water (Hamilton et al., 2017; Moore et al., 2016; Newman et al., 2016; Sundblad et al., 2014).

The life cycle of many reef fishes consists of a pelagic larval stage, followed by a demersal juvenile stage on shallow, low-relief substrate with adult life stages on deeper, high-relief reefs (Dahlgren & Eggleston, 2000). Owing to these complex life cycles, drivers of distribution and abundance of reef fish are expected to vary between life-history stages (Dahlgren & Eggleston, 2000; Galaiduk et al., 2018; Mumby, 2006; Nakamura et al., 2008; Williams & Russ, 1994). For example, settlement choice of pelagic larvae and post-settlement survivorship of juveniles depends on the availability of nursery habitats (Feary et al., 2007; Jones et al., 2004; Lindholm et al., 2001). Therefore, evaluation of distribution patterns and EFH specific to life stages are valuable information to inform marine spatial management planning and can effectively be utilised to enhance survival during vulnerable life stages (Elith & Leathwick, 2009; Moore et al., 2009; Thrush & Dayton, 2010).

The crimson snapper, *Lutjanus erythropterus* (Bloch, 1790), and the saddletail snapper, *L. malabaricus* (Bloch & Schneider, 1801) are sympatric red snapper species which are widely distributed along tropical and subtropical coasts throughout the Indo-Pacific region, including the Fiji Islands, Persian Gulf, Australia, and Japan (Allen, 1985). They are sister taxa (Frédérich & Santini, 2017) and the juveniles are phenotypically cryptic (Fry et al., 2009). Both species support important commercial and recreational fisheries throughout their distributional ranges (Allen, 1985; Blaber et al., 2005; O'Neill et al., 2011). Fisheries catches and research sampling data suggest that the adults co-exist in inter-reefal habitats on hard substrates ranging from depths of 20 to 240m (Blaber et al., 2005; Brouard & Grandperrin, 1985; McPherson et al., 1992; Newman, 2002; Newman & Williams, 1996; Williams & Russ, 1994). In contrast, their juveniles have been recorded in commercial prawn trawls and research survey catches from waters shallower than 30m (Fry et al., 2009; McPherson et al., 1992;

Takahashi et al., 2020). These catch data suggest that *L. erythropterus* and *L. malabaricus* probably undertake ontogenetic movements during their life history. Despite the importance of these species to commercial and recreational fisheries, there has been limited research which investigates their length-specific distribution patterns. Also, little is known about their ecological interactions and niche partitioning between the species and life stages (Blaber et al., 2005; Newman & Williams, 1996; Takahashi et al., 2020).

The objective of this study was to analyse data from Baited Remote Underwater Video systems (BRUVs) to: i) identify the spatial distribution ranges and hotspots of *L. erythropterus* and *L. malabaricus* in Australia across latitudes and depths; ii) corroborate the observed habitat partitioning patterns between life stages, and identify the driving factors of the partitioning; and iii) construct length-specific, continuous predictive maps of their distribution along the Western Australian coast for each species.

6.3 Materials and methods

6.3.1 BRUVs sample and data collection

We analysed data from 19,784 BRUVs samples which were collected between 2000 and 2017 from across Australia in depths ranging from 0 to 590 m across a latitudinal range from 10.41 to 43.78 °S (Figure 6.1). Details regarding the BRUVs design, deployment and video analyses are described in Harvey et al. (2021). The BRUVs data were collated within the GlobalArchive (<https://globalarchive.org>). BRUVs imagery was analysed using the software EventMeasure (<http://www.seagis.com.au>) with relative abundance counts (MaxN) of *L. erythropterus* and *L. malabaricus* being recorded. MaxN is the maximum number of fish observed in the field of view of the BRUVS at one time (Cappo et al., 2001, 2003, 2007). Differences in mean MaxN between the species and coasts were examined using a two-way analysis of variance (2-way ANOVA). MaxN was log-transformed to meet the assumption of normal distribution, and absence records were excluded from the analyses.

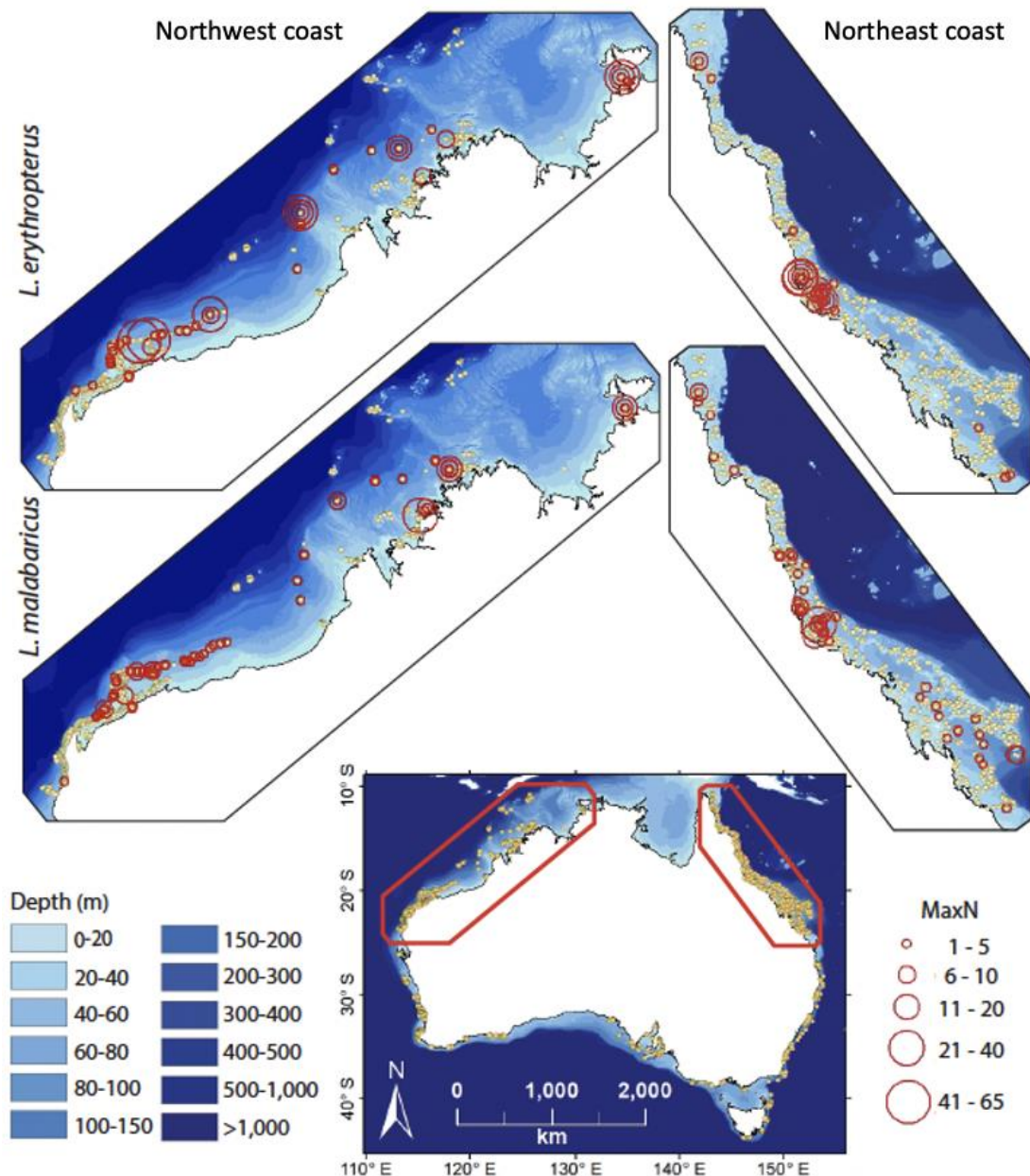


Figure 6.1 Map of Australia indicating the location of BRUVs survey sites (yellow points). Close-up maps detail the northwest (left) and northeast (right) coasts that encompass all the BRUVs sites where *L. erythropterus* (top) and *L. malabaricus* (bottom) were sighted (red circles). The size of the red circles is directly related to the MaxN of each species.

To make measurements of the lengths of fish we used imagery from samples recorded with stereo-BRUVs. Stereo-BRUVs utilise two high-definition video cameras separated by a distance of between 500 and 800 mm, facilitating accurate length measurements at any angle in the field of view when the whole body is captured in the footage (Cappo et al., 2003; Harvey et al., 2010; Harvey & Shortis, 1995). Fork lengths (FL) of fish were also recorded in most of the stereo-BRUVs samples, except where there was a camera failure, or the visibility was too poor to make measurements. Body length was measured on the image where MaxN was

recorded to ensure no individual was recorded more than once. Juveniles of *L. erythropterus* and *L. malabaricus* are phenotypically indistinguishable (cryptic) (Fry et al., 2009). Due to the lack of juvenile discrimination in BRUVs images, fish under 150 mm length were recorded as both *L. erythropterus* and *L. malabaricus*. We acknowledge that this approach limits our analyses to identify species-specific distribution patterns for the juvenile stage, but we believe it is a reasonable approach given that *L. erythropterus* and *L. malabaricus* are sympatric species and the juveniles of both species have been caught in the same trawl nets in Western Australia and elsewhere on the east coast (Fry et al., 2009; McPherson et al., 1992; Takahashi et al., 2020). The subadults and adults were distinguished based on the morphological and behavioural differences, where *L. malabaricus* have larger mouths and more angular heads compared to *L. erythropterus*, and *L. malabaricus* are often found more solitary or in a couple of individuals whereas *L. erythropterus* tend to present in larger numbers. Differences in mean length between the species on the northwest (NW) coast of Australia were examined using a one-way analysis of variance (1-way ANOVA). Fish under 150 mm length were excluded from this analysis as the same individuals were recorded as both *L. erythropterus* and *L. malabaricus*, violating the independence assumption. Due to the lack of length records from the northeast (NE) coast, only the data from NW coast were used for the ANOVA.

A bathymetry raster at 250 m resolution (available from Geoscience Australia, accessed on 20 September 2019) (Whiteway, 2009) was used to derive secondary datasets of environmental predictors of benthic habitat using terrain analysis techniques in ArcGIS 10.6 (see Table 6.1 for the full list and explanations of explanatory variables). Together, these predictors describe the structure and complexity of the seafloor across varying spatial scales and are known to affect the distribution and abundance of fishes (Galaiduk et al., 2017b; Oyafuso et al., 2017; Stamoulis et al., 2018).

6.3.2 Species distribution modelling and predictive mapping

Species distribution models (SDMs) were applied to quantify the relationship between response variables (i.e. occurrence, length of fish) of the BRUVs data and multiple seafloor variables derived from the bathymetry data, such as the direction of slope and curvature of seafloor (Table 6.1). The outputs can be used to make predictions about the distributions of organisms in unsurveyed locations (Cure et al., 2018; Elith & Leathwick, 2009; Galaiduk et al., 2017a; Moore et al., 2009). The occurrence and length of *L. erythropterus* and *L. malabaricus* were modelled separately to inform the body-length distribution maps with predicted data from the occurrence models. Samples from the NW coast of Australia (with a

longitude less than 135°E and a latitude above 25°S) were used in SDMs due to the lack of length records from the NE coast.

Table 6.1. Descriptions of the explanatory variables used for the boosted regression trees (BRT) and generalized additive mixed models (GAMMs)

Explanatory variables	Descriptions
Bathymetry (bathy)	Elevation in metres relative to the Australian Height Datum.
Aspect (asp)	A circular azimuthal direction of the steepest slope, calculated on a 3 x 3-pixel area. Values closest to 0 and 360 represent north-facing slopes. Values close to 90, 180, and 270 represent east-, south-, and west- facing slopes respectively.
Slope (slp)	First derivative of elevation. Average change in elevation, calculated on a 3 x 3 pixel area.
Plan curvature (plan)	second derivative of depth: concavity/convexity perpendicular to the slope.
Profile (prof)	second derivative of depth: concavity/convexity parallel to the slope.
Curvature (curv)	Combined index of profile and plan curvature.
Range (rng05, rng10, rng30, rng50)	Maximum minus the minimum elevation in the local neighbourhood (local relief) of 5, 10, 30 and 50-grid cell kernel radius.
Standard deviation of water depth (std05, std10, std30, std50)	Standard deviation of the local neighbourhood water depth of 5, 10, 30 and 50-grid cell kernel radius.

A total of 5,225 BRUVs data were collected from the NW coast, however, only a subset of these surveys yielded at least one sighting of either *L. erythropterus* and/or *L. malabaricus* on the NW coast. Occurrence data from those surveys that yielded at least one species of interest, comprised a total of 1,611 individual BRUVs deployments. These deployments were utilised to construct SDMs. If the species were observed in the BRUVs recording, it was assigned as a presence record, and all the other BRUV locations were utilised as absence points. Occurrence and length of *L. erythropterus* and *L. malabaricus* were modelled separately to inform the body-length distribution maps with data from the occurrence models.

The presence/absence (PA) of *L. erythropterus* and *L. malabaricus* were modelled using boosted regression trees (BRT) (i.e. fitting a large number of binary splits), a technique that offers flexibility due to the large proportion of zeros, extreme outliers and interaction terms (Elith et al., 2008; Leathwick et al., 2006a). Regression based models are potentially sensitive

to correlated explanatory variables. As a consequence variables with a Spearman's Rank correlation coefficient of over 0.7 were excluded from further analyses (Leathwick et al., 2006b). The PA dataset was randomly divided into training (70%) and test (30%) data to obtain the estimation of prediction error from independent test data. The optimal proportion of training data is ~70% for 5 - 6 predictors, which was the case for this study (Fielding & Bell, 1997; Huberty, 1994). The training data was fitted with Bernoulli distributions, using the *gbm* package (Ridgeway, 2013), and the functions developed by Elith et al. (2008) in R. The optimal model parameters were selected by running the models using the range of parameters and assessing the number of trees retrieved as well as the area under curve (AUC) from 10-fold cross validation (CV) for the model prediction powers. We used the parameters of tree complexity at 2, bag fraction at 0.75 and learning rate at 0.001 to ensure that a minimum of 1000 trees would be retrieved. Variable selection was performed by removing the variables with the least relative percentage contributions to the model. The changes in holdout deviances were assessed each time the models were simplified using 10-fold CV. Through these procedures, the most parsimonious model was selected for each species, with all the remaining explanatory variables contributing at least 10% to the model. The final model for each species was validated using test data by examining AUC, confusion matrix and model accuracy parameters, such as sensitivity, specificity, and the Kappa statistic. AUC is a measure of the model's prediction power, ranging from 0.5 to 1. An AUC of 0.5 suggests that the predictive ability could be achieved by chance alone, 0.7 – 0.8 is considered to be an acceptable prediction, 0.8-0.9 to be excellent, and over 0.9 to be outstanding (Hosmer et al., 2013). The threshold at which sensitivity was equal to specificity was used to ensure high sensitivity, while specificity was also considered (Figure S 6.1), because high false negative rates would be more 'costly' in conservation-terms than false positives (i.e. EFH would not be explicitly incorporated into fisheries and conservation management priorities) (Fielding & Bell, 1997).

Body lengths of 209 individuals of *L. erythropterus* and 151 individuals of *L. malabaricus* were measured on the NW coast of Australia and modelled using generalized additive mixed models (GAMMs). Generalized additive models (GAMs) and GAMMs are a particularly powerful tool to model the complex, non-linear relationships of marine species to environmental predictors by utilizing a smoothing function, and it has been previously used to predict fish lengths and biomass (Galaiduk et al., 2017a, 2018). GAMMs allow consideration of random effects (Wood, 2006), which in our case is the unique ID of BRUVs as the observation level random effect, to account for non-independence of the length measurements. Outliers were removed and the variables were square-root or log transformed if required to meet the normality assumption. Explanatory variables with Spearman's Rank correlation coefficient of over 0.7 were excluded to remove collinearity. The body length dataset for each

species was randomly divided into training (70%) and test (30%). Spatial autocorrelation was examined using the `gstat` package in R (Pebesma, 2004), in order to account for non-independence of observations, which was minimal overall and most importantly non-existent in the test data (Wainwright & Mulligan, 2013). This indicates the spatial independence of data between samples.

The response and explanatory variables of the training data were fit with a gamma error distribution with log link function, using the `FSSgam` package in R (Fisher et al., 2018). Smoothing was performed during the model fitting process, with the knots (smooth terms) limited to 4 degrees of freedom. The most parsimonious model with delta Akaike Information Criterion corrected for finite sample sizes (AICc) of less than 2 was selected for each species (Table S 6.1) (Burnham & Anderson, 2004). The prediction powers of the selected models were validated by predicting the fish length of test data and assessing normalised root mean square error (nRMSE) and an adjusted R squared value (adj. R²) based on a linear regression between the observed values of the test dataset and values predicted without a null term. Model residuals were plotted against the fitted values of each model to verify an absence of residual patterns. The software RStudio (v.1.0.143) was used to select and validate models, produce plots, and carry out correlation analyses (RStudio Team, 2016).

Raster layers of the explanatory variables used in the final models were prepared, covering the areas of the NW coast of Australia, with latitudes between 13.3 and 25.5°S, longitudes between 112.9 and 130.2°E, and the depth to 131 m (the maximum depth at which body length was recorded). Probability of occurrence and body length were predicted separately using the final validated models of BRT and GAMMs for each species on 250 m grids. Probability of occurrence was converted to 1 and 0 for presence and absence respectively, based on the species-specific, PA conversion thresholds defined during the BRT model evaluation. Length-specific, continuous predictive maps were then constructed on the grids where the presence of these species was predicted. The raster package in R was used for the predictions and map constructions.

6.4 Results

6.4.1 Depth and latitudinal distribution patterns

The southernmost sighting of *L. erythropterus* and *L. malabaricus* was 23.44°S on the NW and 24.12°S on the NE coasts of Australia, despite the continuous, large sampling effort at higher latitudes on both coasts (Figure 6.1, Figure 6.2). The number of BRUVs deployed within the observed latitudinal range of *L. erythropterus* and *L. malabaricus* (< 25°S) was

5,225 on the NW coast at depths ranging from 0.4 to 348 m, and 2,490 on the NE coast at depths ranging from 7 to 104 m (Table 6.2, Figure 6.2–A). A total of 74 BRUVs on the NW coast and 56 BRUVs on the NE coast contained sightings of *L. erythropterus*, accounting for a frequency-of-occurrence of 1.42 and 2.25% respectively (Table 6.2). A total of 123 and 84 BRUVs on the NW and NE coasts contained sightings of *L. malabaricus*, accounting for a frequency-of-occurrence of 2.35 and 3.37% respectively (Table 6.2).

The maximum depth at which *L. erythropterus* and *L. malabaricus* were sighted on the NW coast was 123 m and 129 m, respectively, which were deeper than those on the NE coast (78.5 and 104 m, respectively) (Table 6.2 & Figure 6.2-A). The depth difference is most likely related to the low number of samples derived from deeper waters on the NE coast (Figure 6.2–A & B). While the species were sighted at shallow depths (i.e. as shallow as 4 m), the depth distribution hotspot (i.e. an area with a frequency-of-occurrence of more than 10%) for both species was obtained in waters deeper than 20 m on the NW coast, with the peak of frequency-of-occurrence at depths of 80 – 110 m (Figure 6.2–B). In contrast, the hotspot was shallower on the NE coast starting from a depth of 10 m (Figure 6.2–B). An exceptionally high frequency-of-occurrence of *L. malabaricus* (50 and 100%) was observed on the NE coast at 22 – 24 °S and 80 – 110 m depth, which was reflected by sightings on four out of the 7 BRUVs deployed within the depth range (Figure 6.2–A & B). Excluding the exceptionally high frequency-of-occurrence of *L. malabaricus*, the latitudinal distribution patterns were comparable between each of the species and along each coast, with the hotspot at 12 – 22 °S on the NW coast and 10 – 20 °S on the NE coast (Figure 6.2–B).

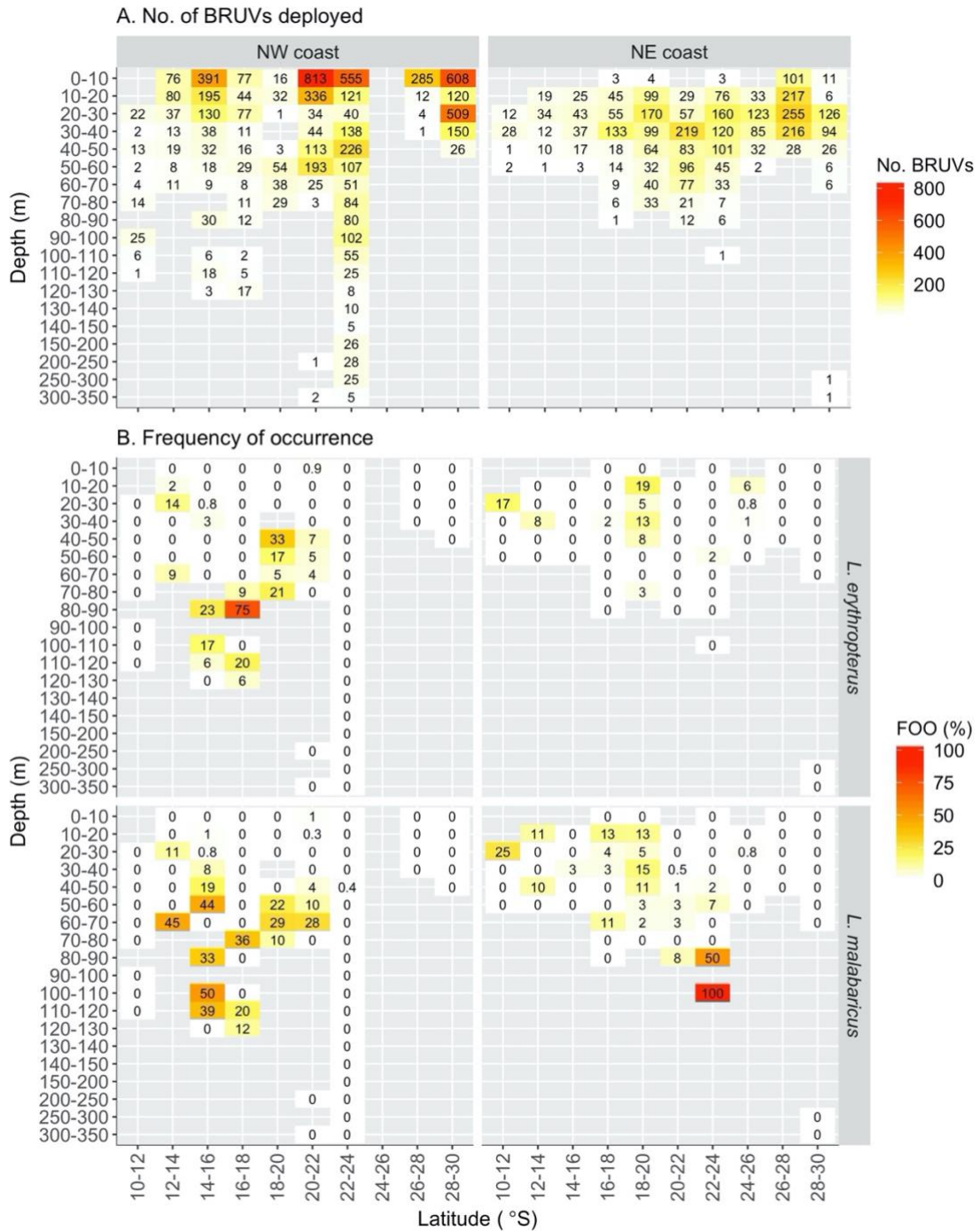


Table 6.2 Summaries of BRUVs counts, MaxN and length of *L. erythropterus* and *L. malabaricus* sighted by BRUVs in northwest (NW) coast and northeast (NE) coast of Australia. Total number of BRUVs is the number of BRUVs deployed above 25 °S on each coast, regardless of the sighting of *L. erythropterus* and *L. malabaricus*. Range and mean of MaxN were generated excluding the absence records. Mean length was calculated without juveniles (under 150 mm). SD, standard deviation.

	NW coast		NE coast	
	LE	LM	LE	LM
Total number of BRUVs (above 25 °S)	5,225		2,490	
Number of BRUVs with a presence record	74	123	56	84
Frequency of occurrence (%)	1.42	2.35	2.25	3.37
Depth range of presence records (m)	4 - 123	4 - 129	11.2 - 78.5	11.2 - 104
Maximum latitude of presence records (°S)	21.64	23.44	24.12	21.64
Total MaxN	407	293	291	218
MaxN range	1 - 64	1 - 25	1 - 28	1 - 25
Mean MaxN (\pm SD)	5.5 (\pm 10.4)	2.38 (\pm 3.18)	5.2 (\pm 6.06)	2.6 (\pm 3.46)
Number of fish with length recorded	209	151	1	6
Length range (mm)	65.14 - 603.42	65.14 - 774.62	394.24	330.83 - 514.9
Mean length (\pm SD) (mm)	391.32 (\pm 88.09)	399.90 (\pm 149.42)	394.24 (NA)	402.43 (\pm 62.83)

6.4.2 MaxN records

The cumulative number of MaxN records were 698 for *L. erythropterus* and 511 for *L. malabaricus*. The mean MaxN of *L. erythropterus* (5.5 and 5.2 on the NW and NE coasts respectively) was significantly higher than those of *L. malabaricus* (2.38 and 2.6 on the NW and NE coasts respectively) on both coasts (Table 6.2) (2-way ANOVA: $F_{(1, 322)} = 18.13$, $p < 0.001$). The difference in mean MaxN was not significant between the coasts (2-way ANOVA: $F_{(1, 322)} = 2.39$, $p = 0.12$), nor were the interactions (2-way ANOVA: $F_{(1, 322)} = 0.67$, $p = 0.42$).

6.4.3 Body length records

Body lengths of 209 individuals of *L. erythropterus* and 151 individuals of *L. malabaricus* were measured on the NW coast. Of these length measurements, sixteen were below 150 mm. Only 9 length records were available from the NE coast due to the low numbers of stereo-BRUVs deployments. The minimum length recorded of a juvenile was 65.14 mm. The maximum recorded length of *L. erythropterus* (603.42 mm) was smaller than those of *L.*

malabaricus (774.62 mm), while their mean lengths were comparable to each other (369.32 mm (\pm 114.31 SD), and 368.54 mm (\pm 168.37 SD), respectively) (Table 6.2) with no significant difference between the species (1-way ANOVA: $F_{(1, 326)} = 0.425$, $p = 0.52$).

6.4.4 Presence/absence models

The initial 14 explanatory variables (Table 6.1) were reduced to six variables after covariates were removed. These were further reduced to four and three influential variables with high contributions to the BRT models of PA of *L. erythropterus* and *L. malabaricus* (Table 6.3). Those influential variables were bathymetry, standard deviation of the local neighbourhood water depth of the 50-grid cell kernel radius (std50), slope, and aspect for *L. erythropterus*; and bathymetry, std50, and slope for *L. malabaricus* (Table 6.3). Bathymetry was the most influential explanatory variable with percentage contributions of 52% for *L. erythropterus* and 51% for *L. malabaricus* (Table 6.3). The probability of occurrence was low at depths shallower than \sim 40 m, and then increased with increasing depth, with a peak at approximately 100 m for both species (Figure 6.3–A). These patterns were also reflected in the predictive maps of the NW coast of Australia, where a low probability of occurrence was predicted at shallow, inshore areas (Figure 6.4–A). Most inshore areas were then predicted to exhibit negligible records after the probability of occurrence was converted to PA, based on the species-specific PA conversion thresholds (Figure 6.4–B). Std50 was the second most influential predictor of occurrence for both species (Table 6.3), where the probability of occurrence was predicted to increase with smaller values of std50 (Figure 6.3–A). A higher probability of occurrence of both species was predicted for gently sloping continental shelf waters. The probability of occurrence of *L. malabaricus* was expected to be higher than those of *L. erythropterus* when fitted with std50 and slope (Figure 6.3–A), which was also reflected in the predictive maps where larger areas with mid to high probability of occurrence (0.3 - 1) were predicted for *L. malabaricus* compared to *L. erythropterus* (Figure 6.4–A). In addition, *L. erythropterus* was also predicted to be mostly associated with the north-facing slope directions (aspect close to zero or 360°) (Figure 6.3–A). The percent contributions of std50, slope, and aspect ranged between 11 and 38%, which were lower than those of bathymetry (Table 6.3), and the changes in probability of occurrence predicted by these variables were also notably less than those of bathymetry (by one order of magnitude) (Figure 6.3–A).

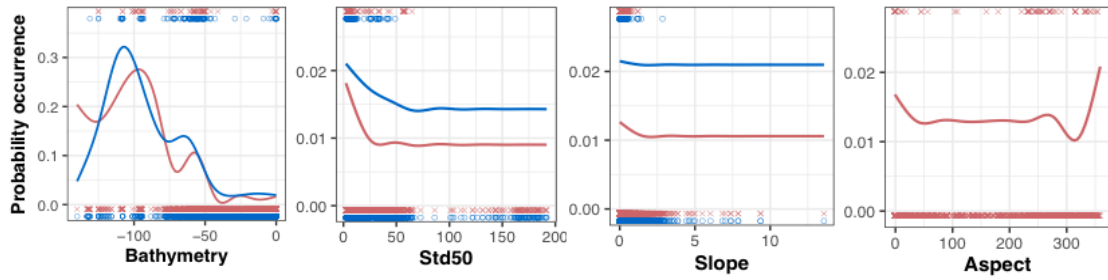
The models for both species achieved a high prediction performance, with an AUC of 0.85 for *L. erythropterus*, and 0.83 for *L. malabaricus* (Table 6.3). The threshold at which sensitivity was equal to specificity was 0.041 for *L. erythropterus* and 0.063 for *L. malabaricus* (Table 6.3). When the predicted probability of occurrence was lower than the threshold, it was converted to an absence in the PA predictive maps (Figure 6.4–B). The sensitivity and

specificity at the threshold were 0.76 for *L. erythropterus* and 0.78 for *L. malabaricus* (Table 6.3 & Figure S 6.1).

Table 6.3 The summary of the final models and model validations of boosted regression trees (BRT) for presence/absence and generalised additive mixed models (GAMMs) for length of *L. erythropterus* and *L. malabaricus* on the northwest coast of Australia. The percentage values for the selected explanatory variables in BRT represent the percentage contributions to the models. Threshold dependent validation parameters, such as specificity and sensitivity, were the values at the threshold where specificity was equal to sensitivity. Normalised root mean square error (nRMSE) and adjusted R squared value (adj. R²) were based on a linear regression between the observed values of the test dataset and values predicted without a null term. Asp, aspect; bathy, bathymetry; prof, profile; slp, slope; std50, standard deviation of the local neighbourhood water depth of 50-grid cell kernel radius; curv, curvature; rng30, maximum minus the minimum elevation in the local neighbourhood (local relief) of 30-grid cell kernel radius; AUC, area under curve.

Response variable	Presence / Absence		Length (mm)	
	<i>L. erythropterus</i>	<i>L. malabaricus</i>	<i>L. erythropterus</i>	<i>L. malabaricus</i>
Species	<i>L. erythropterus</i>	<i>L. malabaricus</i>	<i>L. erythropterus</i>	<i>L. malabaricus</i>
Range	0 / 1		65.14 – 603.42	65.14 – 774.62
Initial explanatory variables	asp, bathy, plan, prof, slp, std50		asp, bathy, curv, sqrt.slp	asp, bathy, curv, sqrt.slp, log.rng30
Selected explanatory variables	bathy (52%) std50 (20%) slp (14%) asp (14%)	bathy (51%) std50 (38%) slp (11%)	bathy	bathy
AUC	0.85	0.83		
Threshold	0.041	0.063		
Sensitivity (= Specificity)	0.76	0.78		
nRMSE (%)			19.05	33.1
adj. R ²			0.59	0.51

A. Probability of occurrence



B. Body length

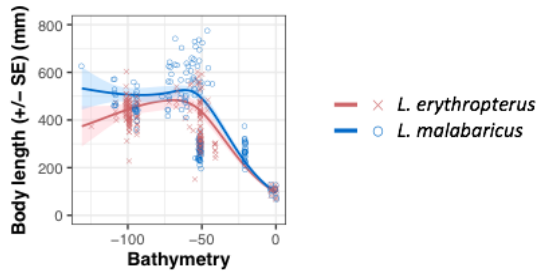


Figure 6.3 Smoother estimates for the explanatory variables as obtained by boosted regression trees (BRT) for occurrence (A), and generalised additive mixed models (GAMMs) for body length (B) of *L. erythropterus* and *L. malabaricus* on the northwest coast of Australia. Marks in the plots represent the sampled data points. In the BRT, marks above the estimated lines represent the presence records, and marks below the lines represent the absence records. The datapoints of juveniles (under 150mm body length) were duplicated for *L. erythropterus* and *L. malabaricus* due to the inability of juvenile discrimination in BRUVs images. Std50, standard deviation of the local neighbourhood water depth of 50-grid cell kernel radius; SE, standard error.

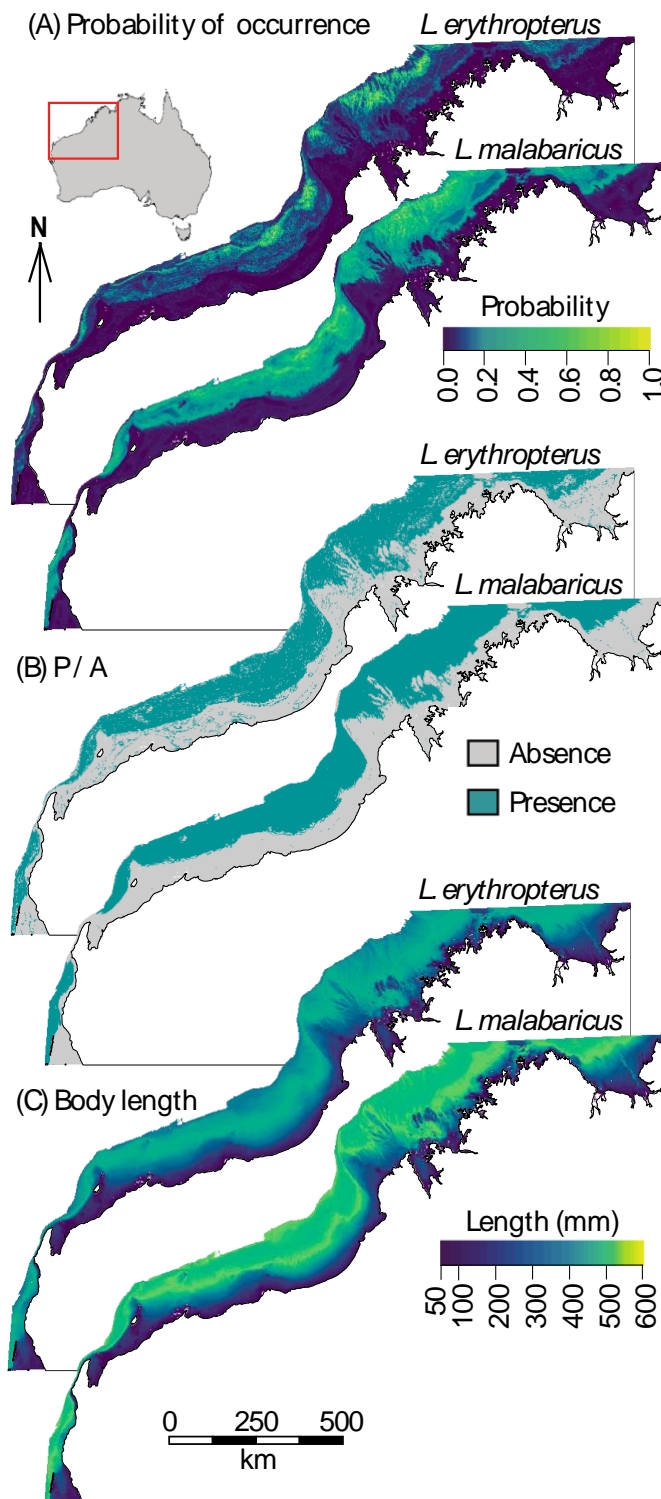


Figure 6.4 Predictive maps of occurrence and body length of *L. erythropterus* and *L. malabaricus* on the northwest coast of Australia. Probability of occurrence (A) was predicted using the selected models of boosted regression trees, which was then converted to presence and absence (P/A) (B) based on the threshold (sensitivity = specificity) of 0.041 and 0.063 for *L. erythropterus* and *L. malabaricus* respectively. Body length (C) was predicted using the final models of the generalised additive mixed models. The predicted area covers the depth to 131 m, latitude between 13.3 and 25.5 °S, and longitude between 112.9 and 130.2 °E.

6.4.5 Body length models

GAMMs for body length identified bathymetry as the significant influential predictor of length of both species on the NW coast of Australia (Table 6.3), with the length increasing from 100 mm to approximately 500 mm as depth increased from 0 to ~ 60 m (Figure 6.3–B). Body length of *L. erythropterus* exhibited a slight decline to below 400 mm as the depth increased from ~ 60 m to the maximum depth observed (131 m), whereas those of *L. malabaricus* plateaued (Figure 6.3–B). Larger body length was predicted for *L. malabaricus* compared to *L. erythropterus* at depths deeper than 50 m (Figure 6.3–B).

These patterns identified in the GAMMs curves were also revealed in the length-specific, continuous predictive maps (Figure 6.4–C). Juvenile *L. erythropterus* and *L. malabaricus* were expected to occur in nearshore and inshore areas along the NW coast of Australia. Body length increased with the proxy of distance from the coast (Figure 6.4–C). The size distribution at offshore areas was larger for *L. malabaricus* than *L. erythropterus* (Figure 6.4–C). The maximum length predicted in the mapped area was 483.48 mm and 588.36 mm for *L. erythropterus* and *L. malabaricus* respectively.

Normalised root mean square error (nRMSE) between the observed and predicted length was 19.1% for *L. erythropterus* and 33.1% for *L. malabaricus* (Table 6.3). Adjusted R^2 of the linear regression between observed and predicted values were 0.59 for *L. erythropterus* and 0.51 for *L. malabaricus* (Table 6.3). Lower nRMSE and higher R^2 achieved by the model for *L. erythropterus* compared to the model for *L. malabaricus* indicate a higher prediction performance of the former model.

6.4.6 Predictive maps of Presence/Absence and body length combined

Large, offshore areas of the NW coast of Australia were expected to be inhabited by medium to large sized fish at depths over ~30 m for both species (Figure 6.5). In contrast, limited areas for juvenile fish were predicted when the predictions of PA were taken into account (Figure 6.5), due to the absent predictions at the majority of inshore, shallow water sampled areas (Figure 6.4–B). More patches of nursery grounds were revealed for *L. erythropterus* compared to *L. malabaricus*, possibly due to the lower PA conversion threshold of *L. erythropterus* (Figure 6.5).

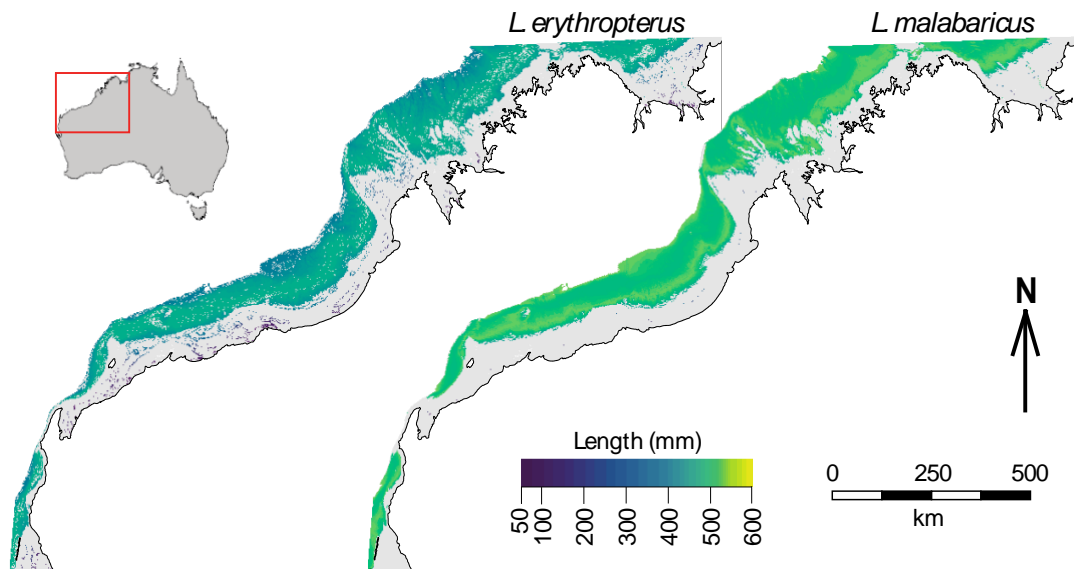


Figure 6.5 Predictive maps of the body length and occurrence combined for *L. erythropterus* (left) and *L. malabaricus* (right) on the northwest coast of Australia. Grey area indicates the area where absence of the species was predicted. The predicted area covers the depth up to 131 m, latitude between 13.3 and 25.5 °S, and longitude between 112.9 and 130.2 °E.

6.5 Discussion

Understanding the patterns of distribution and EFH for different life stages of fishes informs and enables the implementation of effective spatial and temporal management (Laman et al., 2018; Moore et al., 2016). Studying EFH for smaller individuals (i.e. juveniles), and in deep or turbid water is particularly challenging due to the large sample sizes required to collect sufficient occurrence data (Fry et al., 2009; Moore et al., 2016; Vasconcelos et al., 2010). The large BRUVs dataset collated in the GlobalArchive and analysed in this study provided an opportunity to overcome some of these challenges. The frequencies-of-occurrence of *L. erythropterus* and *L. malabaricus* ranged between 1.42 and 3.37% on the NW and NE coasts of Australia, and under 0.5% in shallow waters (< 30 m) on the NW coast where juveniles were expected to occur. Despite the low frequency-of-occurrence, this data derived from this study was able to predict the distribution patterns of *L. erythropterus* and *L. malabaricus* across Australia at an extended depth range and demonstrated ontogenetic movement patterns with the continuous predictive maps on the NW coast of Australia.

Latitudinal hotspots where the frequency-of-occurrence was more than 10% were limited to latitudes less than 20 °S and 24 °S on the NW and NE coasts, respectively. The maximum latitude observed in this study was 24 °S, whereas the most southern sightings previously recorded are at 33 °S off Sydney for both species (Australian Museum Ichthyology Collection, Catalogue number IB.4236 and I.28743-028 for *L. erythropterus* and *L. malabaricus*

respectively). Given the continuous, large sampling effort at higher latitudes, this finding suggests that the EFH of *L. erythropterus* and *L. malabaricus* is likely to be restricted to the tropics despite their wide distributional range from Sydney to southern Japan (Allen, 1985). The latitudinal distribution range is typically the result of thermal tolerance, growth and niche constraints. Consequently, poleward shifts in species distribution and tropicalisation of temperate reefs have been increasingly documented in response to the rising sea water temperature and climate change (Cheung et al., 2012; Wernberg et al., 2013; Wuenschel et al., 2012; Yamano et al., 2011). The latitudinal hotspot we identified for *L. erythropterus* and *L. malabaricus* suggests that they are likely to possess a prominent thermal threshold and may undergo potential poleward shifts as water temperature rises if suitable habitat and diet requirements can be encountered at higher latitudes. The results of this study suggest that areas in higher latitudes (> 20 °S and 24 °S on the NW and NE coasts) could potentially become occupied by these species under climate change scenarios. Long-term continuous observations from monitoring programs are required to detect such changes.

On the NW coast of Australia, the depth hotspot for the two species was between 20 and 130 m with the peak of frequency-of-occurrence at 80 – 110 m despite their depth distribution starting from as shallow as 4 m depth. The maximum depth of *L. erythropterus* and *L. malabaricus* revealed in this study was 123 m and 129 m respectively, which are comparable with records from global and national databases (i.e. FishBase (www.fishbase.org), Fish of Australia (<http://fishesofaustralia.net.au/>)) and consistent with previous studies, ranging between 100 and 140 m (Allen, 1985; Bray & Gomon, 2018; Froese & Pauly, 2018). However, in contrast to the clear latitudinal threshold recorded in this study, the depth distributional patterns require careful interpretation. While the BRUVs deployment depths exceeded 300 m, the number of samples in deeper waters beyond the maximum depth observed on each coast is limited. Given the frequency-of-occurrence in deeper waters remained relatively high, it is likely that the depth limits of the NW and NE coast populations may exceed our findings. Furthermore, the depth distribution patterns (both hotspots and maximum depth) on the NE coast were shallower compared to those on the NW coast, which may be attributed to the difference in deep water sampling effort and also the characteristics of benthic topography between the coasts (i.e. an extensive barrier reef system on the NE coast as opposed to a broad open continental shelf system on the NW coast). Similarly, the maximum reported depth of *L. malabaricus* was 240 m in Vanuatu (Brouard & Grandperrin, 1985), whereas there is no evidence this species occurs at these depths in Australian waters. These findings suggest the importance of location-specific investigations as well as increased sampling effort at deeper water sites to better understand their distribution at extended depths.

Generalised additive mixed models (GAMMs) and body length predictive maps indicated clear ontogenetic movement to deeper water as fish increase in length and presumably age, which is consistent with the life cycle migration patterns found in many reef fishes including other lutjanid species (Cocheret de la Morinière et al., 2003; Dahlgren & Eggleston, 2000; Szedlmayer & Lee, 2004). The increase in body length occurred from shallow waters to 50 m depth for both species, and juveniles were predicted to be found at inshore shallow waters less than 30 m depth. This prediction is consistent with data from a range of studies on *L. erythropterus* and *L. malabaricus*. For example, juveniles were captured in commercial prawn trawls and research survey catches from waters shallower than 30 m (Fry et al., 2009; McPherson et al., 1992; Takahashi et al., 2020) and adults have been reported from a depth range of 20 to 240 m (Blaber et al., 2005; Brouard & Grandperrin, 1985; McPherson et al., 1992; Newman, 2002; Williams & Russ, 1994). These findings indicate that both BRUVs and catch data can be utilised to identify ontogenetic movements if an extensive range of length data is available. However, BRUVs have the advantage of being non-intrusive and non-extractive and can be utilized across management zones (Cappo et al., 2003). In addition to the ontogenetic habitat partitioning, Takahashi et al. (2020) identified significant diet partitioning between the life stages of *L. erythropterus* and *L. malabaricus*. These findings suggest that habitat and diet are strongly connected, and that life history niche partitioning plays an important role not only to provide refuge from predation but also to segregate food resources to minimise intra-specific competition.

Reef fish are also generally understood to migrate from low to high relief substrate as they grow (Dahlgren & Eggleston, 2000; Williams & Russ, 1994). Consequently, we included several substrate complexity variables, such as slope and curvature, in the models. However, the most parsimonious models of both species were underpinned by a single variable, bathymetry. Further sampling to increase the sample size of length records, especially for juveniles, may be required to better understand the association between substrate complexity and body size of *L. erythropterus* and *L. malabaricus*.

SDMs have been increasingly applied to identify EFH and predict the distribution of marine species, and the abundance or PA of a species are the common response variables applied (Bellido et al., 2008; Laman et al., 2018; Moore et al., 2016). EFH specific to each life-stage have been investigated by modelling the abundance of adult and juveniles separately (Compton et al., 2012; Cure et al., 2018; Sagarese et al., 2014) or modelling the body size (i.e. length, biomass; Galaiduk et al., 2017a). In contrast, few studies, including this study, have utilised both occurrence (i.e. abundance, PA) and body size (i.e. length, biomass) to construct the length-specific continuous predictive maps while taking into account the occurrence

probabilities (Galaiduk et al., 2018). Our occurrence data provided useful information on the distribution patterns of *L. erythropterus* and *L. malabaricus*, with the hotspot at depths over 50 m. However, if only the occurrence data were considered, the EFH of juveniles (i.e. nursery grounds) would not have been elucidated due to the reduced amount of data available in these shallow water environments. This highlights that SDMs with the response variables of both occurrence and body size complement each other and should be considered essential if the study aims to identify size specific EFH and produce continuous predictive maps.

The low frequency-of-occurrence in shallow waters (< 40 m) on the NW coast was evident by both frequency-of-occurrence heatmaps and the results of boosted regression trees (BRT). This has resulted in an absence prediction in most inshore nursery areas, and failure to reveal ontogenetic movement patterns when the length and occurrence predictions were combined. Occurrence rates of juvenile fish may be relatively underestimated as visibility at inshore nursery grounds is generally poorer (i.e. high turbidity areas) than those at offshore locations. There may also be bias in the range of shallow depth environments sampled. Furthermore, Dunlop et al. (2015) identified agonistic behaviours of larger, predatory species, resulting in many smaller-bodied fish departing the field of view and confounding their relative abundance using downward facing BRUVs. Alternatively, Coghlan et al. (2017) used horizontally facing BRUVs and did not detect the significant influence of agonistic behaviours on relative abundance and composition of small-bodied fish, possibly because those fish pursued by predators remained sampled in the background of the field of view. These findings imply that agonistic interactions occur closer to the bait (i.e. bait guarding), and juvenile abundance and occurrence rates could be underestimated when the field of view is restricted with downward facing BRUVs or low visibility, which is common at inshore nursery grounds.

Our study also encountered an additional challenge with sampling juveniles due to the cryptic features of *L. erythropterus* and *L. malabaricus* juveniles. Due to the inability of juvenile discrimination in BRUVs images, fish under 150 mm length were recorded as both *L. erythropterus* and *L. malabaricus*, which has resulted in an additional bias, as well as limitations on our analyses to identify any inter-specific interactions during the juvenile stage. These potential sources of bias imply that there needs to be a cautious interpretation of the occurrence predictions for juveniles. For instance, the use of the length predictive maps without the occurrence prediction combined is required if the purpose is to define priority nursery areas. Despite such challenges associated with juvenile sampling, we obtained sufficient length records of juveniles and produced models of length distributions with high prediction accuracy, highlighting the robustness of SDMs and the utility of the large and extensive databases (Harvey et al., 2021).

In addition to the spatial distribution and life cycle migration patterns of *L. erythropterus* and *L. malabaricus*, this study also indicated differences in schooling behaviour and size distributions between the species. For instance, *L. erythropterus* exhibited lower frequency-of-occurrence and higher mean MaxN on both the NW and NE coasts of Australia compared to *L. malabaricus*, which is likely to be associated with a higher schooling tendency for *L. erythropterus*. Furthermore, our length predictive maps identified larger adult sizes of *L. malabaricus* compared to *L. erythropterus* throughout their distribution range, which are consistent with previous studies (Fry et al., 2009). Schooling behaviour is a common strategy to avoid predation, and to capture schooling prey for predatory fish, whereas weak schooling is advantageous to capture isolated (individual) prey (Magurran & Seghers, 1991; Major, 1978). Body morphology, such as body size, jaw structure and dentition, also plays an important role in shaping the diet choice of teleosts (Clifton & Motta, 1998; Wainwright & Richard, 1995). Therefore, the results of this study suggest different predation strategies, with *L. erythropterus* and *L. malabaricus* targeting different prey items. Different diet compositions between *L. erythropterus* and *L. malabaricus* have been revealed in previous studies, where a variety of malacostracans (e.g. crabs, prawns, mantis shrimps) were identified in the gut contents of *L. malabaricus*, but were notably absent in *L. erythropterus* (Salini et al., 1994; Takahashi et al., 2020). Instead, *L. erythropterus* consumed soft bodied prey, such as tunicates, comb jellies and medusa, as well as other fish species (Takahashi et al., 2020). Weaker schooling behaviour and a larger body size of *L. malabaricus* may be advantageous to capture individual, fast-moving malacostracans. These findings suggest a close association between behaviours, body sizes and diet specialisation, as well as the ecological adaptation for niche partitioning and thus coexistence of these two sympatric species.

In conclusion, we identified the distribution patterns of *L. erythropterus* and *L. malabaricus* across an extensive latitude and depth range in Australia. Their latitudinal hotspot and threshold were restricted to the tropics, which is likely to be linked to their thermal threshold, providing baseline information to understand potential future poleward shifts in response to climate change. Clear evidence of ontogenetic migration from inshore shallow waters to the offshore mesophotic zone (i.e. 30 – 150 m) was detected, and the first length-specific predictive maps of these species were revealed on the NW coast of Australia. This provides valuable information to identify spatial areas of importance that could be used in management arrangements to effectively protect the EFH of vulnerable juveniles as well as mesophotic reefs for adult populations. These types of management arrangements can be facilitated via a number of mechanisms within an overarching ecosystem-based fisheries management framework and can include spatio-temporal closures to fishing in nursery areas during recruitment seasons (Paradinas et al., 2015), restrictions to the use of specific gear types such

as trawl nets to reduce the footprint of interaction, and the implementation of bycatch reduction devices to limit the bycatch of juvenile fish (Barnette, 2001; Kennelly, 1995; Stobutzki et al., 2001). The SDMs achieved high predictive accuracy despite the low frequency-of-occurrence of these species particularly at juvenile stages, highlighting the robustness of SDMs. Differences in schooling behaviour and size distribution were also evident, which were likely to be associated with diet partitioning. Given that *L. erythropterus* and *L. malabaricus* are phylogenetically, morphologically and ecologically closely allied species, this study provided new insights on the specialised adaptation and ecological interactions of sympatric reef fish species within an ecosystem. Inter-specific interactions during the juvenile stage could not be examined in our study due to their cryptic features. Juveniles can only be discriminated using DNA barcoding (Elliott, 1996), and they are often found in commercial prawn trawl and research survey catches (Fry et al., 2009; McPherson et al., 1992; Takahashi et al., 2020). Therefore, the recording of geographic coordinates and body length of juveniles encountered, followed by DNA or morphometrics analysis to discriminate the species is required from future studies in order to fill knowledge gaps.

6.6 Supplementary materials

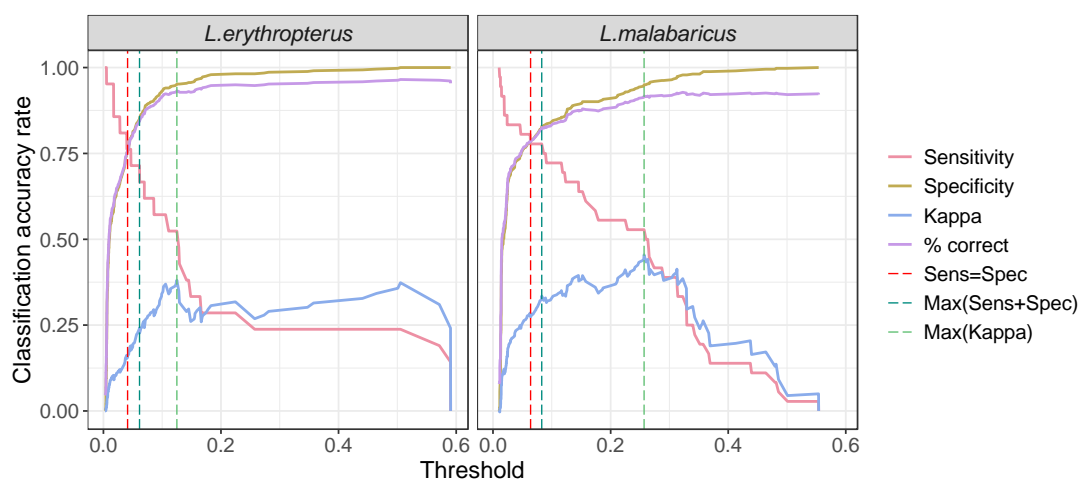


Figure S 6.1 Various measures of classification accuracy at different thresholds, based on boosted regression trees (BRT) for presence/absence of *L. erythropterus* (left) and *L. malabaricus* (right) on the northwest coast of Australia. For both species, higher sensitivity was achieved at sensitivity = specificity (red dotted line) compared to those at max (sensitivity + specificity; dark green dotted line) and maximum Kappa (light green dotted line). Therefore, the threshold selection criterion of sensitivity = specificity was used in this study to ensure lower false negative rates and to minimise the chance of a management area leaving populations unprotected.

Table S 6.1 A summary of candidate models to predict body length of *L. erythropterus* and *L. malabaricus*, with the delta Akaike Information Criterion corrected for finite sample sizes (AICc) of less than 2. The models in bold were selected due to the low AICc and least number of explanatory variables (most parsimonious). Normalised root mean square error (nRMSE) and adjusted R squared value (adj. R²) were based on a linear regression between the observed values of the test dataset and values predicted without a null term. Bathy, bathymetry; curv, curvature; sqrt.slp, square root-transformed slope; log.rng30, log-transformed, maximum minus the minimum elevation in the local neighbourhood (local relief) of 30-grid cell kernel radius.

Species	Selected models	AICc	delta AICc	nRMSE (%)	adj. R ²
<i>L. erythropterus</i>	bathy	1647.26	0	19.05	0.59
	bathy + curv	1647.44	0.17	17.83	0.64
	bathy + sqrt.slp	1647.5	0.23	18.41	0.62
	bathy + curv + sqrt.slp	1647.69	0.42	17.53	0.65
<i>L. malabaricus</i>	bathy + log.rng30	1279.41	0	30.73	0.57
	bathy + sqrt.slp	1279.67	0.26	30.13	0.59
	bathy	1280.93	1.53	33.1	0.51

Chapter 7 General discussion

Understanding the ecological interactions and niche requirements of sympatric, cryptic species provides insights into how species can coexist within an ecosystem (Diamond, 1978; Hardin, 1960). Knowledge of the niche requirements and partitioning of commercially valuable species at different life stages is also valuable for EBFM planning (Lindholm et al., 2001; Piggott et al., 2020; Vasconcelos et al., 2010). However, biological and ecological assessments need to consider the complexity of marine fish life cycles that often comprise a pelagic larval stage, a demersal juvenile stage on shallow, low-relief substrate, and an adult stage on deeper, high-relief reefs (Dahlgren & Eggleston, 2000). Ecological studies on juvenile fish are limited due to the challenges of sampling, capturing and distinguishing between juveniles of some species (Piggott et al., 2020). Dietary studies of juvenile fish are hindered by the challenge of identifying small-sized prey items. Furthermore, marine ecosystems are extraordinarily diverse with many cryptic teleost species (Bickford et al., 2007; Knowlton, 2000; Palumbi, 1994), which pose challenges in species identification and in understanding species-specific niche requirements.

To overcome these challenges and fill gaps in knowledge, I investigated the morphology and ecology of a suite of cryptic teleosts, which are of significance to commercial and recreational fisheries. The primary questions that I asked were;

1. Can morphometric analysis accurately discriminate between morphologically cryptic species of fish which are important to commercial and recreational fishing? Can they be used as a robust, simple identification tool that provides a cost-effective alternative to DNA barcoding?
2. What are the niche requirements of the sympatric, cryptic *Lutjanus* species at juvenile and adult life stages? Is there any inter- and intra-specific niche partitioning?

In this general discussion, I summarise the key findings, significance and challenges of this thesis, and identify the future directions in the context of future research needs and applications (Figure 7.1).

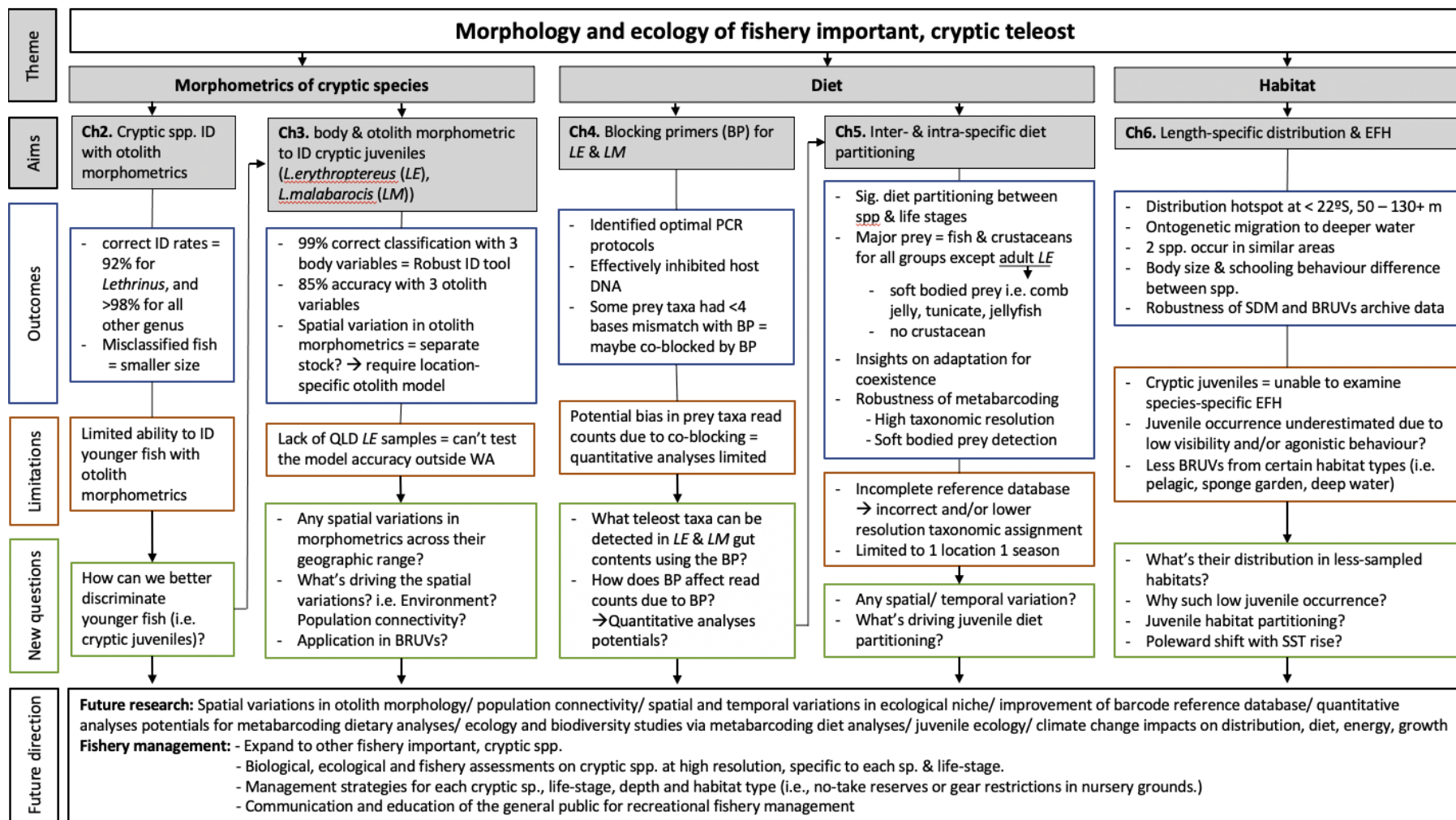


Figure 7.1 Flow diagram outlining the conclusions and future directions identified in this thesis.

7.1 Major findings and significance of the thesis

The data synthesised in my thesis provides a strong case for the use of morphometric analyses to distinguish cryptic species. This is an essential step in understanding and interpreting ecological relationships. The importance and significance of these processes were highlighted in Chapter 5 and 6 where distinct intra- and inter-specific niche requirements of two cryptic species were identified. These differing niches have implications for the management of these species.

7.1.1 Multivariate morphometric analysis is a robust tool to discriminate fishery important, cryptic species

In Chapter 2 and 3, I investigated the efficacy of multivariate data analysis of morphometric measurements of fish to discriminate 11 morphologically cryptic species from five teleost families (Figure 7.1). The high species prediction accuracy (92.46 – 99.86%) for all five families clearly demonstrated that multivariate morphometric analysis is a robust approach to discriminate cryptic species, and a viable alternative to DNA barcoding, which is relatively expensive and time-demanding. In both chapters, the allocation success rates of the CAP models using different combinations of morphometric variables were assessed, considering the practicality and efficiency of the models. Through these processes, I identified the most parsimonious model for each genus, as well as the species prediction accuracy of models when specific variables are missing representing some of the challenges associated with data collection (i.e. chipped otoliths, missing otolith length and weight data).

In Chapter 2, I examined otolith morphometric models on adult teleosts across a wide range of sizes, and identified lower species prediction accuracy for smaller individuals (Figure 7.1). Similarly, in Chapter 3 multivariate models using otolith morphometrics for cryptic lutjanid juveniles had a species prediction accuracy of 85%, but an almost complete discrimination success rate (i.e. 99%) was achieved using body morphometric data (Figure 7.1). These results suggest that: 1) morphometric analysis using head measurements is more effective than using otoliths measurements alone to discriminate cryptic juveniles; and 2) careful interpretation of allocation success results is required, considering the size distribution of specimens examined.

Morphometric approach is undoubtedly more cost-effective compared to molecular approach. The HotSHOT DNA extraction method was applied to identify the cryptic lutjanid juveniles in Chapter 3 and 5. Although this is rapid and cost-efficient compared to other extraction methods (Meeker et al. 2007), it required several items of molecular laboratory equipment (i.e.

thermocycler, electrophoresis tanks and gel imaging system) and a minimum of a day to process 30 samples, with the sequencing cost of AUD7 per sample. In contrast, morphometric analyses required a few minutes to take the measurements with callipers and fit the data in a CAP model to obtain the species identification. Given that otoliths of the study species were routinely collected for fisheries assessments, no additional time was required for otolith dissection. Furthermore, species identification from morphometric analyses can be obtained in field.

The application of these models as a species identification guideline is not limited to the field and laboratory. New cryptic species of teleosts are being discovered at exponential rates, aided by the advancement in molecular studies (Bickford et al., 2007; Bucklin et al., 2011). When a new species is discovered, otolith morphometric models can be applied to revise species identifications using otoliths from archived collections. It can also be applied in dietary studies to identify prey teleost taxa as otoliths are resistant to digestion and can be collected from gastrointestinal contents and faeces (Bowen, 2000; Gales, 1988; Škeljo & Ferri, 2012).

7.1.2 Ecological insights of morphologically cryptic species

Based on the niche principle, niche partitioning is a fundamental process for species to co-exist within an ecosystem (Gause, 1934). Ecomorphology theory posits that the more similar the morphology is, the more similar the niche requirements (Hulsey & León, 2005; Meyer, 1989; Wainwright & Richard, 1995). The combination of these theories generated the hypothesis that cryptic species differentiate their niche requirements to co-exist, and that differentiation is subtle, if any, due to their similar morphology. This hypothesis was tested through metabarcoding dietary studies on adult and juvenile *L. erythropterus* and *L. malabaricus* (Chapter 4 and 5). Inter-specific diet partitioning patterns were significant during both adult and juvenile stages (Figure 7.1), supporting niche principles. The patterns were less distinctive during the juvenile stages, which was possibly due to the lack of morphological differentiation (which can only be distinguished by applying morphometric analyses or DNA barcoding (Chapter 3)), supporting ecomorphology theory. Hence, the hypothesis was accepted.

‘Integrative taxonomy’ is a concept where cryptic species are discriminated by compositing different data types such as genetics, morphology, ecology, behaviour and geography (Edwards & Knowles, 2014; Padiál et al., 2010). My findings highlight the utility of this approach. Diet partitioning patterns during the adult stage were identified in Chapter 5. They were characterised by the high diversity of malacostracan crustaceans for *L. malabaricus* and

soft bodied invertebrates (e.g., tunicates, comb jellies and medusae) for *L. erythropterus* (Figure 7.1). Interestingly, these diet differentiations are supported by several characteristics which are specific to each species. For instance, adult *L. malabaricus* have a longer body length (determined in Chapter 6) and larger mouth compared to *L. erythropterus*. In addition, weaker schooling behaviour of *L. malabaricus* was observed compared to that observed for *L. erythropterus* (Chapter 6). The larger body and mouth and weaker schooling behaviour of *L. malabaricus* may be advantageous to capture individual, fast-moving, hard-shelled crustaceans, whereas *L. erythropterus*, with a smaller mouth, may have shifted their choice of prey to slower, soft-bodied invertebrates. The habitat of their major prey categories also coincides with the fine scale, vertical habitat partitioning of these two species. *Lutjanus malabaricus* is considered a true demersal species whereas *L. erythropterus* is considered benthopelagic (S. Newman, C. Wakefield personal *in-situ* observations from underwater video). Correspondingly, malacostracan crustaceans are benthic or epibenthic while soft bodied invertebrates generally occupy the water column. Associations between these factors, such as diet, habitat, morphology and behaviour, support the concept of integrative taxonomy (Edwards & Knowles, 2014; Padial et al., 2010), and highlight the complex ecological interactions and adaptations required for the coexistence of cryptic species within an ecosystem.

Inter-specific diet partitioning was revealed not only during the adult stage of *L. erythropterus* and *L. malabaricus*, but also during the morphologically cryptic juvenile stage (Chapter 5) (Figure 7.1). While adult ecological interactions of *L. erythropterus* and *L. malabaricus* are explicit, the mechanisms of partitioning and coexistence of the juveniles remain unclear, due to the lack of morphological differences and little data or information being available to determine if any fine scale differentiations in habitat and/or behaviour exist. Niche partitioning occurs in one or more dimensions such as diet, space and time (Fišer et al., 2018; Navarro et al., 2013). Fry et al. (2009) identified the peak spawning season of *L. erythropterus* to range from July to December and for *L. malabaricus* to extend from September to March for the northern Australian population. The shift in spawning seasons may have been selected to allow new recruits to access adequate resources for growth and survival, which consequently reduces interspecific competition and facilitates the co-existence of the cryptic species in nursery grounds. Temporal variations in diet and juvenile occurrences were not examined in Chapter 5 and 6 respectively, and these should be assessed in future studies to better understand the evolutionary and niche mechanisms of the cryptic juveniles (Figure 7.1).

Information on niche partitioning of cryptic species provides insights on the evolutionary mechanisms that underpin cryptic morphological diversity. These mechanisms may be

explained using one of the three hypotheses suggested by Fiser et al. (2018). Firstly, the *recent divergence* hypothesis refers to a speciation event that occurred recently and where morphological differentiation is not yet evident. Secondly, the *phylogenetic niche conservatism* hypothesis posits that species diverged by micro niche partitioning, yet morphological differentiation is constrained by selection such as similar niches or mimicking for survival advantage (i.e. reduced predation). Thirdly, the *morphological convergence* hypothesis postulates that distantly related species evolved a similar morphology based on selection. *Lutjanus erythropterus* and *L. malabaricus* are sister taxa, which speciated less than 5 Ma ago during the Plio-Pleistocene period (Frédérich & Santini, 2017). This would exclude the possibility of a case of *morphological convergence* and point towards the *recent divergence* hypothesis. However, given the diet partitioning and the associated differentiations shown in this study, *phylogenetic niche conservatism* is likely to be the case for these species.

7.1.3 Ontogenetic shifts in niche

My research revealed ontogenetic shifts in both diet and habitat use of *L. erythropterus* and *L. malabaricus*, using metabarcoding and species distribution model approaches (Chapter 5 and 6, respectively) (Figure 7.1). These findings highlight a close association between diet and habitat and suggest that ontogenetic migration is based not only on finding a refuge from predation, but also on accessing food resources and minimising intraspecific competition. My SDMs generated length-specific distribution predictive maps for these species, indicating a clear ontogenetic migration pattern and essential fish habitat requirement for the morphologically cryptic juveniles (Chapter 6). These maps provide valuable information for EBFM planning specific to different life stages, which are further discussed below.

7.2 Future implications, management and conservation

The interpretation of my data provides an understanding of the speciation mechanisms and specialised niche differentiations of *L. erythropterus* and *L. malabaricus*, which has important implications for fisheries and biodiversity management (Figure 7.1). For instance, in Chapter 5, I revealed that *L. malabaricus* adults predominantly feed on benthic malacostracan crustaceans, whereas the diet of *L. erythropterus* adults consist of prey taxa that are often suspended in the water column. As a result, the former may be more dependent on benthic habitat, and consequently more susceptible to certain fishing methods with adverse effect on the benthos (i.e. bottom trawling), than the latter. However, noting the adaptive capacity of fishers that operate fish trawl nets and the technology available to monitor where the gear is

in the water column (board sensors), means that any species in the water column is vulnerable to fish trawl gear. This does, however, suggest that different cryptic species might require different ecosystem-based management strategies. Furthermore, *L. erythropterus* and *L. malabaricus* have a different size distribution (Chapter 6), size at sexual maturity and spawning seasons (Fry et al., 2009), implying different optimal requirements in regard to catch size limits and/or seasonal closures. These data clearly highlight the relevance of high-resolution assessments on species-specific biology, ecology and fisheries, as well as separate management and conservation strategies for each cryptic species (Bickford et al., 2007; Craig et al., 2009).

The first, fundamental step to achieve this is accurate species discrimination of cryptic species during assessments, which is possible with minimal time requirements and can be undertaken in a cost-effective manner using morphometric analyses (Chapter 2 and 3). The body morphometric multivariate model for cryptic juveniles of *L. erythropterus* and *L. malabaricus* (Chapter 3) is particularly useful to separate these species and assess the relative impacts of different elements of any bycatch components within prawn trawl nets (Stobutzki et al., 2001; Tonks et al., 2008). Despite these findings and the high commercial and recreational value of *L. erythropterus* and *L. malabaricus*, these species are often categorised as “red snappers” and are combined into a single species group within catch data in some parts of the world (Blaber et al., 2005; Leigh & O’Neill, 2016). The results of my thesis allow a mechanism to separate these catches into species-specific elements for assessment and management purposes.

The ontogenetic shifts in niche requirements, which I identified in Chapter 5 and 6, also have important implications for effective ecosystem-based management strategies targeting different life stages. For instance, recruitment success rates and survival of juveniles are highly dependent on nursery ground conditions, possibly due to the use of that habitat as a shelter from predators (Almany, 2004; Feary et al., 2007; Jones et al., 2004; Lindholm et al., 2001). Therefore, in areas where fishing effort is high and concentrated, alternative management strategies that seek to minimise any adverse effects on juvenile EFH and to enhance the survival rates of juveniles may be required. These alternative management strategies include closed areas (juvenile protected areas), and potentially the prohibition of some fishing techniques (i.e. bottom trawling) to limit adverse impacts. The length-specific distribution predictive maps (Chapter 6) that I have derived can be used to determine any priority management areas to effectively protect critical life stages.

Fishery management must consider not only commercial, but also recreational fisheries given their large annual total catch and economic value (Arlinghaus et al., 2019; Cooke & Cowx, 2006; Raguragavan et al., 2013; Ryan et al., 2019; Tate et al., 2019). There is a common belief

among the general public that recreational fishers have a lower impact on fish stocks and ecosystems compared to commercial fishers (Arlinghaus et al., 2019; Cooke & Cowx, 2006). However, that may not necessarily be the case. For example, there are misconceptions about the relative impacts of bottom trawling on fish stocks. In many cases, the footprint of fish trawling is much lower than is perceived (Amoroso et al., 2018). However, significant habitat destruction, such as reduced seagrass cover caused by the propellers and anchors of recreational fishery boats has impacted juvenile EFH in some species, by negatively affecting juvenile growth and abundance (Hansen et al., 2019; Lloret et al., 2008; Whitfield & Becker, 2014). Furthermore, the annual recreational catch of individual fishers may seem small but can add up to a substantial total catch (i.e. over 1.32 million individual finfish (kept or released) in 2017/18 in Western Australia) (Tate et al., 2019). Thus, collecting accurate, species-level catch data in recreational fisheries is critical. However, recreational catches are often underreported, particularly for undersized juveniles, which are caught-and-released (Cooke & Schramm, 2007; Santos et al., 2017). Additionally, several cryptic species, including *L. erythropterus* and *L. malabaricus*, are grouped for catch data and analyses as recreational fishers may not be able to distinguish them (West et al., 2012). This issue may be solved with *in-situ* image analyses through smartphone applications based on artificial intelligence algorithms to identify the species and report the catch with fish length and GPS coordinates (Lukhtanov, 2019; Wäldchen & Mäder, 2018).

Another challenge in recreational fisheries management is that recreational fishers consist of a diverse group with different experience, equipment, origin (i.e. locals versus tourists), and objectives such as social benefit, quantity of catch or a single large trophy. Consequently, they have different (and often conflicting) levels of conservation interests and participation in management processes (Arlinghaus et al., 2019). Therefore, common management targets for commercial fisheries, such as maximum sustainable yield, cannot be directly transferred to the recreational fishery management context. These factors highlight the importance of communication and education of the general public to increase their understanding and awareness of regulations and their rationale (Bennett et al., 2017; Hunt et al., 2013). Using various resources including media, education at schools, community outreach to remote areas and smartphone applications could help to ultimately achieve management and conservation objectives.

7.3 Limitations of this thesis and future research directions

7.3.1 Spatial and temporal comparisons

The life history, ecology and behaviour of marine teleosts are influenced by temporal and spatial changes in factors such as water temperature, food and habitat availability, oceanography and population connectivity (Birt et al., 2012; Malcolm et al., 2007; Myers et al., 2016; West et al., 2003). This highlights the importance of considering intra-specific variations through time and space when conducting studies. I acknowledge that the data collected, analysed and presented in my thesis were limited to specific time periods and locations (Figure 7.1). For instance, spatial variations in otolith morphometry of *L. malabaricus* juveniles were identified between Western Australia (WA) and Queensland (QLD) in Chapter 3, which are possibly attributable to environmental factors and restricted gene flow (Campana & Casselman, 1993; Thomas et al., 2014; Zhuang et al., 2015). This emphasises the need to validate location-specific species identification models throughout their distributional ranges, as well as to investigate population structures. Similarly, temporal and spatial variation in community structure and prey composition have also been described in previous studies (Bostrom et al., 2012; Marsh et al., 2017; Myers et al., 2016). However, sampling for the dietary study in Chapter 5 was restricted to the Pilbara region of WA and the winter months of one year. The length specific predictive maps in Chapter 6 were also limited to WA, within certain depth ranges. Further studies are required to investigate the spatial and temporal variation in both diet and distribution patterns.

7.3.2 Further studies on juvenile ecology

While my research provides a better understanding of juvenile fish ecology, a few challenges were encountered (Figure 7.1). In Chapter 6, the frequency-of-occurrence of *L. erythropterus* and *L. malabaricus* juveniles in Baited Remote Underwater Video systems (BRUVs) samples was significantly lower than those of adults, which was possibly underestimated due to poorer visibility at inshore nursery grounds (i.e. high turbidity areas), reduced sampling in inshore nursery grounds, and/or agonistic behaviours of larger, predatory species, and/or displacement by larger sized fish at the time of MaxN (a limitation of BRUVs) (Coghlan et al., 2017; Dunlop et al., 2015; Stoner et al., 2008). Secondly, inter-specific habitat partitioning patterns during the juvenile stage could not be assessed due to the inability of cryptic juvenile discrimination in BRUVs images. Further studies are required to better understand the species-specific, fine-scale essential fish habitat, particularly in nearshore waters. This could be achieved by

collecting more juvenile occurrence data in targeted surveys using trawls in association with BRUVs, followed by species identification with a morphometric analysis. Unbaited Remote Underwater Video systems (RUVs) could also be trialled and they may potentially improve the juvenile occurrence rates as the lack of bait might result in fewer predatory fish that juveniles might avoid (Myers et al., 2016; Piggott et al., 2020). Given nearly total species prediction success with only three body morphometric variables (Chapter 3), species discrimination in video images using this approach maybe achievable, although it requires further validation.

7.3.3 Dietary metabarcoding studies

The metabarcoding approach in dietary studies poses numerous advantages, yet there are also limitations associated with this technique (Figure 7.1). Firstly, an incomplete reference database could result in a higher taxonomic level assignment or potential misclassification, thus requiring increased effort to build a comprehensive species database. Secondly, quantitative analyses are limited due to a number of sources causing bias on sequence read counts, such as different DNA abundance in templates, primer choice including blocking primers, and the different states of digestion of prey materials (Deagle et al., 2019; Elbrecht & Leese, 2015; Piñol et al., 2015). Positive correlations between relative read abundance (RRA), and independent measures of abundances have been identified in previous studies (Deagle et al., 2019; Deagle & Tollit, 2007; Leray & Knowlton, 2015). However, there is a need to assess the viability of RRA as a proxy for relative abundance of prey taxa, for each prey/predator species, and for each primer including blocking primers. Dietary metabarcoding analyses has a limitation to detect cannibalism as it cannot determine whether host DNA sequences were from cannibalised prey or host tissue. Cannibalistic behaviours occur in teleost fish, particularly in culture tanks and/or early life stages such as during metamorphosis, yet those in *L. erythropterus* and *L. malabaricus* have not been reported in wild (Manica, 2002). The risk of filial cannibalism for juveniles is likely to be reduced through ontogenetic habitat partitioning determined in Chapter 6. In summary, future studies in the field of DNA metabarcoding for dietary analyses include building a comprehensive database and validation of RRA using a range of taxa-specific and universal primers and blocking primers (Figure 7.1).

7.3.4 Expansions to other taxa and monitoring studies

In order to further advance ecological knowledge, and to assist fishery assessments and management plans, the integrative approaches applied in this thesis (i.e. morphometric

analyses, metabarcoding, SDMs, BRUVs GlobalArchive data) can be expanded to other taxa (Figure 7.1). Furthermore, these ecological studies may provide an insight into wider ecosystem processes. For instance, prey species composition obtained by metabarcoding dietary studies can profile a wide diversity of the ecosystem that extends beyond the studied taxa, and could contribute to biodiversity monitoring programs (Sousa et al., 2019). The latitudinal distribution range and hotspots of *L. erythropterus* and *L. malabaricus* obtained in Chapter 6 provide baseline information for long-term observations to understand potential responses to climate change. This study can be expanded to other taxa to provide baseline distribution and hotspot information to support both current management approaches and understand any potential impacts of climate change.

7.4 Thesis conclusion

How can we effectively discriminate among fishery important, cryptic species for assessment purposes? How can cryptic species co-exist within an ecosystem? How can we manage species and populations across different life history stages within an EBFM framework? These questions arise from fundamental principles linked to conservation, fisheries management, and applied ecology. I have addressed these questions throughout this thesis through morphometric analyses and ecological studies on sympatric, cryptic teleost species that are important to fisheries. Morphometrics analyses on 11 cryptic teleost species from five genera have validated robust, and cost-effective species identification tools, which can be applied in future studies and assessments of those species. My research also revealed the mechanisms that allow two cryptic *Lutjanus* species to minimise inter- and intra-specific competitions and co-exist within an ecosystem by having different food, habitat, morphology, and behaviours, facilitating effective resource sharing. The new ecological knowledge for these species suggests that each cryptic species and life history stage have different levels of susceptibility to environmental changes and therefore may require different management strategies. The robust species identification tools as well as the detailed ecological knowledge of cryptic teleosts that this thesis identified provide significant contributions to fishery science and ecosystem-based management strategies.

Bibliography

- Allen, G. R. (1985). *Snappers of the world. FAO Species Catalogue, Vol.6.* FAO.
- Almany, G. R. (2004). Differential effects of habitat complexity, predators and competitors on abundance of juvenile and adult coral reef fishes. *Oecologia*, *141*(1), 105–113.
<https://doi.org/10.1007/s00442-004-1617-0>
- Altschul, S. F., Gish, W., Miller, W., Myers, E. W., & Lipman, D. J. (1990). Basic local alignment search tool. *Journal of Molecular Biology*, *215*, 403–410.
[https://doi.org/10.1016/S0022-2836\(05\)80360-2](https://doi.org/10.1016/S0022-2836(05)80360-2)
- Amoroso, R. O., Pitcher, C. R., Rijnsdorp, A. D., McConnaughey, R. A., Parma, A. M., Suuronen, P., Eigaard, O. R., Bastardie, F., Hintzen, N. T., Althaus, F., Baird, S. J., Black, J., Buhl-Mortensen, L., Campbell, A. B., Catarino, R., Collie, J., Cowan, J. H., Durholtz, D., Engstrom, N., ... Jennings, S. (2018). Bottom trawl fishing footprints on the world's continental shelves. *Proceedings of the National Academy of Sciences of the United States of America*, *115*(43), E10275–E10282.
<https://doi.org/10.1073/pnas.1802379115>
- Anderson, M. J., Gorley, R. N., & Clarke, K. R. (2008). *PERMANOVA+ for PRIMER: Guide to Software and Statistical Methods.* PRIMER-E.
- Anderson, M. J., & Willis, T. J. (2003). Canonical analysis of principal coordinates: A useful method of constrained ordination for ecology. *Ecology*, *84*(2), 511–525.
[https://doi.org/10.1890/0012-9658\(2003\)084\[0511:CAOPCA\]2.0.CO;2](https://doi.org/10.1890/0012-9658(2003)084[0511:CAOPCA]2.0.CO;2)
- Arlinghaus, R., Abbott, J. K., Fenichel, E. P., Carpenter, S. R., Hunt, L. M., Alós, J., Klefoth, T., Cooke, S. J., Hilborn, R., Jensen, O. P., Wilberg, M. J., Post, J. R., & Manfredo, M. J. (2019). Governing the recreational dimension of global fisheries. *Proceedings of the National Academy of Sciences of the United States of America*, *116*(12), 5209–5213.
<https://doi.org/https://doi.org/10.1073/pnas.1902796116>
- Ashrafi, S., Bontadina, F., Kiefer, A., Pavlinic, I., & Arlettaz, R. (2010). Multiple morphological characters needed for field identification of cryptic long-eared bat species around the Swiss Alps. *Journal of Zoology*, *281*, 241–248.
<https://doi.org/10.1111/j.1469-7998.2010.00697.x>
- Baker, A. M., Bartlett, C., Bunn, S. E., Goudkamp, K., Sheldon, F., & Huges, J. M. (2003).

- Cryptic species and morphological plasticity in long-lived bivalves (Unionoida: Hyriidae) from inland Australia. *Molecular Ecology*, 12, 2707–2717.
<https://doi.org/10.1046/j.1365-294X.2003.01941.x>
- Bani, A., Poursaeid, S., & Tuset, V. M. (2013). Comparative morphology of the sagittal otolith in three species of south Caspian gobies. *Journal of Fish Biology*, 82(4), 1321–1332. <https://doi.org/10.1111/jfb.12073>
- Barnette, M. C. (2001). A review of the fishing gear utilized within the Southeast Region and their potential impacts on essential fish habitat. In *NOAA Technical Memorandum NMFS-SEFC* (Issue 449).
- Begg, G. A., Campana, S. E., Fowler, A. J., & Suthers, I. M. (2005). Otolith research and application: Current directions in innovation and implementation. *Marine and Freshwater Research*, 56(5), 477–483. <https://doi.org/10.1071/MF05111>
- Bellido, J. M., Brown, A. M., Valavanis, V. D., Giráldez, A., Pierce, G. J., Iglesias, M., & Palialexis, A. (2008). Identifying essential fish habitat for small pelagic species in Spanish Mediterranean waters. *Hydrobiologia*, 612(1), 171–184.
<https://doi.org/10.1007/s10750-008-9481-2>
- Bellwood, D. R., Hughes, T. P., Folke, C., & Nyström, M. (2004). Confronting the coral reef crisis. *Nature*, 429(6994), 827–833. <https://doi.org/10.1038/nature02691>
- Bennett, N. J., Roth, R., Klain, S. C., Chan, K., Christie, P., Clark, D. A., Cullman, G., Curran, D., Durbin, T. J., Epstein, G., Greenberg, A., Nelson, M. P., Sandlos, J., Stedman, R., Teel, T. L., Thomas, R., Veríssimo, D., & Wyborn, C. (2017). Conservation social science: Understanding and integrating human dimensions to improve conservation. *Biological Conservation*, 205, 93–108.
<https://doi.org/10.1016/j.biocon.2016.10.006>
- Benson, D. A., Cavanaugh, M., Clark, K., Karsch-mizrachi, I., Lipman, D. J., Ostell, J., & Sayers, E. W. (2017). GenBank. *Nucleic Acids Research*, 45, D37–D42.
<https://doi.org/10.1093/nar/gkw1070>
- Berry, T. E., Osterrieder, S. K., Murray, D. C., Coghlan, M. L., Richardson, A. J., Greal, A. K., Stat, M., Bejder, L., & Bunce, M. (2017). DNA metabarcoding for diet analysis and biodiversity : A case study using the endangered Australian sea lion (*Neophoca cinerea*). *Ecology and Evolution*, 7, 5435–5453. <https://doi.org/10.1002/ece3.3123>

- Berry, T. E., Saunders, B. J., Coghlan, M. L., Stat, M., Jarman, S., Richardson, A. J., Davies, C. H., Berry, O., Harvey, E. S., & Bunce, M. (2019). Marine environmental DNA biomonitoring reveals seasonal patterns in biodiversity and identifies ecosystem responses to anomalous climatic events. *PLoS Genetics*, *15*(2), e1007943. <https://doi.org/10.1371/journal.pgen.1007943>
- Bickford, D., Lohman, D. J., Sodhi, N. S., Ng, P. K. L., Meier, R., Winker, K., Ingram, K. K., & Das, I. (2007). Cryptic species as a window on diversity and conservation. *Trends in Ecology and Evolution*, *22*(3), 148–155. <https://doi.org/10.1016/j.tree.2006.11.004>
- Birt, M. J., Harvey, E. S., & Langlois, T. J. (2012). Within and between day variability in temperate reef fish assemblages: Learned response to baited video. *Journal of Experimental Marine Biology and Ecology*, *416–417*, 92–100. <https://doi.org/10.1016/j.jembe.2012.02.011>
- Blaber, S. J. M., Dichmont, C. M., Buckworth, R. C., Badrudin, Sumiono, B., Nurhakim, S., Iskandar, B., Fegan, B., Ramm, D. C., & Salini, J. P. (2005). Shared stocks of snappers (Lutjanidae) in Australia and Indonesia: Integrating biology, population dynamics and socio-economics to examine management scenarios. *Reviews in Fish Biology and Fisheries*, *15*, 111–127. <https://doi.org/10.1007/s11160-005-3887-y>
- Bolger, A. M., Lohse, M., & Usadel, B. (2014). Trimmomatic: A flexible trimmer for Illumina sequence data. *Bioinformatics*, *30*(15), 2114–2120. <https://doi.org/10.1093/bioinformatics/btu170>
- Bostrom, M. K., Ostman, O., Bergenius, M. A. J., & Lunneryd, S. G. (2012). Cormorant diet in relation to temporal changes in fish communities. *ICES Journal of Marine Science*, *69*, 175–183. <https://doi.org/10.4135/9781412953924.n678>
- Bowen, W. D. (2000). Reconstruction of pinniped diets: Accounting for complete digestion of otoliths and cephalopod beaks. *Canadian Journal of Fisheries and Aquatic Sciences*, *57*(5), 898–905. <https://doi.org/10.1139/f00-032>
- Bray, D. J., & Gomon, M. F. (2018). *Fishes of Australia*. Museums Victoria and OzFishNet. <http://fishesofaustralia.net.au/>
- Brewer, D. T., Blaber, S. J. M., & Salini, J. P. (1991). Predation on penaeid prawns by fishes in Albatross Bay, Gulf of Carpentaria. *Marine Biology*, *109*, 231–240. <https://doi.org/10.1007/BF01319391>

- Brouard, F., & Grandperrin, R. (1985). *Deep-bottom fishes of the outer reef slope in Vanuatu. South Pacific Commission 7th Regional Technical Meeting on Fisheries.*
- Bucklin, A., Steinke, D., & Blanco-Bercial, L. (2011). DNA barcoding of marine metazoa. *Annual Review of Marine Science*, 3, 471–508. <https://doi.org/10.1146/annurev-marine-120308-080950>
- Burnham, K. P., & Anderson, D. R. (2004). Multimodel inference: Understanding AIC and BIC in model selection. *Sociological Methods and Research*, 33(2), 261–304. <https://doi.org/10.1177/0049124104268644>
- Buschmann, T. (2017). DNABarcodes: An R package for the systematic construction of DNA sample tags. *Bioinformatics*, 33, 920–922. <https://doi.org/10.1093/bioinformatics/btw759>
- Callahan, B. J., McMurdie, P. J., & Holmes, S. P. (2017). Exact sequence variants should replace operational taxonomic units in marker-gene data analysis. *ISME Journal*, 11(12), 2639–2643. <https://doi.org/10.1038/ismej.2017.119>
- Callahan, B. J., McMurdie, P. J., Rosen, M. J., Han, A. W., Johnson, A. J. A., & Holmes, S. P. (2016). DADA2: High-resolution sample inference from Illumina amplicon data. *Nature Methods*, 13, 581–583. <https://doi.org/10.1038/nmeth.3869>
- Campana, S. E. (2005). Otolith science entering the 21st century. *Marine and Freshwater Research*, 56(5), 485–495. <https://doi.org/10.1071/MF04147>
- Campana, S. E., & Casselman, J. M. (1993). Stock discrimination using otolith shape analysis. *Canadian Journal of Fisheries and Aquatic Sciences*, 50(5), 1062–1083. <https://doi.org/10.1139/f93-123>
- Cappo, M., Harvey, E. S., Malcolm, H., & Speare, P. (2003). Potential of video techniques to monitor diversity, abundance and size of fish in studies of marine protected areas. *World Congress on Aquatic Protected Areas*, 455–464.
- Cappo, M., Harvey, E. S., & Shortis, M. (2007). Counting and measuring fish with baited video techniques - an overview. *Australian Society for Fish Biology 2006 Workshop Proceedings*, 101–114. https://doi.org/10.1007/978-1-62703-724-2_1
- Cappo, M., Speare, P., Wassenberg, T. J., Harvey, E. S., Rees, M., Heyward, A., & Pitcher, R. (2001). Use of Baited Remote Underwater Video Stations (BRUVS) to survey

- demersal fish – how deep and meaningful? In E. S. Harvey & M. Cappo (Eds.), *Direct sensing of the size frequency and abundance of target and non-target fauna in Australian Fisheries - a national workshop* (pp. 63–71).
- Casey, J. M., Meyer, C. P., Morat, F., Brandl, S. J., Planes, S., & Parravicini, V. (2019). Reconstructing hyperdiverse food webs: gut content metabarcoding as a tool to disentangle trophic interactions on coral reefs. *Methods in Ecology and Evolution*, *10*(8), 1157–1170. <https://doi.org/10.1111/2041-210X.13206>
- Cazorla, D., & Acosta, M. (2003). Multivariate Morphometric Discrimination Among Three Species of *Lutzomyia* subgenus *Micropygomyia* (Diptera: Psychodidae). *Journal of Medical Entomology*, *40*, 750–754. <https://doi.org/10.1603/0022-2585-40.6.750>
- Chen, S. H., Lin, C. Y., Cho, C. S., Lo, C. Z., & Hsiung, C. A. (2003). Primer Design Assistant (PDA): A web-based primer design tool. *Nucleic Acids Research*, *31*(13), 3751–3754. <https://doi.org/10.1093/nar/gkg560>
- Cheung, W. W. L., Meeuwig, J. J., Feng, M., Harvey, E. S., Lam, V. W. H., Langlois, T., Slawinski, D., Sun, C., & Pauly, D. (2012). Climate-change induced tropicalisation of marine communities in Western Australia. *Marine and Freshwater Research*, *63*(5), 415–427. <https://doi.org/10.1071/MF11205>
- Choat, J. H., Klanten, O. S., Van Herwerden, L., Robertson, D. R., & Clements, K. D. (2012). Patterns and processes in the evolutionary history of parrotfishes (Family Labridae). *Biological Journal of the Linnean Society*, *107*(3), 529–557. <https://doi.org/10.1111/j.1095-8312.2012.01959.x>
- Ciannelli, L., Fauchald, P., Chan, K. S., Agostini, V. N., & Dingsør, G. E. (2008). Spatial fisheries ecology: Recent progress and future prospects. *Journal of Marine Systems*, *71*(3–4), 223–236. <https://doi.org/10.1016/j.jmarsys.2007.02.031>
- Clarke, K. R., Gorley, R. N., Somerfield, P. J., & Warwick, R. M. (2014). *Change in marine communities: An approach to statistical analysis and interpretation, 3rd edition*. PRIMER-E: Plymouth.
- Clifton, K. B., & Motta, P. J. (1998). Feeding morphology, diet, and ecomorphological relationships among Five Caribbean Labrids (Teleostei, Labridae). *Copeia*, *4*, 953–966.
- Cocheret De La Morinière, E., Pollux, B. J. A., Nagelkerken, I., & Van Der Velde, G. (2003). Diet shifts of Caribbean grunts (Haemulidae) and snappers (Lutjanidae) and the

- relation with nursery-to-coral reef migrations. *Estuarine, Coastal and Shelf Science*, 57(5–6), 1079–1089. [https://doi.org/10.1016/S0272-7714\(03\)00011-8](https://doi.org/10.1016/S0272-7714(03)00011-8)
- Cocheret de la Morinière, E., Pollux, B. J. A., Nagelkerken, I., Velde, G. Van Der, & Morinie, E. C. De. (2003). Diet shifts of Caribbean grunts (Haemulidae) and snappers (Lutjanidae) and the relation with nursery-to-coral reef migrations. *Estuarine, Coastal and Shelf Science*, 57, 1079–1089. [https://doi.org/10.1016/S0272-7714\(03\)00011-8](https://doi.org/10.1016/S0272-7714(03)00011-8)
- Coghlan, A. R., McLean, D. L., Harvey, E. S., & Langlois, T. J. (2017). Does fish behaviour bias abundance and length information collected by baited underwater video? *Journal of Experimental Marine Biology and Ecology*, 497(May 2016), 143–151. <https://doi.org/10.1016/j.jembe.2017.09.005>
- Collins, F. H., & Paskewitz, S. M. (1996). A review of the use of ribosomal DNA (rDNA) to differentiate among cryptic Anopheles species. *Insect Molecular Biology*, 5(1), 1–9. <https://doi.org/10.1111/j.1365-2583.1996.tb00034.x>
- Colwell, R. K. (2013). *EstimateS: Statistical estimation of species richness and shared species from samples. Version 9. User's Guide*. <http://purl.oclc.org/estimates>
- Compton, T. J., Morrison, M. A., Leathwick, J. R., & Carbines, G. D. (2012). Ontogenetic habitat associations of a demersal fish species, *Pagrus auratus*, identified using boosted regression trees. *Marine Ecology Progress Series*, 462, 219–230. <https://doi.org/10.3354/meps09790>
- Conover, D. O., Travis, J., & Coleman, F. C. (2000). Essential fish habitat and marine reserves: An introduction to the second mote symposium in fisheries ecology. *Bulletin of Marine Science*, 66(3), 527–534.
- Cooke, S. J., & Cowx, I. G. (2006). Contrasting recreational and commercial fishing: Searching for common issues to promote unified conservation of fisheries resources and aquatic environments. *Biological Conservation*, 128(1), 93–108. <https://doi.org/10.1016/j.biocon.2005.09.019>
- Cooke, S. J., & Schramm, H. L. (2007). Catch-and-release science and its application to conservation and management of recreational fisheries. *Fisheries Management and Ecology*, 14(2), 73–79. <https://doi.org/10.1111/j.1365-2400.2007.00527.x>
- Cox, E. F. (1994). Resource use by corallivorous butterflyfishes (Family Chaetodontidae) in Hawaii. *Bulletin of Marine Science*, 54, 535–545.

- Craig, M. T., Graham, R. T., Torres, R. A., Hyde, J. R., Freitas, M. O., Ferreira, B. P., Hostim-Silva, M., Gerhardinger, L. C., Bertoncini, A. A., & Robertson, D. R. (2009). How many species of goliath grouper are there? Cryptic genetic divergence in a threatened marine fish and the resurrection of a geopolitical species. *Endangered Species Research*, 7(3), 167–174. <https://doi.org/10.3354/esr00117>
- Crowder, L., & Norse, E. (2008). Essential ecological insights for marine ecosystem-based management and marine spatial planning. *Marine Policy*, 32(5), 772–778. <https://doi.org/10.1016/j.marpol.2008.03.012>
- Cure, K., Hobbs, J. P. A., Langlois, T. J., Abdo, D. A., Bennett, S., & Harvey, E. S. (2018). Distributional responses to marine heat waves: insights from length frequencies across the geographic range of the endemic reef fish *Choerodon rubescens*. *Marine Biology*, 165(1). <https://doi.org/10.1007/s00227-017-3259-x>
- Dahlgren, C. P., & Eggleston, D. B. (2000). Ecological Processes underlying ontogenetic habitat shifts in a coral reef fish. *Ecology*, 81(8), 2227–2240. [https://doi.org/10.1890/0012-9658\(2000\)081\[2227:EPUOHS\]2.0.CO;2](https://doi.org/10.1890/0012-9658(2000)081[2227:EPUOHS]2.0.CO;2)
- Dance, M. A., Rooker, J. R., Kline, R. J., Quigg, A., Stunz, G. R., Wells, R. J. D., Lara, K., Lee, J., & Suarez, B. (2021). Importance of low-relief nursery habitat for reef fishes. *Ecosphere*, 12(6), e03542. <https://doi.org/10.1002/ecs2.3542>
- Darwin, C. M. A. (1859). *On the origin of species by means of natural selection*.
- Deagle, B. E., Chiaradia, A., McInnes, J., & Jarman, S. N. (2010). Pyrosequencing faecal DNA to determine diet of little penguins: Is what goes in what comes out? *Conservation Genetics*, 11(5), 2039–2048. <https://doi.org/10.1007/s10592-010-0096-6>
- Deagle, B. E., Gales, N. J., Evans, K., Jarman, S. N., Robinson, S., Trebilco, R., & Hindell, M. A. (2007). Studying seabird diet through genetic analysis of faeces : A case study on Macaroni Penguins (*Eudyptes chrysolophus*). *PLoS ONE*, 2(9), e831. <https://doi.org/10.1371/journal.pone.0000831>
- Deagle, B. E., Kirkwood, R., & Jarman, S. N. (2009). Analysis of Australian fur seal diet by pyrosequencing prey DNA in faeces. *Molecular Ecology*, 18(9), 2022–2038. <https://doi.org/10.1111/j.1365-294X.2009.04158.x>
- Deagle, B. E., Thomas, A. C., & McInnes, J. C. (2019). Counting with DNA in metabarcoding studies: how should we convert sequence reads to dietary data?

Molecular Ecology, 28, 391–406. <https://doi.org/doi.org/10.1111/mec.14734>

- Deagle, B. E., Thomas, A. C., Shaffer, A. K., Trites, A. W., & Jarman, S. N. (2013). Quantifying sequence proportions in a DNA-based diet study using Ion Torrent amplicon sequencing: Which counts count? *Molecular Ecology Resources*, 13(4), 620–633. <https://doi.org/10.1111/1755-0998.12103>
- Deagle, B. E., & Tollit, D. J. (2007). Quantitative analysis of prey DNA in pinniped faeces: potential to estimate diet composition? *Conservation Genetics*, 8, 743–747. <https://doi.org/10.1007/s10592-006-9197-7>
- Demartini, E. E., Anderson, T. W., Kenyon, J. C., Beets, J. P., & Friedlander, A. M. (2010). Management implications of juvenile reef fish habitat preferences and coral susceptibility to stressors. *Marine and Freshwater Research*, 61(5), 532–540. <https://doi.org/10.1071/MF09141>
- Diamond, J. M. (1978). Niche shifts and the rediscovery of interspecific competition. *American Scientist*, 66(3), 322–331.
- Drummond, A. J., Ashton, B., Buxton, S., Cheung, M., Cooper, A., Heled, J., Kearse, M., Moir, R., Stones-Havas, S., Sturrock, S., Thierer, T., & Wilson, A. (2010). *Geneious v5.1*.
- Duffy, J. E., Lefcheck, J. S., Stuart-Smith, R. D., Navarrete, S. A., & Edgar, G. J. (2016). Biodiversity enhances reef fish biomass and resistance to climate change. *Proceedings of the National Academy of Sciences of the United States of America*, 113(22), 6230–6235. <https://doi.org/10.1073/pnas.1524465113>
- Dunlop, K. M., Marian Scott, E., Parsons, D., & Bailey, D. M. (2015). Do agonistic behaviours bias baited remote underwater video surveys of fish? *Marine Ecology*, 36(3), 810–818. <https://doi.org/10.1111/maec.12185>
- Edwards, D. E., & Knowles, L. L. (2014). Species detection and individual assignment in species delimitation: can integrative data increase efficacy? *Proceedings of the Royal Society B: Biological Sciences*, 281, 20132765. <https://doi.org/10.4135/9781412972093.n399>
- Elbrecht, V., & Leese, F. (2015). Can DNA-based ecosystem assessments quantify species abundance? Testing primer bias and biomass-sequence relationships with an innovative metabarcoding protocol. *PLoS ONE*, 10(7), 1–16.

<https://doi.org/10.1371/journal.pone.0130324>

- Elith, J., & Leathwick, J. R. (2009). Species distribution models: Ecological explanation and prediction across space and time. *Annual Review of Ecology and Systematics*, *40*, 677–697. <https://doi.org/10.1146/annurev.ecolsys.110308.120159>
- Elith, J., Leathwick, J. R., & Hastie, T. (2008). A working guide to boosted regression trees. *Journal of Animal Ecology*, *77*(4), 802–813. <https://doi.org/10.1111/j.1365-2656.2008.01390.x>
- Elliott, N. G. (1996). Allozyme and mitochondrial DNA analysis of the tropical saddle-tail sea perch, *Lutjanus malabaricus* (Schneider), from Australian Waters. *Marine and Freshwater Research*, *47*, 869–876.
- Elliott, N. G., Haskard, K., & Koslow, J. A. (1995). Morphometric analysis of orange roughy (*Hoplostethus atlanticus*) off the continental slope of southern Australia. *Journal of Fish Biology*, *46*(2), 202–220. <https://doi.org/10.1111/j.1095-8649.1995.tb05962.x>
- Elmqvist, T., Folke, C., Nyström, M., Peterson, G., Bengtsson, J., Walker, B., & Norberg, J. (2003). Response diversity, ecosystem change, and resilience. *Frontiers in Ecology and the Environment*, *1*(9), 488–494. [https://doi.org/10.1890/1540-9295\(2003\)001\[0488:RDECAR\]2.0.CO;2](https://doi.org/10.1890/1540-9295(2003)001[0488:RDECAR]2.0.CO;2)
- FAO. (2014). The state of world fisheries and aquaculture. In *Food and Agriculture Organization of the United Nations, Rome*. <https://doi.org/92-5-105177-1>
- Feary, D. A., Almany, G. R., McCormick, M. I., & Jones, G. P. (2007). Habitat choice, recruitment and the response of coral reef fishes to coral degradation. *Oecologia*, *153*(3), 727–737. <https://doi.org/10.1007/s00442-007-0773-4>
- Fielding, A. H., & Bell, J. F. (1997). A review of methods for the assessment of prediction errors in conservation presence/absence models. *Environmental Conservation*, *24*(1), 38–49. <https://doi.org/10.1017/S0376892997000088>
- Fišer, C., Robinson, C. T., & Malard, F. (2018). Cryptic species as a window into the paradigm shift of the species concept. *Molecular Ecology*, *27*(3), 613–635. <https://doi.org/10.1111/mec.14486>
- Fisher, R. A. (1936). The use of multiple measurements in taxonomic problems. *Annals of Eugenics*, *7*, 179–188.

- Fisher, R. A. (1938). The statistical utilization of multiple measurements. *Annals of Eugenics*, 8, 376–386.
- Fisher, R., Wilson, S. K., Sin, T. M., Lee, A. C., & Langlois, T. J. (2018). A simple function for full-subsets multiple regression in ecology with R. *Ecology and Evolution*, 8(12), 6104–6113. <https://doi.org/10.1002/ece3.4134>
- Frédérich, B., & Santini, F. (2017). Macroevolutionary analysis of the tempo of diversification in snappers and fusiliers (Percomorpha: Lutjanidae). *Belgian Journal of Zoology*, 147(1), 17–35. <https://doi.org/10.26496/bjz.2017.2>
- Froese, R., & Pauly, D. (2018). *FishBase*. World Wide Web Electronic Publication. www.fishbase.org
- Fry, G. C., & Milton, D. A. (2009). Age, growth and mortality estimates for populations of red snappers *Lutjanus erythropterus* and *L. malabaricus* from northern Australia and eastern Indonesia. *Fisheries Science*, 75(5), 1219–1229. <https://doi.org/10.1007/s12562-009-0157-2>
- Fry, G. C., Milton, D. A., Van Der Velde, T., Stobutzki, I., Andamari, R., Badrudin, & Sumiono, B. (2009). Reproductive dynamics and nursery habitat preferences of two commercially important Indo-Pacific red snappers *Lutjanus erythropterus* and *L. malabaricus*. *Fisheries Science*, 75, 145–158. <https://doi.org/10.1007/s12562-008-0034-4>
- Galaiduk, R., Radford, B. T., & Harvey, E. S. (2018). Utilizing individual fish biomass and relative abundance models to map environmental niche associations of adult and juvenile targeted fishes. *Scientific Reports*, 8(1), 1–13. <https://doi.org/10.1038/s41598-018-27774-7>
- Galaiduk, R., Radford, B. T., Saunders, B. J., Newman, S. J., & Harvey, E. S. (2017a). Characterizing ontogenetic habitat shifts in marine fishes: Advancing nascent methods for marine spatial management. *Ecological Applications*, 27(6), 1776–1788. <https://doi.org/10.1002/eap.1565>
- Galaiduk, R., Radford, B. T., Wilson, S. K., & Harvey, E. S. (2017b). Comparing two remote video survey methods for spatial predictions of the distribution and environmental niche suitability of demersal fishes. *Scientific Reports*, 7(1), 1–11. <https://doi.org/10.1038/s41598-017-17946-2>

- Gales, R. P. (1988). The use of otoliths as indicators of Little Penguin *Eudyptula minor* diet. *International Journal of Avian Science*, *130*, 418–426.
- Gause, G. F. (1934). *The struggle for existence* (Williams and Wilkins (ed.)).
- Haak, C. R., Power, M., Cowles, G. W., & Danylchuk, A. J. (2019). Hydrodynamic and isotopic niche differentiation between juveniles of two sympatric cryptic bonefishes, *Albula vulpes* and *Albula goreensis*. *Environmental Biology of Fishes*, *102*(2), 129–145. <https://doi.org/10.1007/s10641-018-0810-7>
- Hamilton, R. J., Almany, G. R., Brown, C. J., Pita, J., Peterson, N. A., & Howard Choat, J. (2017). Logging degrades nursery habitat for an iconic coral reef fish. *Biological Conservation*, *210*, 273–280. <https://doi.org/10.1016/j.biocon.2017.04.024>
- Hansen, J. P., Sundblad, G., Bergström, U., Austin, Å. N., Donadi, S., Eriksson, B. K., & Eklöf, J. S. (2019). Recreational boating degrades vegetation important for fish recruitment. *Ambio*, *48*(6), 539–551. <https://doi.org/10.1007/s13280-018-1088-x>
- Hardin, G. (1960). The competitive exclusion principle. *Science*, *131*, 1292–1297.
- Harper, G. L., King, R. A., Dodd, C. S., Harwood, J. D., Glen, D. M., Bruford, M. W., & Symondson, W. O. C. (2005). Rapid screening of invertebrate predators for multiple prey DNA targets. *Molecular Ecology*, *14*(3), 819–827. <https://doi.org/10.1111/j.1365-294x.2005.02442.x>
- Harvey, E. S., Goetze, J., McLaren, B., Langlois, T., & Shortis, M. R. (2010). The influence of range, angle of view, image resolution and image compression on underwater stereo-video measurements: high definition and broadcast resolution video cameras compared. *Marine Technology Society Journal*, *44*(1), 75–85.
- Harvey, E. S., McLean, D. L., Goetze, J. S., Saunders, B. J., Langlois, T. J., Monk, J., Barrett, N., Wilson, S. K., Holmes, T. H., Ierodiaconou, D., Jordan, A. R., Meekan, M. G., Malcolm, H. A., Heupel, M. R., Harasti, D., Huveneers, C., Knott, N. A., Fairclough, D. V., Currey-Randall, L. M., ... Newman, S. J. (2021). The BRUVs workshop – An Australia-wide synthesis of baited remote underwater video data to answer broad-scale ecological questions about fish, sharks and rays. *Marine Policy*, *127*(January), 104430. <https://doi.org/10.1016/j.marpol.2021.104430>
- Harvey, E. S., & Shortis, M. R. (1995). A System for stereo-video measurement of sub-tidal organisms: Implications for assessments of reef fish stocks. *Marine Technology Society*

Journal, 29, 10–22. <https://doi.org/10.1007/s00227-010-1404-x>

- Hey, J., Waples, R. S., Arnold, M. L., Butlin, R. K., & Harrison, R. G. (2003). Understanding and confronting species uncertainty in biology and conservation. *Trends in Ecology and Evolution*, 18(11), 597–603. <https://doi.org/10.1016/j.tree.2003.08.014>
- Hilborn, R., Maguire, J. J., Parma, A. M., & Rosenberg, A. A. (2001). The precautionary approach and risk management: Can they increase the probability of successes in fishery management? *Canadian Journal of Fisheries and Aquatic Sciences*, 58(1), 99–107. <https://doi.org/10.1139/f00-225>
- Holmlund, C. M., & Hammer, M. (1999). Ecosystem services generated by fish populations. *Ecological Economics*, 29(2), 253–268. [https://doi.org/10.1016/S0921-8009\(99\)00015-4](https://doi.org/10.1016/S0921-8009(99)00015-4)
- Hosmer, D. W., Lemeshow, S., & Sturdivant, R. X. (2013). *Applied Logistic Regression* (Third edit). John Wiley & Sons, Incorporated.
- Huberty, C. J. (1994). *Applied Discriminant Analysis*. Wiley Interscience.
- Hulsey, C. D., & León, F. J. G. D. E. (2005). Cichlid jaw mechanics : linking morphology to feeding specialization. *Functional Ecology*, 19, 487–494. <https://doi.org/10.1111/j.1365-2435.2005.00987.x>
- Hunt, L. M., Sutton, S. G., & Arlinghaus, R. (2013). Illustrating the critical role of human dimensions research for understanding and managing recreational fisheries within a social-ecological system framework. *Fisheries Management and Ecology*, 20(2–3), 111–124. <https://doi.org/10.1111/j.1365-2400.2012.00870.x>
- Iwatsuki, Y. (2013). Review of the *Acanthopagrus latus* complex (Perciformes: Sparidae) with descriptions of three new species from the Indo-West Pacific Ocean. *Journal of Fish Biology*, 83(1), 64–95. <https://doi.org/10.1111/jfb.12151>
- Jarman, S. N., Deagle, B. E., & Gales, N. J. (2004). Group-specific polymerase chain reaction for DNA-based analysis of species diversity and identity in dietary samples. *Molecular Ecology*, 13(5), 1313–1322. <https://doi.org/10.1111/j.1365-294X.2004.02109.x>
- Jarman, S. N., McInnes, J. C., Faux, C., Polanowski, A. M., Marthick, J., Deagle, B. E., Southwell, C., & Emmerson, L. (2013). Adélie penguin population diet monitoring by

- analysis of food DNA in scats. *PLoS ONE*, 8(12), e82227.
<https://doi.org/10.1371/journal.pone.0082227>
- Jarman, S. N., Redd, K. S., & Gales, N. J. (2006). Group-specific primers for amplifying DNA sequences that identify Amphipoda, Cephalopoda, Echinodermata, Gastropoda, Isopoda, Ostracoda and Thoracica. *Molecular Ecology Notes*, 6(1), 268–271.
<https://doi.org/10.1111/j.1471-8286.2005.01172.x>
- Jemaa, S., Bacha, M., Khalaf, G., & Amara, R. (2015). Evidence for population complexity of the European anchovy (*Engraulis encrasicolus*) along its distributional range. *Fisheries Research*, 168, 109–116. <https://doi.org/10.1016/j.fishres.2015.04.004>
- Johnson, N. S., Lewandoski, S. A., & Merkes, C. (2021). Assessment of sea lamprey (*Petromyzon marinus*) diet using DNA metabarcoding of feces. *Ecological Indicators*, 125, 107605. <https://doi.org/10.1016/j.ecolind.2021.107605>
- Jones, G. P., McCormick, M. I., Srinivasan, M., Eagle, J. V., & Paine, R. T. (2004). Coral decline threatens fish biodiversity in marine reserves. *Proceedings of the National Academy of Sciences*, 101, 8251–8253. <https://doi.org/10.1073/pnas.0401277101>
- Kämpke, T., Kieninger, M., & Mecklenburg, M. (2001). Efficient primer design algorithms. *Bioinformatics*, 17(3), 214–225. <https://doi.org/10.1093/bioinformatics/17.3.214>
- Kennelly, S. J. (1995). The issue of bycatch in Australia's demersal trawl fisheries. *Reviews in Fish Biology and Fisheries*, 5(2), 213–234. <https://doi.org/10.1007/BF00179757>
- Kindt, R. (2020). *BiodiversityR: Package for community ecology and suitability analysis* (2.12-1).
- Knowlton, N. (2000). Molecular genetic analyses of species boundaries in the sea. *Hydrobiologia*, 420(1), 73–90. <https://doi.org/10.1023/A:1003933603879>
- Kume, G., Kobari, T., Hirai, J., Kuroda, H., Takeda, T., Ichinomiya, M., Komorita, T., Aita-Noguchi, M., & Hyodo, F. (2021). Diet niche segregation of co-occurring larval stages of mesopelagic and commercially important fishes in the Osumi Strait assessed through morphological, DNA metabarcoding, and stable isotope analyses. *Marine Biology*, 168(6), 1–14. <https://doi.org/10.1007/s00227-020-03810-x>
- Kwak, S. N., Klumpp, D. W., & Park, J. M. (2015). Feeding relationships among juveniles of abundant fish species inhabiting tropical seagrass beds in Cockle Bay, North

- Queensland, Australia. *New Zealand Journal of Marine and Freshwater Research*, 49(2), 205–223. <https://doi.org/10.1080/00288330.2014.990467>
- Laman, E. A., Rooper, C. N., Turner, K., Rooney, S., Cooper, D. W., & Zimmermann, M. (2018). Using species distribution models to describe essential fish habitat in Alaska. *Canadian Journal of Fisheries and Aquatic Sciences*, 75(8), 1230–1255. <https://doi.org/10.1139/cjfas-2017-0181>
- Latour, R. J., Brush, M. J., & Bonzek, C. F. (2003). Toward ecosystem-based fisheries management. *Fisheries*, 28(9), 10–22. [https://doi.org/10.1577/1548-8446\(2003\)28\[10:TEFM\]2.0.CO;2](https://doi.org/10.1577/1548-8446(2003)28[10:TEFM]2.0.CO;2)
- Leathwick, J. R., Elith, J., Francis, M. P., Hastie, T., & Taylor, P. (2006a). Variation in demersal fish species richness in the oceans surrounding New Zealand: An analysis using boosted regression trees. *Marine Ecology Progress Series*, 321, 267–281. <https://doi.org/10.3354/meps321267>
- Leathwick, J. R., Elith, J., & Hastie, T. (2006b). Comparative performance of generalized additive models and multivariate adaptive regression splines for statistical modelling of species distributions. *Ecological Modelling*, 199(2), 188–196. <https://doi.org/10.1016/j.ecolmodel.2006.05.022>
- Leigh, G. M., & O'Neill, M. F. (2016). *Gulf of Carpentaria finfish trawl fishery: maximum sustainable yield*. Department of Agriculture and Fisheries, Queensland.
- Leray, M., Agudelo, N., Mills, S. C., & Meyer, C. P. (2013). Effectiveness of annealing blocking primers versus restriction enzymes for characterization of generalist diets: Unexpected prey revealed in the gut contents of two coral reef fish species. *PLoS ONE*, 8(4), e58076. <https://doi.org/10.1371/journal.pone.0058076>
- Leray, M., Alldredge, A. L., Yang, J. Y., Meyer, C. P., Holbrook, S. J., Schmitt, R. J., Knowlton, N., & Brooks, A. J. (2019). Dietary partitioning promotes the coexistence of planktivorous species on coral reefs. *Molecular Ecology*, 28(10), 2694–2710. <https://doi.org/10.1111/mec.15090>
- Leray, M., Boehm, J. T., Mills, S. C., & Meyer, C. P. (2012). Moorea BIOCOTE barcode library as a tool for understanding predator-prey interactions: Insights into the diet of common predatory coral reef fishes. *Coral Reefs*, 31(2), 383–388. <https://doi.org/10.1007/s00338-011-0845-0>

- Leray, M., & Knowlton, N. (2015). DNA barcoding and metabarcoding of standardized samples reveal patterns of marine benthic diversity. *Proceedings of the National Academy of Sciences*, *112*, 2076–2081. <https://doi.org/10.1073/pnas.1424997112>
- Libungan, L. A., & Pálsson, S. (2015). ShapeR: An R package to study otolith shape variation among fish populations. *PLoS ONE*, *10*(3), e0121102. <https://doi.org/10.1371/journal.pone.0121102>
- Lindholm, J. B., Auster, P. J., Ruth, M., & Kaufman, L. (2001). Modeling the effects of fishing and implications for the design of marine protected areas: Juvenile fish responses to variations in seafloor habitat. *Conservation Biology*, *15*(2), 424–437. <https://doi.org/10.1046/j.1523-1739.2001.015002424.x>
- Link, J. S. (2002). What does ecosystem-based fisheries management mean? *Fisheries*, *27*(4), 18–21.
- Lloret, J., Zaragoza, N., Caballero, D., & Riera, V. (2008). Impacts of recreational boating on the marine environment of Cap de Creus (Mediterranean Sea). *Ocean and Coastal Management*, *51*(11), 749–754. <https://doi.org/10.1016/j.ocecoaman.2008.07.001>
- Longenecker, K. (2007). Devil in the details: High-resolution dietary analysis contradicts a basic assumption of reef-fish diversity models. *Copeia*, *2007*(3), 543–555. [https://doi.org/doi.org/10.1643/0045-8511\(2007\)2007\[543:DITDHD\]2.0.CO;2](https://doi.org/doi.org/10.1643/0045-8511(2007)2007[543:DITDHD]2.0.CO;2)
- Longmore, C., Fogarty, K., Neat, F., Brophy, D., Trueman, C., Milton, A., & Mariani, S. (2010). A comparison of otolith microchemistry and otolith shape analysis for the study of spatial variation in a deep-sea teleost, *Coryphaenoides rupestris*. *Environmental Biology of Fishes*, *89*(3), 591–605. <https://doi.org/10.1007/s10641-010-9674-1>
- Lowe, J. R., Williamson, D. H., Ceccarelli, D. M., Evans, R. D., & Russ, G. R. (2020). Environmental disturbance events drive declines in juvenile wrasse biomass on inshore coral reefs of the Great Barrier Reef. *Environmental Biology of Fishes*, *103*, 1279–1293. <https://doi.org/10.1007/s10641-020-01022-2>
- Lukhtanov, V. A. (2019). Species Delimitation and Analysis of Cryptic Species Diversity in the XXI Century. *Entomological Review*, *99*(4), 463–472. <https://doi.org/10.1134/S0013873819040055>
- Lynam, C. P., Llope, M., Möllmann, C., Helaouët, P., Bayliss-Brown, G. A., & Stenseth, N. C. (2017). Interaction between top-down and bottom-up control in marine food webs.

- Proceedings of the National Academy of Sciences of the United States of America*, 114(8), 1952–1957. <https://doi.org/10.1073/pnas.1621037114>
- Magurran, A. E., & Seghers, B. H. (1991). Variation in schooling and aggression amongst guppy (*Poecilia reticulata*) Populations in Trinidad. *Behaviour*, 118(3), 214–234.
- Major, P. F. (1978). Predator-prey interactions in two schooling fishes, *Caranx ignobilis* and *Stolephorus purpureus*. *Animal Behaviour*, 26(PART 3), 760–777. [https://doi.org/10.1016/0003-3472\(78\)90142-2](https://doi.org/10.1016/0003-3472(78)90142-2)
- Malcolm, H. A., Gladstone, W., Lindfield, S., Wraith, J., & Lynch, T. P. (2007). Spatial and temporal variation in reef fish assemblages of marine parks in New South Wales, Australia - Baited video observations. *Marine Ecology Progress Series*, 350, 277–290. <https://doi.org/10.3354/meps07195>
- Manel, S., Guerin, P. E., Mouillot, D., Blanchet, S., Velez, L., Albouy, C., & Pellissier, L. (2020). Global determinants of freshwater and marine fish genetic diversity. *Nature Communications*, 11(1), 1–9. <https://doi.org/10.1038/s41467-020-14409-7>
- Manica, A. (2002). Filial cannibalism in teleost fish. *Biological Reviews*, 77, 261–277. <https://doi.org/10.1017/S1464793101005905>
- Marsh, J. M., Mueter, F. J., Iken, K., & Danielson, S. (2017). Ontogenetic, spatial and temporal variation in trophic level and diet of Chukchi Sea fishes. *Deep-Sea Research Part II: Topical Studies in Oceanography*, 135, 78–94. <https://doi.org/10.1016/j.dsr2.2016.07.010>
- McInnes, J. C., Alderman, R., Lea, M. A., Raymond, B., Deagle, B. E., Phillips, R. A., Stanworth, A., Thompson, D. R., Catry, P., Weimerskirch, H., Suazo, C. G., Gras, M., & Jarman, S. N. (2017). High occurrence of jellyfish predation by black-browed and Campbell albatross identified by DNA metabarcoding. *Molecular Ecology*, 26(18), 4831–4845. <https://doi.org/10.1111/mec.14245>
- McPherson, G. R., Squire, L., & O'Brien, J. (1992). Reproduction of three dominant *Lutjanus* species of the Great Barrier Reef inter-reef fishery. *Asian Fisheries Science*, 5, 15–24.
- Meeker, D. N., Hutchinson, S. A., Ho, L., & Trede, N. S. (2007). Method for isolation of PCR-ready genomic DNA from zebrafish tissues. *BioTechniques*, 43, 610–614. <https://doi.org/10.2144/000112619>

- Methot, R. D., & Wetzel, C. R. (2013). Stock synthesis: A biological and statistical framework for fish stock assessment and fishery management. *Fisheries Research*, *142*, 86–99. <https://doi.org/10.1016/j.fishres.2012.10.012>
- Meyer, A. (1989). Cost of morphological specialization: feeding performance of the two morphs in the trophically polymorphic cichlid fish, *Cichlasoma citrinellum*. *Oecologia*, *80*, 431–436. <https://doi.org/doi.org/10.1007/BF00379047>
- Moberg, F., & Folke, C. (1999). Ecological goods and services of coral reef ecosystems. *Ecological Economics*, *29*(2), 215–233. [https://doi.org/10.1016/S0921-8009\(99\)00009-9](https://doi.org/10.1016/S0921-8009(99)00009-9)
- Moore, C. H., Drazen, J. C., Radford, B. T., Kelley, C., & Newman, S. J. (2016). Improving essential fish habitat designation to support sustainable ecosystem-based fisheries management. *Marine Policy*, *69*, 32–41. <https://doi.org/10.1016/j.marpol.2016.03.021>
- Moore, C. H., Harvey, E. S., & Van Niel, K. P. (2009). Spatial prediction of demersal fish distributions: Enhancing our understanding of species-environment relationships. *ICES Journal of Marine Science*, *66*(9), 2068–2075. <https://doi.org/10.1093/icesjms/fsp205>
- Mousavi-Derazmahalleh, M., Stott, A., Lines, R., Peverley, G., Nester, G., Simpson, T., Zawierta, M., De La Pierre, M., Bunce, M., & Christophersen, C. T. (2021). eDNAFlow, an automated, reproducible and scalable workflow for analysis of environmental DNA sequences exploiting Nextflow and Singularity. *Molecular Ecology Resources*, *21*(5), 1697–1704. <https://doi.org/10.1111/1755-0998.13356>
- Mumby, P. J. (2006). Connectivity of reef fish between mangroves and coral reefs: Algorithms for the design of marine reserves at seascape scales. *Biological Conservation*, *128*, 215–222. <https://doi.org/10.1016/j.biocon.2005.09.042>
- Myers, E. M. V., Harvey, E. S., Saunders, B. J., & Travers, M. J. (2016). Fine-scale patterns in the day, night and crepuscular composition of a temperate reef fish assemblage. *Marine Ecology*, *37*(3), 668–678. <https://doi.org/10.1111/maec.12336>
- Nagelkerken, I., Van Der Velde, G., Wartenbergh, S. L. J., Nugues, M. M., & Pratchett, M. S. (2009). Cryptic dietary components reduce dietary overlap among sympatric butterflyfishes (Chaetodontidae). *Journal of Fish Biology*, *75*(6), 1123–1143. <https://doi.org/10.1111/j.1095-8649.2009.02303.x>
- Nakamura, Y., Horinouchi, M., Shibuno, T., Tanaka, Y., Miyajima, T., Koike, I., Kurokura,

- H., & Sano, M. (2008). Evidence of ontogenetic migration from mangroves to coral reefs by black-tail snapper *Lutjanus fulvus*: stable isotope approach. *Marine Ecology Progress Series*, 355, 257–266. <https://doi.org/10.3354/meps07234>
- Navarro, J., Votier, S. C., Aguzzi, J., Chiesa, J. J., Forero, M. G., & Phillips, R. A. (2013). Ecological segregation in space, time and trophic niche of sympatric planktivorous petrels. *PLoS ONE*, 8(4). <https://doi.org/10.1371/journal.pone.0062897>
- Nester, G. M., De Brauwer, M., Koziol, A., West, K. M., DiBattista, J. D., White, N. E., Power, M., Heydenrych, M. J., Harvey, E., & Bunce, M. (2020). Development and evaluation of fish eDNA metabarcoding assays facilitate the detection of cryptic seahorse taxa (family: Syngnathidae). *Environmental DNA*, April, 1–13. <https://doi.org/10.1002/edn3.93>
- Newman, S. J. (2002). Growth rate, age determination, natural mortality and production potential of the scarlet seaperch, *Lutjanus malabaricus* Schneider 1801, off the Pilbara coast of north-western Australia. *Fisheries Research*, 58, 215–225.
- Newman, S. J., Cappo, M., & Williams, D. M. B. (2000). Age, growth, mortality rates and corresponding yield estimates using otoliths of the tropical red snappers, *Lutjanus erythropterus*, *L. malabaricus* and *L. sebae*, from the central Great Barrier Reef. *Fisheries Research*, 48(1), 1–14. [https://doi.org/10.1016/S0165-7836\(00\)00115-6](https://doi.org/10.1016/S0165-7836(00)00115-6)
- Newman, S. J., Skepper, C. L., Mitsopoulos, G. E. A., Wakefield, C. B., Meeuwig, J. J., & Harvey, E. S. (2011). Assessment of the potential impacts of trap usage and ghost fishing on the Northern Demersal Scalefish Fishery. *Reviews in Fisheries Science*, 19(2), 74–84. <https://doi.org/10.1080/10641262.2010.543961>
- Newman, S. J., Wakefield, C. B., Williams, A. J., O'Malley, J. M., Nicol, S. J., DeMartini, E. E., Halafihi, T., Kaltavara, J., Humphreys, R. L., Taylor, B. M., Andrews, A. H., & Nichols, R. S. (2015). International workshop on methodological evolution to improve estimates of life history parameters and fisheries management of data-poor deep-water snappers and groupers. *Marine Policy*, 60, 182–185. <https://doi.org/10.1016/j.marpol.2015.06.020>
- Newman, S. J., Williams, A. J., Wakefield, C. B., Nicol, S. J., Taylor, B. M., & O'Malley, J. M. (2016). Review of the life history characteristics, ecology and fisheries for deep-water tropical demersal fish in the Indo-Pacific region. *Reviews in Fish Biology and Fisheries*, 26(3), 537–562. <https://doi.org/10.1007/s11160-016-9442-1>

- Newman, S. J., & Williams, D. M. B. (1996). Variation in reef associated assemblages of the Lutjanidae and Lethrinidae at different distances offshore in the central Great Barrier Reef. *Environmental Biology of Fishes*, 46(2), 123–138.
<https://doi.org/10.1007/BF00005214>
- NOAA, Magnuson-Stevens Fishery Management and Conservation Act amended through 11 October 1996. NOAA Technical Memorandum NMFS-F/SPO-23. U.S. Department of Commerce. (1996).
- O'Neill, M. F. O., Leigh, G. M., Martin, J. M., Newman, S. J., Chambers, M., Dichmont, C. M., & Buckworth, R. C. (2011). *Sustaining productivity of tropical red snappers using new monitoring and reference points* (Issue 20). The State of Queensland, Department of Employment, Economic Development and Innovation.
- Oyafuso, Z. S., Drazen, J. C., Moore, C. H., & Franklin, E. C. (2017). Habitat-based species distribution modelling of the Hawaiian deepwater snapper-grouper complex. *Fisheries Research*, 195(October 2016), 19–27. <https://doi.org/10.1016/j.fishres.2017.06.011>
- Padial, J. M., Miralles, A., De la Riva, I., & Vences, M. (2010). The integrative future of taxonomy. *Frontiers in Zoology*, 7, 1–15. <https://doi.org/10.1186/1742-9994-7-16>
- Palumbi, S. R. (1994). Genetic divergence, reproductive isolation, and marine speciation. *Annual Review of Ecology and Systematics*, 25, 547–572.
- Paradinas, I., Conesa, D., Pennino, M. G., Muñoz, F., Fernández, A. M., López-Quílez, A., & Bellido, J. M. (2015). Bayesian spatio-temporal approach to identifying fish nurseries by validating persistence areas. *Marine Ecology Progress Series*, 528, 245–255. <https://doi.org/10.3354/meps11281>
- Pebesma, E. J. (2004). Multivariable geostatistics in S: the gstat package. *Computers and Geosciences*, 30(7), 683–691. <https://doi.org/10.1016/j.cageo.2004.03.012>
- Peters, K. J., Ophelkeller, K., Bott, N. J., Deagle, B. E., Jarman, S. N., & Goldsworthy, S. D. (2014). Fine-scale diet of the Australian sea lion (*Neophoca cinerea*) using DNA-based analysis of faeces. *Marine Ecology*, 36, 347–367.
<https://doi.org/doi.org/10.1111/maec.12145>
- Piggott, C. V. H., Depczynski, M., Gagliano, M., & Langlois, T. J. (2020). Remote video methods for studying juvenile fish populations in challenging environments. *Journal of Experimental Marine Biology and Ecology*, 532, 151454.

<https://doi.org/10.1016/j.jembe.2020.151454>

- Pimentel, C. R., & Joyeux, J. C. (2010). Diet and food partitioning between juveniles of mutton *Lutjanus analis*, dog *Lutjanus jocu* and lane *Lutjanus synagris* snappers (Perciformes: Lutjanidae) in a mangrove-fringed estuarine environment. *Journal of Fish Biology*, *76*(10), 2299–2317. <https://doi.org/10.1111/j.1095-8649.2010.02586.x>
- Piñol, J., Mir, G., Gomez-Polo, P., & Agustí, N. (2015). Universal and blocking primer mismatches limit the use of high-throughput DNA sequencing for the quantitative metabarcoding of arthropods. *Molecular Ecology Resources*, *15*(4), 819–830. <https://doi.org/10.1111/1755-0998.12355>
- Plagányi, É. E., Punt, A. E., Hillary, R., Morello, E. B., Thébaud, O., Hutton, T., Pillans, R. D., Thorson, J. T., Fulton, E. A., Smith, A. D. M., Smith, F., Bayliss, P., Haywood, M., Lyne, V., & Rothlisberg, P. C. (2014). Multispecies fisheries management and conservation: Tactical applications using models of intermediate complexity. *Fish and Fisheries*, *15*(1), 1–22. <https://doi.org/10.1111/j.1467-2979.2012.00488.x>
- Pochon, X., Bott, N. J., Smith, K. F., & Wood, S. A. (2013). Evaluating detection limits of next-generation sequencing for the surveillance and monitoring of international marine pests. *PLoS ONE*, *8*, e73935. <https://doi.org/10.1371/journal.pone.0073935>
- Pompanon, F., Deagle, B. E., Symondson, W. O. C., Brown, D. S., Jarman, S. N., & Taberlet, P. (2012). Who is eating what: diet assessment using next generation sequencing. *Molecular Ecology*, *21*, 1931–1950. <https://doi.org/10.1111/j.1365-294X.2011.05403.x>
- Ponton, D., Carassou, L., Raillard, S., & Borsa, P. (2013). Geometric morphometrics as a tool for identifying emperor fish (Lethrinidae) larvae and juveniles. *Journal of Fish Biology*, *83*(1), 14–27. <https://doi.org/10.1111/jfb.12138>
- Popper, A. N., Ramcharitar, J., & Campana, S. E. (2005). Why otoliths? Insights from inner ear physiology and fisheries biology. *Marine and Freshwater Research*, *56*(5), 497–504. <https://doi.org/10.1071/MF04267>
- Pratchett, M. S. (2005). Dietary overlap among coral-feeding butterflyfishes (Chaetodontidae) at Lizard Island, northern Great Barrier Reef. *Marine Biology*, *148*, 373–382. <https://doi.org/10.1007/s00227-005-0084-4>
- Prochazka, K. (1998). Spatial and trophic partitioning in cryptic fish communities of shallow

- subtidal reefs in False Bay, South Africa. *Environmental Biology of Fishes*, 51(2), 201–220. <https://doi.org/10.1023/A:1007407200708>
- Quéméré, E., Aucourd, M., Troispoux, V., Brosse, S., Murienne, J., Covain, R., Le Bail, P. Y., Olivier, J., Tysklind, N., & Galan, M. (2021). Unraveling the dietary diversity of Neotropical top predators using scat DNA metabarcoding: A case study on the elusive Giant Otter. *Environmental DNA*, 3, 889–900. <https://doi.org/10.1002/edn3.195>
- Raguragavan, J., Hailu, A., & Burton, M. (2013). Economic valuation of recreational fishing in Western Australia: Statewide random utility modelling of fishing site choice behaviour. *Australian Journal of Agricultural and Resource Economics*, 57(4), 539–558. <https://doi.org/10.1111/1467-8489.12009>
- Razgour, O., Clare, E. L., Zeale, M. R. K., Hanmer, J., Schnell, I. B., Rasmussen, M., Gilbert, T. P., & Jones, G. (2011). High-throughput sequencing offers insight into mechanisms of resource partitioning in cryptic bat species. *Ecology and Evolution*, 1, 556–570. <https://doi.org/10.1002/ece3.49>
- Ridgeway, G. (2013). *Generalized boosted regression models. Documentation on the R package "gbm", version 2.1*. <http://code.google.com/p/gradientboostedmodels/>
- Rooker, J. R. (1995). Feeding ecology of the schoolmaster snapper, *Lutjanus apodus* (Walbaum), from southwestern Puerto Rico. *Bulletin of Marine Science*, 56, 881–894.
- RStudio Team. (2016). *RStudio: Integrated Development for R*. RStudio, Inc. <http://www.rstudio.com/>
- Rundle, H. D., & Nosil, P. (2005). Ecological speciation. *Ecology Letters*, 8(3), 336–352. <https://doi.org/10.1111/j.1461-0248.2004.00715.x>
- Ryan, K. L., Hall, N. G., Lai, E. K. M., Smallwood, C. B., Tate, A., Taylor, S. M., & Wise, B. S. (2019). State-wide survey of boat-based recreational fishing in Western Australia 2017/18. In *Fisheries Research Report No. 297* (Issue 297). http://www.fish.wa.gov.au/Documents/research_reports/frr297.pdf
- Sadighzadeh, Z., Tuset, V. M., Valinassab, T., Dadpour, M. R., & Lombarte, A. (2012). Comparison of different otolith shape descriptors and morphometrics for the identification of closely related species of *Lutjanus* spp. from the Persian Gulf. *Marine Biology Research*, 8(9), 802–814. <https://doi.org/10.1080/17451000.2012.692163>

- Sagarese, S. R., Frisk, M. G., Cerrato, R. M., Sosebee, K. A., Musick, J. A., & Rago, P. J. (2014). Application of generalized additive models to examine ontogenetic and seasonal distributions of spiny dogfish (*Squalus acanthias*) in the Northeast (US) shelf large marine ecosystem. *Canadian Journal of Fisheries and Aquatic Sciences*, *71*(6), 847–877. <https://doi.org/10.1139/cjfas-2013-0342>
- Sale, P. F. (1974). Overlap in resource use, and interspecific competition. *Oecologia*, *17*, 245–256. <https://doi.org/10.1007/BF00344924>
- Sale, P. F. (1978). Coexistence of coral reef fishes - a lottery for living space. *Environmental Biology of Fishes*, *3*, 85–102. <https://doi.org/10.1007/BF00006310>
- Salini, J. P., Blaber, S. J. M., & Brewer, D. T. (1990). Diets of piscivorous fishes in a tropical Australian estuary, with special reference to predation on penaeid prawns. *Marine Biology*, *105*(3), 363–374. <https://doi.org/10.1007/BF01316307>
- Salini, J. P., Blaber, S. J. M., & Brewer, D. T. (1994). Diets of trawled predatory fish of the Gulf of Carpentaria, Australia, with particular reference to predation on prawns. *Australian Journal of Marine and Freshwater Research*, *45*, 397–411. <https://doi.org/10.1071/MF9940397>
- Salini, J. P., Ovenden, J. R., Street, R., Pendrey, R., Haryanti, & Ngurah. (2006). Genetic population structure of red snappers (*Lutjanus malabaricus* Bloch & Schneider, 1801 and *Lutjanus erythropterus* Bloch, 1790) in central and eastern Indonesia and northern Australia. *Journal of Fish Biology*, *68*, 217–234. <https://doi.org/10.1111/j.0022-1112.2006.001060.x>
- Sanders, K. L., Malhotra, A., & Thorpe, R. S. (2006). Combining molecular, morphological and ecological data to infer species boundaries in a cryptic tropical pitviper. *Biological Journal of the Linnean Society*, *87*(3), 343–364. <https://doi.org/10.1111/j.1095-8312.2006.00568.x>
- Santos, R. O., Rehage, J. S., Adams, A. J., Black, B. D., Osborne, J., & Kroloff, E. K. N. (2017). Quantitative assessment of a data-limited recreational bonefish fishery using a time-series of fishing guides reports. *PLoS ONE*, *12*(9), 1–19. <https://doi.org/10.1371/journal.pone.0184776>
- Saunders, T., Lunow, C., Trinnie, F., Wakefield, C. B., & Newman, S. J. (2018). *Lutjanus malabaricus*. In C. Stewardson, C. Andrews, C. Ashby, M. Haddon, K. Hartmann, P. Hone, P. Horvat, S. Mayfield, A. Roelofs, K. Sainsbury, T. Saunders, J. Stewart, S.

- Nicol, & B. Wise (Eds.), *Status of Australian fish stock reports 2018*, Fisheries Research and Development Corporation.
- Schluter, D. (2000). Ecological character displacement in adaptive radiation. *The American Naturalist*, 156, S4–S16. <https://doi.org/10.2307/3079223>
- Scriven, J. J., Whitehorn, P. R., Goulson, D., & Tinsley, M. C. (2016). Niche partitioning in a sympatric cryptic species complex. *Ecology and Evolution*, 6(5), 1328–1339. <https://doi.org/10.1002/ece3.1965>
- Sheppard, S. K., Bell, J., Sunderland, K. D., Fenlon, J., Skervin, D., & Symondson, W. O. C. (2005). Detection of secondary predation by PCR analyses of the gut contents of invertebrate generalist predators. *Molecular Ecology*, 14(14), 4461–4468. <https://doi.org/10.1111/j.1365-294X.2005.02742.x>
- Siegenthaler, A., Wangenstein, O. S., Benvenuto, C., Campos, J., & Mariani, S. (2019). DNA metabarcoding unveils multiscale trophic variation in a widespread coastal opportunist. *Molecular Ecology*, 28(2), 232–249. <https://doi.org/10.1111/mec.14886>
- Sievers, K. T., Abesamis, R. A., Bucol, A. A., & Russ, G. R. (2020). Unravelling seascape patterns of cryptic life stages: Non-reef habitat use in juvenile parrotfishes. *Diversity*, 12, 1–18. <https://doi.org/10.3390/d12100376>
- Škeljo, F., & Ferri, J. (2012). The use of otolith shape and morphometry for identification and size-estimation of five wrasse species in predator-prey studies. *Journal of Applied Ichthyology*, 28(4), 524–530. <https://doi.org/10.1111/j.1439-0426.2011.01925.x>
- Sousa, L. L., Silva, S. M., & Xavier, R. (2019). DNA metabarcoding in diet studies: Unveiling ecological aspects in aquatic and terrestrial ecosystems. *Environmental DNA*, 1(3), 199–214. <https://doi.org/10.1002/edn3.27>
- Stamoulis, K. A., Delevaux, J. M. S., Williams, I. D., Poti, M., Lecky, J., Costa, B., Kendall, M. S., Pittman, S. J., Donovan, M. K., Wedding, L. M., & Friedlander, A. M. (2018). Seascape models reveal places to focus coastal fisheries management. *Ecological Applications*, 28(4), 910–925. <https://doi.org/10.1002/eap.1696>
- Stewardson, C., Andrews, J., Ashby, C., Haddon, M., Hartmann, K., Hone, P., Horvat, P., Mayfield, S., Roelofs, A., Sainsbury, K., Saunders, T., Stewart, J., Nicol, S., & Wise, B. (2018). *Status of Australian fish stocks reports 2018*, Fisheries Research and Development Corporation.

- Stobutzki, I., Miller, M., & Brewer, D. (2001). Sustainability of fishery bycatch: A process for assessing highly diverse and numerous bycatch. *Environmental Conservation*, 28(2), 167–181. <https://doi.org/10.1017/S0376892901000170>
- Stoner, A. W., Laurel, B. J., & Hurst, T. P. (2008). Using a baited camera to assess relative abundance of juvenile Pacific cod: Field and laboratory trials. *Journal of Experimental Marine Biology and Ecology*, 354(2), 202–211. <https://doi.org/10.1016/j.jembe.2007.11.008>
- Stransky, C., & MacLellan, S. E. (2005). Species separation and zoogeography of redfish and rockfish (genus *Sebastes*) by otolith shape analysis. *Canadian Journal of Fisheries and Aquatic Sciences*, 62, 2265–2276. <https://doi.org/10.1139/f05-143>
- Stroud, J. T., & Losos, J. B. (2016). Ecological opportunity and adaptive radiation. *Annual Review of Ecology, Evolution, and Systematics*, 47, 507–532. <https://doi.org/10.1146/annurev-ecolsys-121415-032254>
- Su, M., Liu, H., Liang, X., Gui, L., & Zhang, J. (2017). Dietary analysis of marine fish species: Enhancing the detection of prey-specific DNA sequences via high-throughput sequencing using blocking primers. *Estuaries and Coasts*, 41, 560–571. <https://doi.org/10.1007/s12237-017-0279-1>
- Sundblad, G., Bergstrom, U., Sandstrom, A., & Eklov, P. (2014). Nursery habitat availability limits adult stock sizes of predatory coastal fish. *ICES Journal of Marine Science*, 71, 672–680.
- Szedlmayer, S. T., & Lee, J. D. (2004). Diet shifts of juvenile red snapper (*Lutjanus compechanus*) with changes in habitat and fish size. *Fishery Bulletin*, 102(2), 366–375.
- Takahashi, M., DiBattista, J. D., Jarman, S., Newman, S. J., Wakefield, C. B., Harvey, E. S., & Bunce, M. (2020). Partitioning of diet between species and life history stages of sympatric and cryptic snappers (Lutjanidae) based on DNA metabarcoding. *Scientific Reports*, 10, 4319. <https://doi.org/10.1038/s41598-020-60779-9>
- Tate, A., Ryan, K. L., Smallwood, C. B., Desfosses, C. J., Taylor, S. M., & Blight, S. J. (2019). Review of recreational fishing surveys in Western Australia. In *Fisheries Research Report No. 301* (Issue 301). http://www.fish.wa.gov.au/Documents/research_reports/frr301.pdf
- Thomas, R. C., Willette, D. A., Carpenter, K. E., & Santos, M. D. (2014). Hidden diversity

- in sardines: Genetic and morphological evidence for cryptic species in the goldstripe sardinella, *Sardinella gibbosa* (Bleeker, 1894). *PLoS ONE*, 9(1), 1–10.
<https://doi.org/10.1371/journal.pone.0084719>
- Thrush, S. F., & Dayton, P. K. (2010). What can ecology contribute to ecosystem-based management? *Annual Review of Marine Science*, 2(1), 419–441.
<https://doi.org/10.1146/annurev-marine-120308-081129>
- Tittensor, D. P., Micheli, F., Nyström, M., & Worm, B. (2007). Human impacts on the species-area relationship in reef fish assemblages. *Ecology Letters*, 10(9), 760–772.
<https://doi.org/10.1111/j.1461-0248.2007.01076.x>
- Tittensor, D. P., Mora, C., Jetz, W., Lotze, H. K., Ricard, D., Berghe, E. Vanden, & Worm, B. (2010). Global patterns and predictors of marine biodiversity across taxa. *Nature*, 466(7310), 1098–1101. <https://doi.org/10.1038/nature09329>
- Tonks, M. L., Griffiths, S. P., Heales, D. S., Brewer, D. T., & Dell, Q. (2008). Species composition and temporal variation of prawn trawl bycatch in the Joseph Bonaparte Gulf, northwestern Australia. *Fisheries Research*, 89(3), 276–293.
<https://doi.org/10.1016/j.fishres.2007.09.007>
- Tracey, S. R., Lyle, J. M., & Duhamel, G. (2006). Application of elliptical Fourier analysis of otolith form as a tool for stock identification. *Fisheries Research*, 77(2), 138–147.
<https://doi.org/10.1016/j.fishres.2005.10.013>
- Tsoumani, M., Apostolidis, A. P., & Leonardos, I. D. (2013). Biogeography of *Rutilus* species of the southern Balkan Peninsula as inferred by multivariate analysis of morphological data. *Journal of Zoology*, 289(3), 204–212.
<https://doi.org/10.1111/j.1469-7998.2012.00979.x>
- Tuset, V. M., Rosin, P. L., & Lombarte, A. (2006). Sagittal otolith shape used in the identification of fishes of the genus *Serranus*. *Fisheries Research*, 81(2–3), 316–325.
<https://doi.org/10.1016/j.fishres.2006.06.020>
- Usmar, N. R. (2012). Ontogenetic diet shifts in snapper (*Pagrus auratus*: Sparidae) within a New Zealand estuary. *New Zealand Journal of Marine and Freshwater Research*, 46(1), 31–46. <https://doi.org/10.1080/00288330.2011.587824>
- Valentini, A., Pompanon, F., & Taberlet, P. (2009). DNA barcoding for ecologists. *Trends in Ecology and Evolution*, 24, 110–117. <https://doi.org/10.1016/j.tree.2008.09.011>

- Vasconcelos, R. P., Reis-Santos, P., Maia, A., Fonseca, V., França, S., Wouters, N., Costa, M. J., & Cabral, H. N. (2010). Nursery use patterns of commercially important marine fish species in estuarine systems along the Portuguese coast. *Estuarine, Coastal and Shelf Science*, 86(4), 613–624. <https://doi.org/10.1016/j.ecss.2009.11.029>
- Vega, G. C., & Wiens, J. J. (2012). Why are there so few fish in the sea? *Proceedings of the Royal Society B: Biological Sciences*, 279(1737), 2323–2329. <https://doi.org/10.1098/rspb.2012.0075>
- Vestheim, H., Deagle, B. E., & Jarman, S. N. (2011). Application of blocking oligonucleotides to improve signal-to-noise ratio in a PCR. In D. J. Park (Ed.), *PCR Protocols. Method in Molecular Biology (Methods and Protocols)* (3rd Ed., Vol. 687, pp. 265–274). Humana Press. <https://doi.org/10.1007/978-1-60761-944-4>
- Vestheim, H., & Jarman, S. N. (2008). Blocking primers to enhance PCR amplification of rare sequences in mixed samples - A case study on prey DNA in Antarctic krill stomachs. *Frontiers in Zoology*, 5(12), 1–11. <https://doi.org/10.1186/1742-9994-5-12>
- Wainwright, J., & Mulligan, M. (2013). Environmental modelling : finding simplicity in complexity. In J. Wainwright & M. Mulligan (Eds.), *A John Wiley & Sons, Ltd.* (2nd ed.). Wiley-Blackwell. https://doi.org/10.4324/9780203302217_chapter_12
- Wainwright, P. C., & Richard, B. A. (1995). Predicting patterns of prey use from morphology of fishes. *Environmental Biology of Fishes*, 44, 97–113. <https://doi.org/10.1007/BF00005909>
- Wakefield, C. B., Moran, M. J., Tapp, N. E., & Jackson, G. (2007). Catchability and selectivity of juvenile snapper (*Pagrus auratus*, Sparidae) and western butterfish (*Pentapodus vitta*, Nemipteridae) from prawn trawling in a large marine embayment in Western Australia. *Fisheries Research*, 85(1–2), 37–48. <https://doi.org/10.1016/j.fishres.2006.11.037>
- Wakefield, C. B., Williams, A. J., Newman, S. J., Bunel, M., Dowling, C. E., Armstrong, C. A., & Langlois, T. J. (2014). Rapid and reliable multivariate discrimination for two cryptic Eteline snappers using otolith morphometry. *Fisheries Research*, 151, 100–106. <https://doi.org/10.1016/j.fishres.2013.10.011>
- Wäldchen, J., & Mäder, P. (2018). Machine learning for image based species identification. *Methods in Ecology and Evolution*, 9(11), 2216–2225. <https://doi.org/10.1111/2041-210X.13075>

- Wang, Z. L., Zhang, D. Y., & Wang, G. (2005). Does spatial structure facilitate coexistence of identical competitors? *Ecological Modelling*, *181*(1), 17–23.
<https://doi.org/10.1016/j.ecolmodel.2004.06.020>
- Wangensteen, O. S., & Turon, X. (2017). Metabarcoding techniques for assessing biodiversity of marine animal forests. In S. Rossi, L. Bramanti, A. Gori, & C. Orejas (Eds.), *Marine Animal Forests: The Ecology of Benthic Biodiversity Hotspots* (pp. 455–473). Springer International Publishing.
- Ward, R. D., Zemplak, T. S., Innes, B. H., Last, P. R., & Hebert, P. D. N. (2005). DNA barcoding Australia's fish species. *Philosophical Transactions of the Royal Society B: Biological Sciences*, *360*(1462), 1847–1857. <https://doi.org/10.1098/rstb.2005.1716>
- Wells, R. J. D., Cowan Jr, J. H., & Fry, B. (2008). Feeding ecology of red snapper *Lutjanus campechanus* in the northern Gulf of Mexico. *Marine Ecology Progress Series*, *361*, 213–225. <https://doi.org/10.3354/meps07425>
- Wen, C. K., Almany, G. R., Williamson, D. H., Pratchett, M. S., & Jones, G. P. (2012). Evaluating the effects of marine reserves on diet, prey availability and prey selection by juvenile predatory fishes. *Marine Ecology Progress Series*, *469*, 133–144.
<https://doi.org/10.3354/meps09949>
- Wernberg, T., Smale, D. A., Tuya, F., Thomsen, M. S., Langlois, T. J., De Bettignies, T., Bennett, S., & Rousseaux, C. S. (2013). An extreme climatic event alters marine ecosystem structure in a global biodiversity hotspot. *Nature Climate Change*, *3*(1), 78–82. <https://doi.org/10.1038/nclimate1627>
- West, J. M., Williams, G. D., Madon, S. P., & Zedler, J. B. (2003). Integrating spatial and temporal variability into the analysis of fish food web linkages in Tijuana Estuary. *Environmental Biology of Fishes*, *67*(3), 297–309.
<https://doi.org/10.1023/A:1025843300415>
- West, L. D., Lyle, J. M., Matthews, S. R., Stark, K. E., & Steffe, A. S. (2012). Survey of recreational fishing in the Northern Territory 2009-10. In *Fishery Report No. 109* (Issue 109).
- Whiteway, T. (2009). *Australian bathymetry and topography grid*. Geoscience Australia.
- Whitfield, A. K., & Becker, A. (2014). Impacts of recreational motorboats on fishes: A review. *Marine Pollution Bulletin*, *83*(1), 24–31.

<https://doi.org/10.1016/j.marpolbul.2014.03.055>

- Williams, A. J., Newman, S. J., Wakefield, C. B., Bunel, M., Halafihi, T., Kaltavara, J., & Nicol, S. J. (2015). Evaluating the performance of otolith morphometrics in deriving age compositions and mortality rates for assessment of data-poor tropical fisheries. *ICES Journal of Marine Science*, *72*, 2098–2109.
- Williams, D. M., & Russ, G. R. (1994). Review of data on fishes of commercial and recreational fishing interest in the Great Barrier Reef: a report to the Great Barrier Reef Marine Park Authority. *North*, *33*.
<http://books.google.com.au/books?id=OyMWAQAIAAJ>
- Williamson, D. H., Ceccarelli, D. M., Evans, R. D., Jones, G. P., & Russ, G. R. (2014). Habitat dynamics, marine reserve status, and the decline and recovery of coral reef fish communities. *Ecology and Evolution*, *4*(4), 337–354. <https://doi.org/10.1002/ece3.934>
- Wood, S. N. (2006). *Generalized Additive Models: an introduction with R*. Chapman & Hall/CRC.
- Worm, B., Hilborn, R., Baum, J. K., Branch, T. A., Collie, J. S., Costello, C., Fogarty, M. J., Fulton, E. A., Hutchings, J. A., Jennings, S., Jensen, O. P., Lotze, H. K., Mace, P. M., McClanahan, T. R., Minto, C., Palumbi, S. R., Parma, A. M., Ricard, D., Rosenberg, A. A., ... Zeller, D. (2009). Rebuilding Global Fisheries. *Science*, *325*(5940), 578–585. <https://doi.org/10.1126/science.1173146>
- Wuenschel, M. J., Hare, J. A., Kimball, M. E., & Able, K. W. (2012). Evaluating juvenile thermal tolerance as a constraint on adult range of gray snapper (*Lutjanus griseus*): A combined laboratory, field and modeling approach. *Journal of Experimental Marine Biology and Ecology*, *436–437*, 19–27. <https://doi.org/10.1016/j.jembe.2012.08.012>
- Yamano, H., Sugihara, K., & Nomura, K. (2011). Rapid poleward range expansion of tropical reef corals in response to rising sea surface temperatures. *Geophysical Research Letters*, *38*(4), L04601. <https://doi.org/10.1029/2010GL046474>
- Zhuang, L., Ye, Z., & Zhang, C. (2015). Application of otolith shape analysis to species separation in *Sebastes* spp. from the Bohai Sea and the Yellow Sea, northwest Pacific. *Environmental Biology of Fishes*, *98*(2), 547–558. <https://doi.org/10.1007/s10641-014-0286-z>
- Zischke, M. T., Litherland, L., Tilyard, B. R., Stratford, N. J., Jones, E. L., & Wang, Y.

(2016). Otolith morphology of four mackerel species (*Scomberomorus* spp.) in Australia: Species differentiation and assessment. *Fisheries Research*, 176, 39–47.
<https://doi.org/10.1016/j.fishres.2015.12.003>

Every reasonable effort has been made to acknowledge the owners of copyright material. I would be pleased to hear from any copyright owner who has been omitted or incorrectly acknowledge.